UNIVERSITY OF CALGARY

Synthesis and Properties of Anthraquinone Labelled Nucleobases

by

Sandra Elizabeth Phillips

A THESIS

SUBMITTED TO THE FACULTY OF GRADUATE STUDIES

IN PARTIAL FULFILMENT OF THE REQUIREMENTS FOR THE

DEGREE OF MASTER OF SCIENCE

DEPARTMENT OF CHEMISTRY

CALGARY, ALBERTA

JULY, 2010

Your file Votre référence
ISBN: 978-0-494-69566-1
Our file Notre référence
ISBN: 978-0-494-69566-1

UNIVERSITY OF CALGARY

FACULTY OF GRADUATE STUDIES

The undersigned certify that they have read, and recommend to the Faculty of Graduate Studies for acceptance, a thesis entitled "Synthesis and Properties of Anthraquinone Labelled Nucleobases" submitted by Sandra Elizabeth Phillips in partial fulfilment of the requirements of the degree of Master of Science.

Supervisor, Dr. Todd C. Sutherland
Department of Chemistry

Dr. Thomas Baumgartner
Department of Chemistry

Dr. Chang-Chun Ling
Department of Chemistry

Dr. Elmar Prenner
Department of Biological Sciences

Date

Abstract

The early steps in photosynthesis show charge transfer over large distances, ultimately resulting in energy stored in chemical bonds. These long-range charge transports are accomplished by non-covalently bonded redox sites. Our goal is to understand the charge transfer dynamics that occur through hydrogen bonding interactions. To understand the role that hydrogen bonds play in charge transfer, a series of DNA nucleobases functionalized with anthraquinone (AQ) were synthesized and characterized. The target nucleobase-substituted AQs exhibited a limited solubility in the less polar organic solvents, and did not demonstrate hydrogen bonding in moderately more polar solvent, THF. The electrochemical properties of these compounds were examined and the AQs showed redox potentials that ranged from -0.650 to -1.169 V and electron transfer rates that ranged from 1.69×10^{-5} to 60.1×10^{-5} $cm\cdot s^{-1}$. The reduction mechanism of the AQ exhibited the typical two successive one-electron reductions in aprotic solvents.

Acknowledgements

Foremost, Dr. Todd C. Sutherland for providing guidance during my Masters, but it was especially appreciated during the more challenging moments in this research.

I thank my committee members, Dr. Thomas Baumgartner, Dr. Chang-Chun Ling, and Dr. Elmar Prenner for being part of my academic journey.

I want to also thank the Sutherland group members, with a special thank-you to Anusha Abhayawardhana for acting more as a sister than anything else.

I thank the Department Instrumentation Facility staff for running numerous samples of mine and for maintaining all of the equipment.

I want to thank the office staff, with a very special thank-you to Bonnie King for always keeping on top of a mountain of paperwork and for always staying positive.

I greatly appreciate Bob Stockwell and Magdi Khalil for the keeping the Chemistry Stores well stocked.

I thank my regular coffee and cookie companions, Lauren Mercier, Sandra Ward, and especially Ian Hargreaves.

Table of Contents

List of Tables

List of Figures and Illustrations

List of Symbols, Abbreviations and Nomenclature

Symbol	Definition
A	adenine
A	absorption
A	area
Ac	acetyl
Ac_2O	acetic anhydride
AcOH	acetic acid
AIBN	azobisisobutyronitrile
AQ	anthraquinone
Ar	aryl
BHJ	bulk-heterojunction
BINAP	2,2'-bis(diphenylphosphino)-1,1'-binaphthyl
Bn	benzyl
Boc	butoxycarbonyl
BOM	benzyloxymethyl
Bu	*n*-butyl
Bz	benzoyl
c	concentration
C_{60}	fullerene
cat.	catalytic
$CDCl_3$	deuterated chloroform
$CHCl_3$	chloroform
CV	cyclic voltammetry
D	diffusion coefficient
DA	donor-acceptor
DBU	1,8-diazabicyclo[5.4.0]undec-7-ene
DCC	dicyclohexylcarbodiimide
DEAD	diethyl azodicarboxylate
DMAP	4-dimethylaminopyridine
DMF	dimethylformamide
DMSO	dimethyl sulfoxide
DMSO-d_6	deuterated dimethyl sulfoxide
DNA	deoxyribonucleic acid
DSSC	dye sensitized solar cell
$E_{½}$	half-wave potential
EDC·HCl	1-ethyl-3-(3-dimethylaminopropyl) carbodiimide hydrochloride
EDG	electron donating group
Et	ethyl
Et_3N	triethylamine
EWG	electron withdrawing group
F	Faraday's constant (96 485 C mol^{-1})

Fc	ferrocenyl
h	height
HB	hydrogen bond
HOMO	highest occupied molecular orbital
hυ	light energy
i	current
*i*Pr	*iso*propyl
IR	infra red
ITO	indium tin oxide
k	electron transfer rate
K_a	association constant
ℓ	path length
LUMO	lowest unoccupied molecular orbital
m	slope
m/z	mass to charge ratio
M^+	molecular ion
Me	methyl
MeCN	acetonitrile
MeOH	methanol
NB	nucleobase
NBS	*N*-bromosuccinimide
NMM	*N*-methylmorpholine
NMR	nuclear magnetic resonance
NREL	National Renewable Energy Laboratory
Nu	nucleophile
OPV	oligo(phenylenevinylene)
OSC	organic solar cell
PEDOT	poly(3,4-ethylenedioxythiophene)
PERY	perylene-diimide
Ph	phenyl
PPV	poly(phenylenevinylene)
Pr	*n*-propyl
PSS	poly(styrenesulfonate)
PTAA	polytriarylamine
PyBOP	benzotriazol-1-yl-oxytripyrrolidinophosphonium hexafluorophosphate
R	ideal gas constant (8.314 J K^{-1} mol^{-1})
r	radius
R_f	retention factor
RNA	ribonucleic acid
SAM	self assembling monolayer
T	thymine
t	time
T	temperature

TBAHFP	tetrabutylammonium hexafluorophosphate
TBDMS	*tert*-butyldimethylsilyl
TBDPS	*tert*-butyldiphenylsilyl
*t*Bu	*tert*-butyl
TEG	triethylene glycol
Tf	triflate
TFA	trifluoroacetic acid
THF	tetrahydrofuran
TMS	trimethylsilanylethynyl
Tr	trityl
Ts	tosyl
TsOH	tosic acid
TTV	tetrathiafulvalene
UP	ureidopyrimidinone
UV-vis	ultraviolet-visible spectroscopy
ε	molar absorbtivity
η	energy conversion efficiency
υ	scan rate

Chapter One: **Introduction and Background Information**

1.1 Energy and the environment

A paper, written by Lewis and Nocera,[1] outlines the expected energy consumption, necessary fuel resources and environmental factors for the year 2050.

From 2000 to 2050, the global energy demands are expected to double from a consumption rate of 13.5 TW to 27.5 TW.[1] This increase is due primarily to the growing population and economies of China and India. Sources[1] predict that there is sufficient kfossil fuel stock to supply this amount of energy based on these predictions; unfortunately the cumulative carbon emissions will have effects on the environment.[1] Based on natural removal methods of CO_2, such as photosynthesis, the emissions of the next 50 years will remain for 500-2000 years.[1]

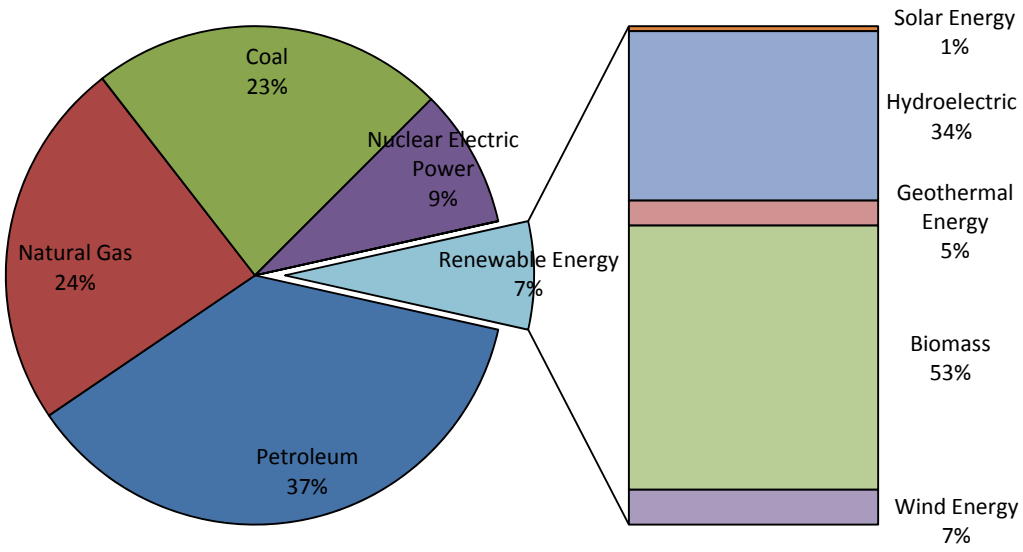

Figure 1-1: The sources of energy consumed in the USA in 2008.[2]

It is hoped that science and innovation will solve this energy dilemma, and this challenge must be met with carbon-neutral or carbon-free technologies. Of the renewable energy

resources, solar power is by far the most abundant source, and thus is the most promising.[1] In 2001, energy was consumed at a rate of 13.0 TW, while the sun radiates the Earth's surface at a rate of 119,000 TW.[3] Challenges that solar power currently face are the manufacturing costs, the efficiency, η, of the solar cell devices, and the actual concentration of the sun's energy on the surface of the Earth.[1] Presently, silicon-based solar cells dominate the market, with a few niche companies specializing in organic solar cells (OSCs).[1] OSCs are growing in popularity in research and in literature, but still need to increase efficiencies and reduce the cost of materials before they are commercially viable, let alone compete with the cost of energy derived from fossil fuels.[1] Currently, the most efficient OSC is 7.9% fabricated by the company Solarmer,[4,5] while the most efficient multicrystalline silicon solar cell rates at 20.4%,[5] and a single crystal silicon compares at 25.0%.[5]

1.2 Types of solar cells (semi conductors)

1.2.1 Inorganic

The major portion of the solar cell market comprises of multicrystalline silicon solar cells because they are less expensive to fabricate than the single crystal varieties.[1]

Another inorganic based solar cell worth mentioning is the multijunction cell. This device, by definition, is composed of two or more layers that each absorbs a different region within the solar spectrum, from approximately 400 – 1800 nm.[6] The most notable multijunction device was fabricated by NREL, which contains three layers (gallium indium phosphide, gallium indium arsenide, and gallium arsenide), and holds the highest efficiency to date of 40.8%.[7] These photovoltaic devices are far too expensive to produce

commercially,[1] but are good candidates for satellites and space exploration as they are lighter than the silicon-based cells.[6]

Instead of making solar cells using the top down approach, the other method is to go from the bottom up. The most common technique is the top down approach, where a mass of silicon is then shaped into a solar cell panel. The bottom up approach describes creating a material via synthetic chemistry that is later fabricated into an OSC. One such family of cells is called the dye sensitized solar cell (DSSC), first constructed by Grätzel *et al.*[8] that utilizes tuned ruthenium based dyes that have been adsorbed onto titanium dioxide particles, as illustrated in Figure 1-2.

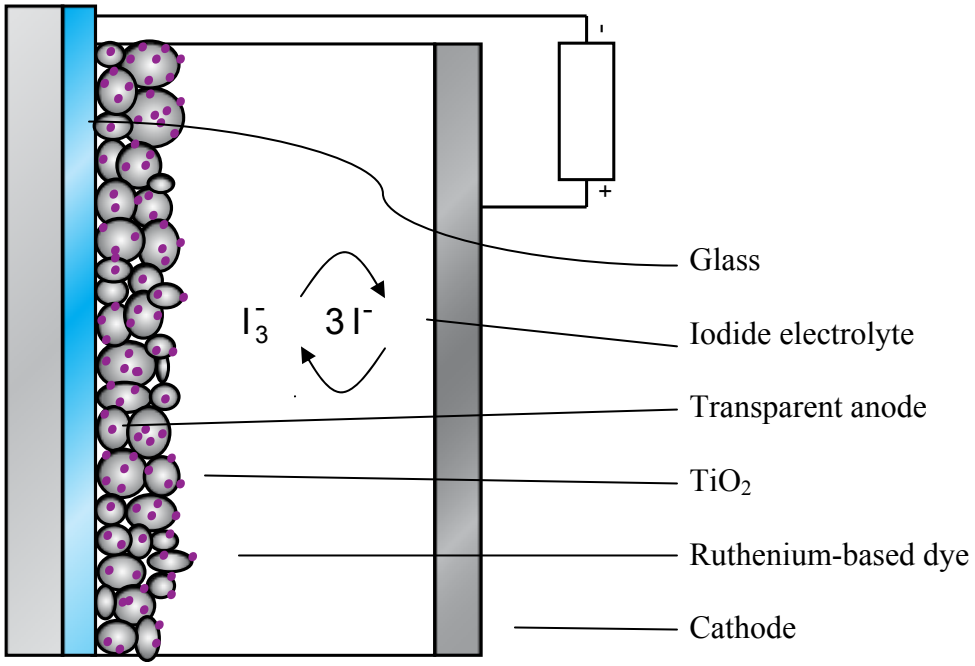

Figure 1-2: The schematics of a dye-sensitized solar cell.[8]

In these cells, the photons are absorbed by the ruthenium (Ru) based dyes, which then inject an electron into the semiconductor, titanium oxide (TiO_2). This electron then passes through the circuit, and reduces the electrolyte, typically iodide, in solution. The reduced

electrolyte then becomes oxidized again when it passes on the electron and regenerates the Ru dye.[8]

1.2.2 Organic

Another bottom up approach employs organic-based solar cells (OSCs). One of the simplest of these photovoltaic devices is the multilayer cell shown in Figure 1-3. A minimum requirement of two organic layers, a donor and an acceptor, are sandwiched between the electrodes.

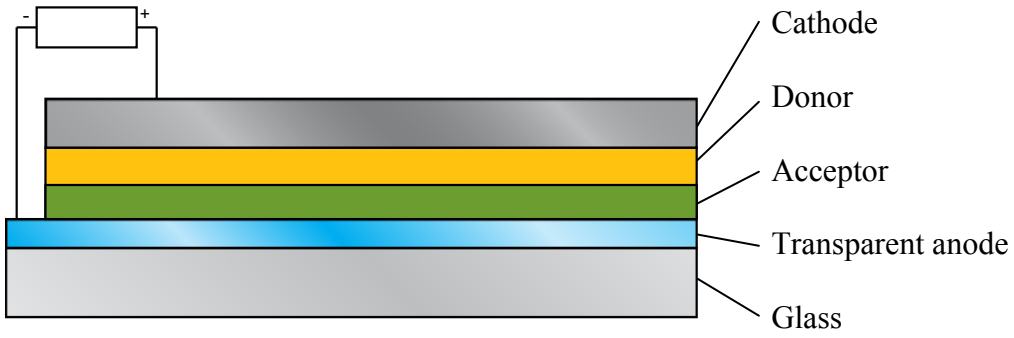

Figure 1-3: The schematics of a simple multilayer organic solar cell.[9,10]

The generation of current between these two layers is explained using four basic steps and is illustrated in Figure 1-4:[11-13]

1. The absorption of a photon creates an exciton in the donor layer. An exciton is an electronically excited molecule that is defined by having an electron from the HOMO (highest occupied molecular orbital) excited into the LUMO (lowest unoccupied molecular orbital).
2. The exciton state diffuses toward the donor-acceptor (DA) interface. The limit to which an exciton can travel is termed the exciton diffusion length and is unique to each donor layer material.

3. At the DA interface, and if energetically favourable, the exciton transfers charge by way of an electron into the acceptor and hole into the donor.
4. The charges travel towards and collect at the electrode contacts. The holes travel towards the cathode and the electrons towards the anode.

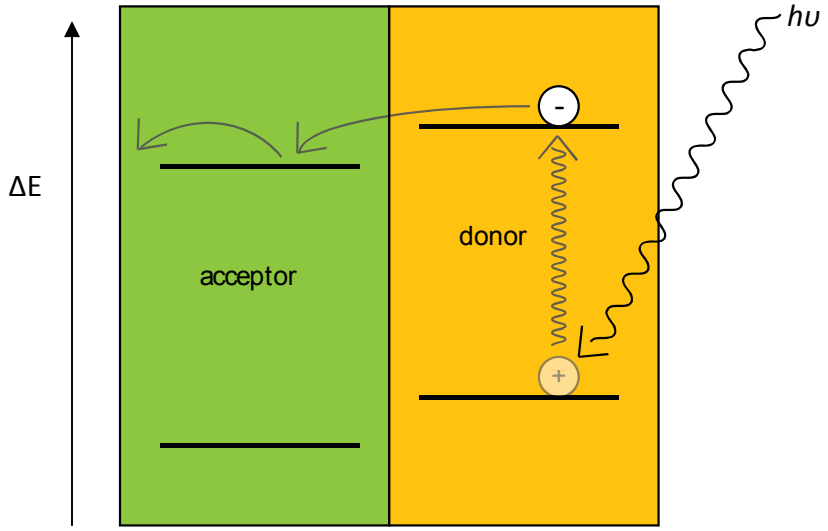

Figure 1-4: The excitation of an electron from the conduction band into the conduction band in an organic solar cell. ΔE is the energy measurement of the HOMOs and the LUMOs, and is typically measured in electron volts (eV).

Some of the most common materials for the active layers for these devices include derivatives of poly(phenylenevinylene) (PPV), fullerene (C_{60}), oligomeric thiophene, phthalocyanine, pentacene, perylene, and polytriarylamine (PTAA) shown in Scheme 1-1.[9,10,14-17]

Scheme 1-1: The chemical structures of the most common materials used in organic solar cells as the active layers. The donor materials are shown in orange, and the acceptor materials are shown in green.[9,10,14-17]

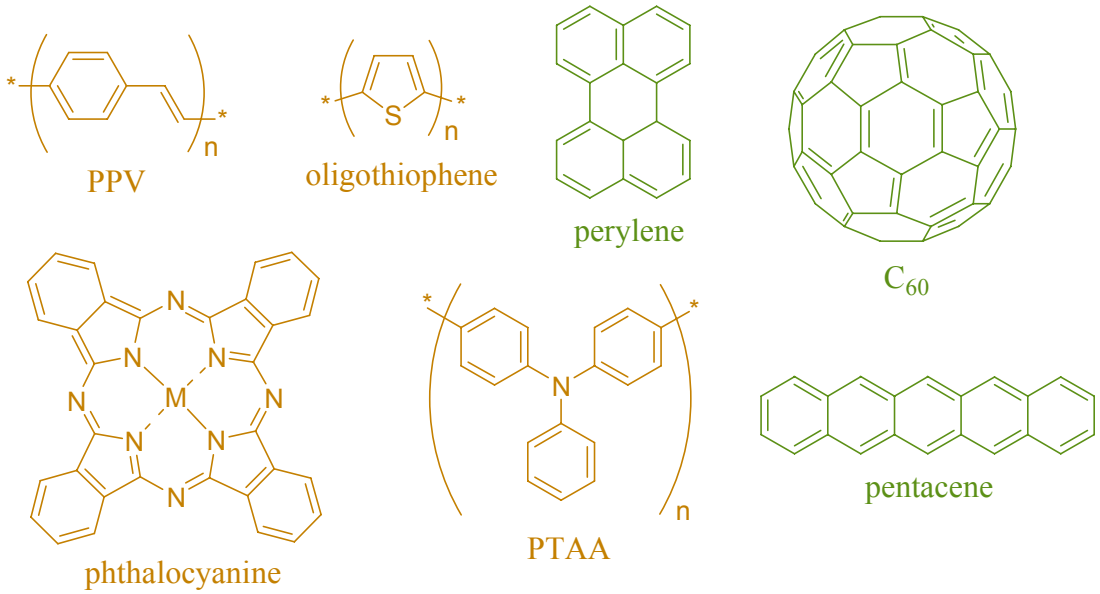

The multilayer OSC has limited efficiency due to the small surface area where the acceptor and donor layers meet where current is generated. The multilayer OSC evolved into the bulk-heterojunction (BHJ) OSC, as shown in Figure 1-5. The active layers of the multilayer device have been blended which greatly increase surface area at the DA interface. As a consequence of this increased DA contact, there is an increase in the current generated. Another improvement of the BHJ devices is the addition of the polymer blend, poly(3,4-ethylenedioxythiophene) and poly(styrenesulfonate) (PEDOT:PSS), shown in Scheme 1-2, which is a highly stable, transparent and conducting polymer. The PEDOT:PSS layer acts as a hole transporter

Scheme 1-2: The molecular structures of the polymer blend poly(3,4-ethylenedioxythiophene) and poly(styrene-*para*-sulfonate).

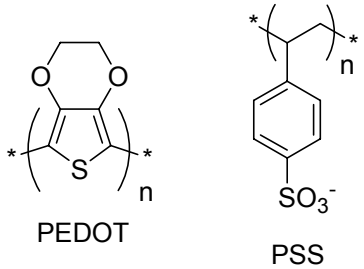

and an electron blocker, and it also improves contact between the active layer and the anode.[12]

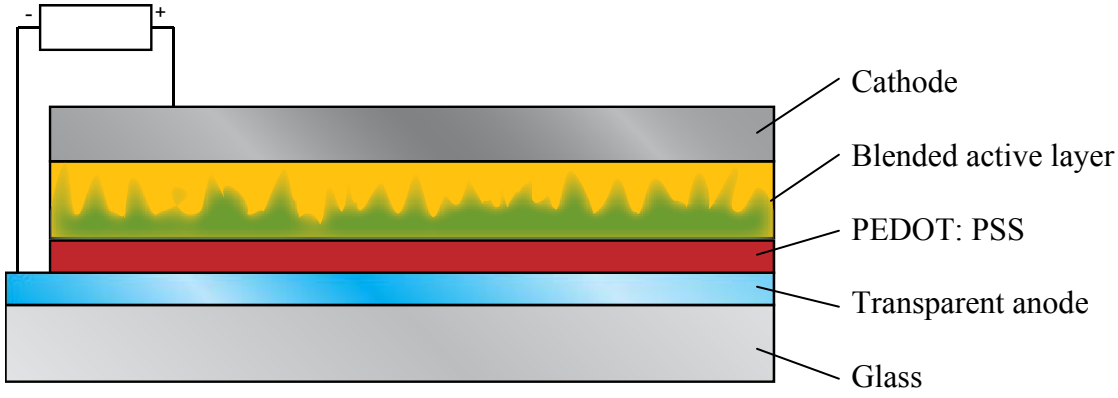

Figure 1-5: The schematics of a simple bulk heterojunction organic solar cell.[9,18]

1.3 Challenges with solar cells

1.3.1 Charge transfer at electrode interfaces

One area that challenges the efficiencies of OSCs is the interface of the electrodes and the organic layers due to their respective hydrophilic and hydrophobic nature. The former is a surface that prefers polar substances, like water, while the latter prefers non-polar substances that are typically organic in nature. As illustrated in Figure 1-5, the addition of the organic layer made up of PEDOT:PSS, which is typically deposited by spin coating the anode, has been introduced to the BHJ cells.[12]

Scheme 1-3: Some examples of self assembling monolayer transparent anode surface coatings that are functionalized with (a) carboxylic acids,[19] and (b) phosphonic acids.[20]

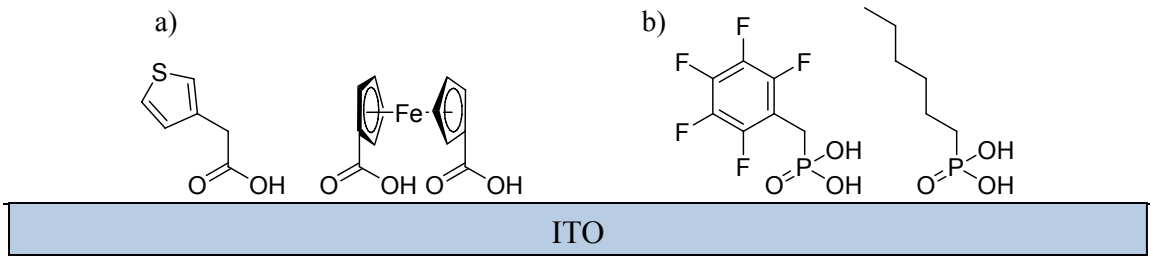

By functionalizing an indium tin oxide (ITO) surface with thiophene and ferrocene as shown in Scheme 1-3a, Armstrong *et al*. report a decrease in circuit resistance by increasing the wettability of the ITO surface towards the organic layers.[19] This functionalization was achieved by simply soaking the ITO in a 1 mM solution of the carboxylic acids in ethanol.[19] Paniagua *et al*. also report increased wettability of the ITO by modifying it with organic phosphonic acid as shown in Scheme 1-3b.[20]

1.3.2 Layer thickness vs. exciton diffusion length

One important consideration with the manufacture of the active layer in BHJ cells, is the thickness of the acceptor and donor domains, as it is dictated by the exciton diffusion length, typically 10-20 nm.[9,18] Once cast, the two organic materials of the BHJ layer can phase separate, shown in Figure 1-6c, which can cause domains on the order of micrometers, which is too large for the excitons to diffuse to the DA interface.[9] Phase separation is caused by a greater affinity of one material with itself, rather than the second material. Another possibility is that one of the two materials will become enveloped in the other, as shown in Figure 1-6b, and not allow for the appropriate charges to pass through to the respective electrode. Matching the thickness of the donor and acceptor to the exciton

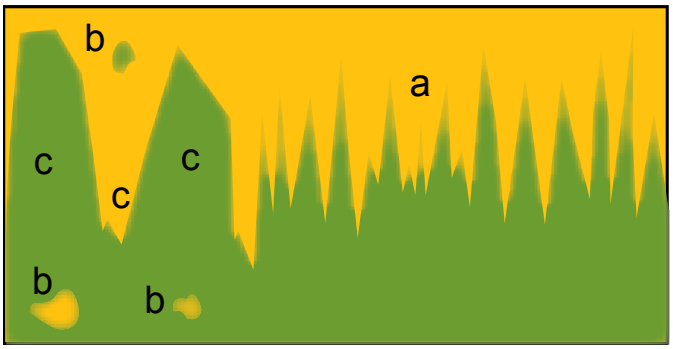

Figure 1-6: a) Ideal bulk heterojunction structure; b) Enveloped islands of n- or donor materials; c) Extreme phase separation of the n- and donor materials.

diffusion length can be fairly complicated, but can be facilitated by matching the n- and donor compounds that do not prefer to phase-separate, or by carefully controlling the active layer's growth.[9]

1.3.3 Impurities of organic layers

When creating polymers, impurities from polymer by-products and catalysts can greatly affect the conductivity of the active layers.[16] Thus, extremely pure materials are required for viable devices and the purification processes adds a significant amount of cost and energy to fabrication of the materials.

1.3.4 Organics are more susceptible to degradation

Another challenge that faces OSCs is the stability of the organic materials used in the OSC. Under conditions of illumination, heat, and in the presence of oxygen or water vapour, these materials can be oxidized resulting in another source of impurities within the active layers.[9] This oxidative degradation alters the properties of each layer by changing the molecular structure of the materials, and consequently the band-gap and conductive properties also degrade.

1.4 Relevant research to this thesis

One idea to limit phase separation is by functionalizing OSC compounds with complementary hydrogen bonding (HBing) groups. This manipulation encourages the self-assembly of the n- and donor materials in the active layer, enabling a better material blend. There are many factors to consider when approaching this strategy. The two most

Scheme 1-4: Meijer's hydrogen bonding ureidopyrimidinone.[21]

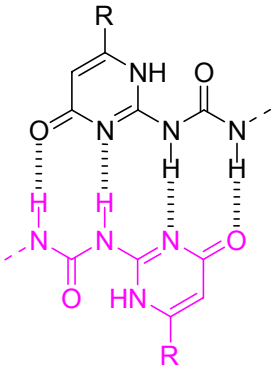

important considerations are that the HBing unit does not absorb light in the same range of the donor layer, or is electrochemically active. The processability of the active layers must be maintained with the addition of the HBing moieties, as the solubility of these highly polar groups is limited in typical organic solvents. Another consideration is how strong are the attractive forces between complementary HBing groups, which is called the association constant, K_a.

Most research done in this field has used Meijer's self-recognizing ureidopyrimidinone (UP) unit as shown in Scheme 1-4[21] Some of the first materials to be treated this way, are fullerenes (C_{60})[22] and oligo(phenylenevinylenes) (OPVs),[23] as shown in Scheme 1-5, due to their popularity within current organic photovoltaic devices. One limitation of using a self-recognizing HBing group, such as UP, is that there will be a statistical distribution of homo-dimers and hetero-dimers.

Sánchez *et al.* were able to spin coat the C_{60}-UP_2 monomer onto glass, which behaved more like a polymer by virtue of the HBing units allowing the formation of HBed oligomers and polymers. C_{60}-UP_2 had an expected association constant of (K_a) $\geq$ 6 x $10^7 M^{-1}$ in chloroform, but was found to be lower and was attributed to impurities. Sánchez *et al.* did not report the experimental K_a for C_{60}-UP_2. Cyclic voltammetry (CV) experiments demonstrated little to no interaction between the HBed C_{60} cages, as would be demonstrated by two distinct, red-ox peaks.[22] This result suggests that the HBed C_{60}

cages were too far apart for the electronic environment to be felt by the other the HBed C_{60} cage.

Scheme 1-5: The (a) ureidopyrimidinone functionalized acceptor compound fullerene[22] and (b) the donor compound oligophenylvinylene.[23]

a)

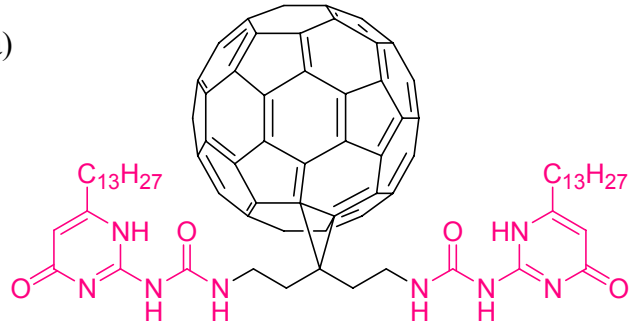

C_{60}-UP_2

b)

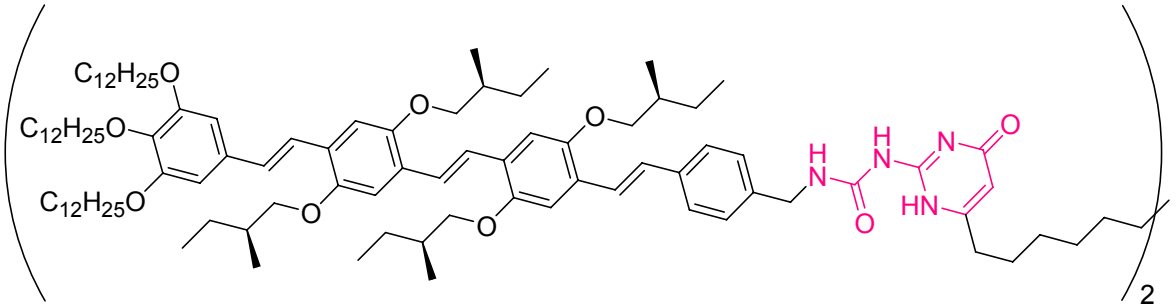

$(OPV\text{-}UP)_2$

Similarly, El-ghayoury *et al*. developed and characterized $(OPV\text{-}UP)_2$, which formed HBed oligomers and polymers and calculated a K_a of approximately $10^{8}{}_{M}{}^{-1}$ in toluene.[23,24] Little communication was found between the HBed OPV units as the emission spectra of the monomers did not differ to that of the spectra of the HBed oligomers. This result is not desirable as the HBing was implemented to create an electronic environment where they can communicate. Additionally, they integrated $(OPV\text{-}UP)_2$ into an OSC and found that the device performance was comparable to polymeric phenylvinylene (PPV), which is significant because it shows no significant

detriment to the device performance.

When combined in solution, C_{60}-UP_2 and $(OPV\text{-}UP)_2$ were found to preferentially form cyclic dimers with each other, as determined by ^1H NMR and shown in Scheme 1-6. The monomers did not undergo an electron transfer, which was attributed to large, but unquantified, distance between the C_{60} and the OPV.[25]

Scheme 1-6: The cyclic dimer formed by C_{60}-UP_2 and $(OPV\text{-}UP)_2$ in a 1:1 solution in chloroform.

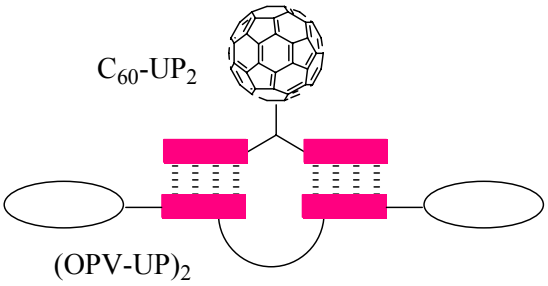

Scheme 1-7: The monomers (a) PERY-UP and (b) OPV-UP[24] studied as dimers in solution.[26]

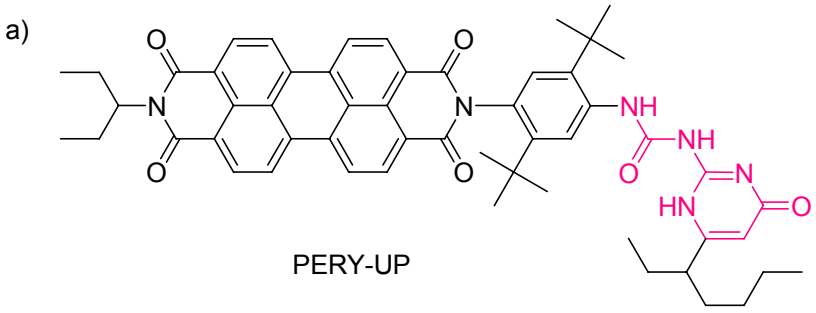

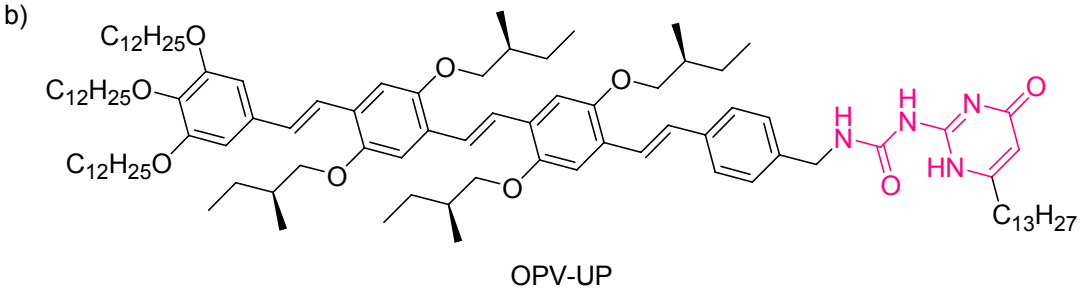

Neuteboom *et al*. combine PERY-UP and OPV-UP[24] in solution, as depicted in Scheme 1-7, and study via fluorescence the photo-induced singlet-energy transfer between the hetero-HBed pair, from OPV-UP to PERY-UP.[26] It is found that although the energy transfer occurs, that charge transfer does not occur due to the relatively large, yet

unquantified, distance between the electroactive moieties. One drawback of the UP HBing unit that has been identified in these studies is the ability to self-recognize.[22-27] In the study performed by Neuteboom *et al*., a statistical mixture of homo- and hetero-dimers were reported.[26]

A similar study has been done where a fullerene and a tetrathiafulvalene (TTF) have been held together with guanidinium and carboxylate salts via HBing and ionic interactions.

Scheme 1-8: Segura *et al*. have joined a C_{60} with a tetrathiafulvalene (TTF) by using a carboxylate (red) and guanidinium (blue) HBing/ionic interactions.[28]

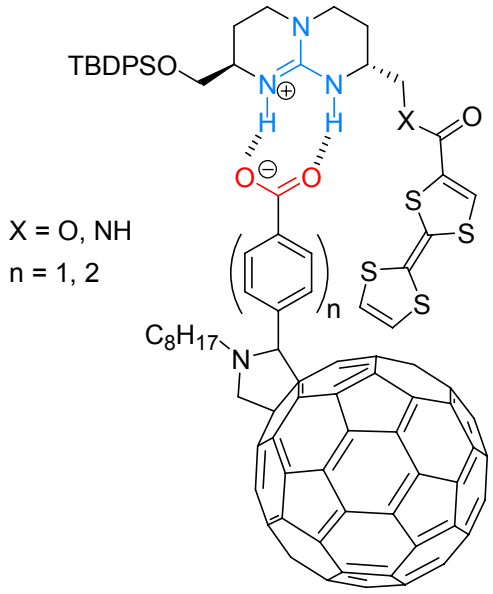

The C_{60} and TTF moieties were combined in varying distances dependant on the number of phenyl spacer units, as shown in Scheme 1-8. Both singlet energy and electron transfer occurred, as determined by emission and electrochemical studies respectively, but at different rates dependant on the distance between the C_{60} and TTF.[28] It was found that the charge recombination rates slowed with increasing distance; for instance the phenyl *vs*. the biphenyl system were calculated to be 8.4×10^6 s^{-1} and 1.0×10^6 s^{-1} respectively. These findings are significant because they were the first supramolecular system that underwent a charge transfer that was induced by irradiation.

Scheme 1-9: Gold electrodes functionalized with self-assembled monolayers that are hydrogen bonded to pentathiophene and fullerene via barbituric acid (green) and melamine (blue).[29]

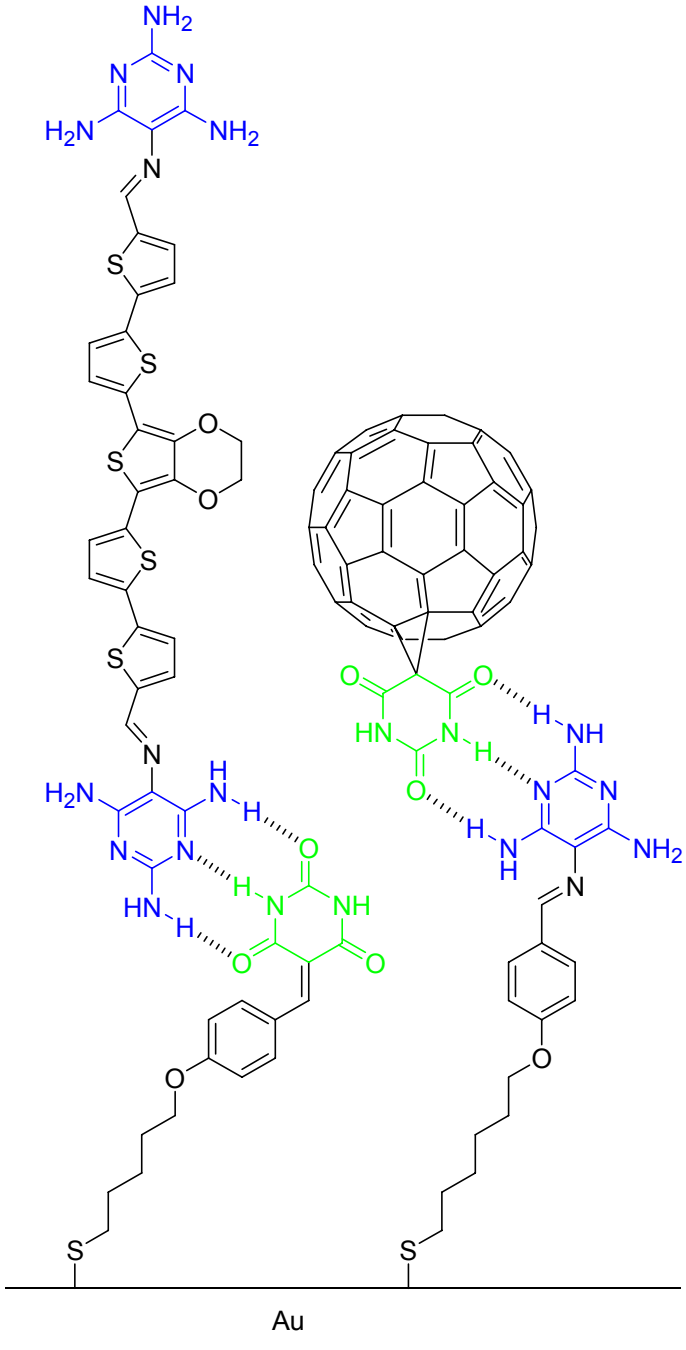

Huang *et al*. created self assembling monolayers (SAMs) on gold electrodes that were functionalized with either HBing melamine or barbituric acid, shown in Scheme 1-9. A

SAM is unique as it is made up of a single layer of molecules upon a surface, in this case gold. Gold was used, as thiols will self-assemble on the surface. These SAMs were then allowed to HB with the appropriately functionalized pentathiophene and C_{60}, shown as Figure 1-9, and by incorporating these HBing groups, the resultant photovoltaic device was more efficient by a factor of 2.5 when compared the non-HBing equivalent system.[29]

Scheme 1-10: The organic electronic device materials functionalized with hydrogen bonds that were investigated by (a) Sessler *et al.*[30] and (b) Harriman *et al.*[31] and using fluorescence quenching studies to examine the energy transfer properties.

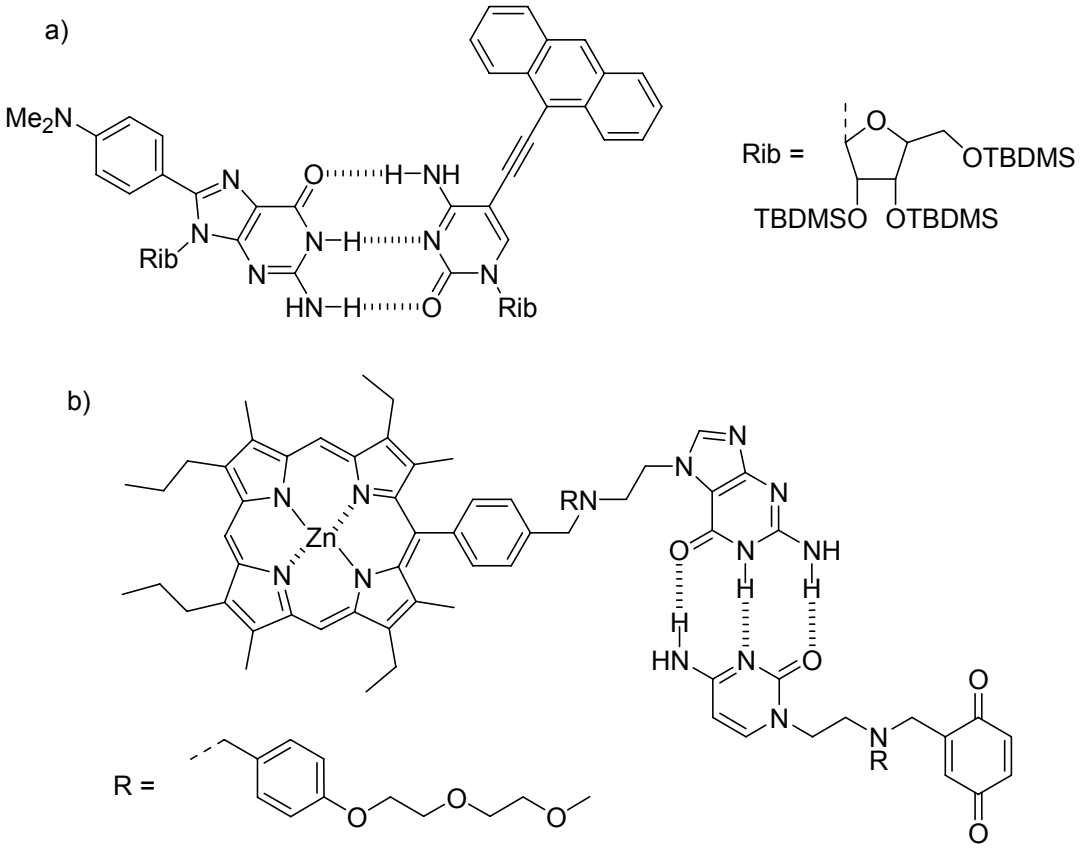

A number of other studies[30-34] and reviews[27,35] concerning HBing organic materials, shown in Scheme 1-10, have been presented, although the majority of these are investigated by fluorescence studies and not electrochemically.

Scheme 1-10 continued: The organic electronic device materials functionalized with hydrogen bonds that were investigated by (c) Myles *et al.*,[32] (d) Zhao *et al.*[33] and (e) Fang et al.[34] using fluorescence quenching studies to examine the energy transfer properties.

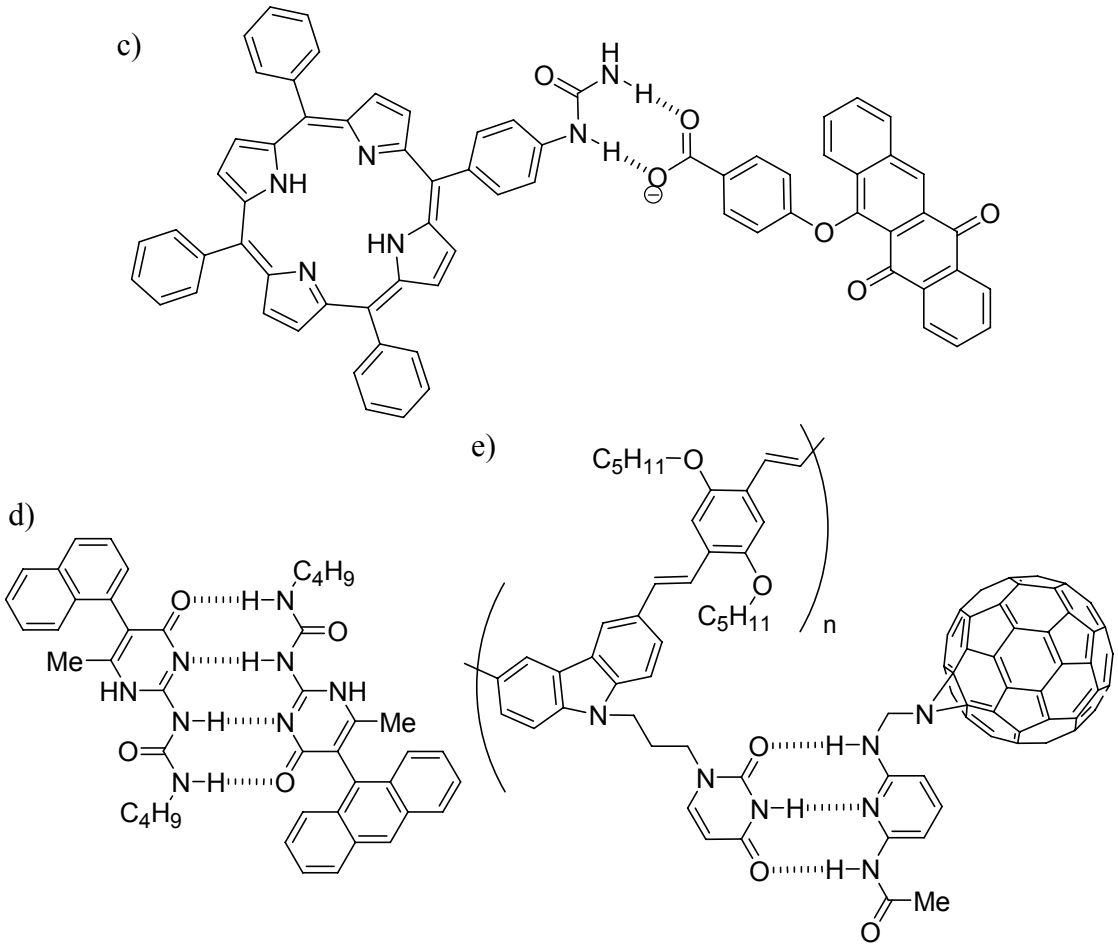

1.5 Kaifer's hydrogen bonding ferrocene

Kaifer synthesized a quadruply HBing monomer, fashioned after Meijer's ureidopyrimidinone, that was further furnished with ferrocenyl (Fc), shown in Scheme 1-11. The added electro-active probe allowed Kaifer to investigate how HBs behave amidst red-ox chemistry. ^{1}H NMR was first used to identify and confirm the presence of the self-assembled dimer by adding acetonitrile, a polar solvent, to disrupt the HBing effect. CV experiments revealed two reduction-oxidation peaks in chloroform, but only one reduction-oxidation pair with the introduction of acetonitrile. This finding of two sets of signals indicates that the ferrocene units were "feeling" the presence of each other during the reduction and oxidation process, as illustrated by Scheme 1-12. Once one ferrocene was oxidized, the second ferrocene felt this increased positive charge and required a greater potential to be oxidized.

Scheme 1-11: Kaifer's electroactive, hydrogen bonded dimer.[36]

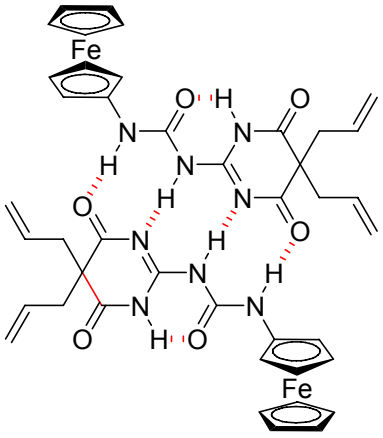

Scheme 1-12: The electrochemical behaviour of Kaifer's homocoupled ferrocene derivatives.

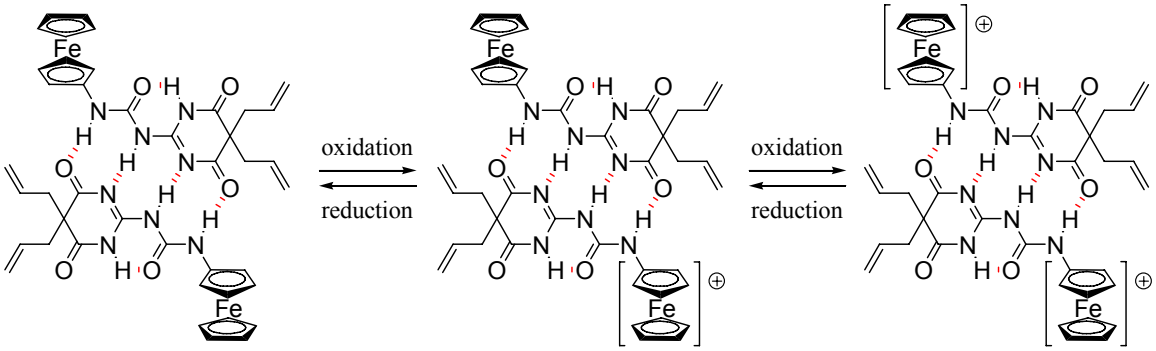

Kaifer's work shows us that self-assembly through HBing is a potential option to construct supramolecular, organic, electronic materials, such as OSC layers. To properly design and execute a working device, further studies are necessary to understand how HBs assist in the reduction and oxidation of materials.

1.6 Goals of Thesis

This thesis is organized to illustrate the separate tasks associated with synthesizing and analyzing an HBing electroactive probe. The second chapter outlines and explains the synthetic methodologies, as well as reactions and characterizations of all synthesized compounds. There is a focus on the challenges of increasing the solubility of intermediate and target molecules, as well as the methods investigated to join the HBing groups and the chosen electroactive compound, anthraquinone. The third chapter includes the physical characterization of the target compounds and some precursor materials for comparison. This chapter explores the ability of the target molecules to undergo directed HBing, and the electrochemical properties of the materials. The last chapter concludes this thesis, and presents possibilities for future work.

Chapter Two: **Synthesis and Experimental**

2.1 Introduction and background

The goal of this chapter is to covalently link an anthraquinone (AQ) to a HBing group as illustrated in Scheme 2-1a to investigate the properties of a HBing redox probe. Several variables come into play in the design of this AQ-HB adduct, namely: 1) the AQ ring position; 2) the linker and functional group chemistry; and 3) the HBing group. Each of the following sub-chapters will discuss one of these three variables.

The linker moiety dictates the chemistry and the functional groups necessary to join the AQ and HBing group. The investigated linking reactions are shown in Table 2-1, and can be divided into four primary groups: 1) propargyl, 2) allyl, 3) ethyl ester, and 4) ethyl ether; and their respective reactions are 1) Sonogashira coupling, 2) the Heck reaction, 3) Steglich esterification, and 4) Mitsunobu coupling.

Scheme 2-1: a) The anthraquinone target structure, and b) the investigated hydrogen bonding groups. The green NH is the site where the nucleobase will be covalently bonded to the linker moiety.

a)

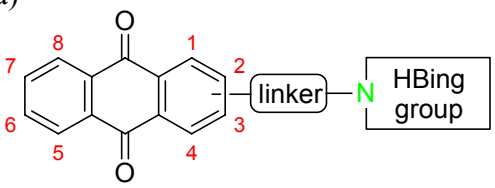

b)

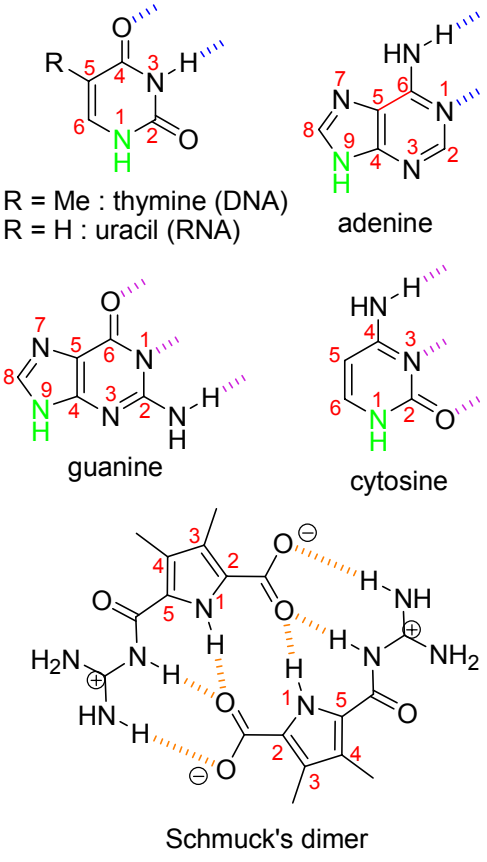

The molecules chosen for the HBing groups are the DNA nucleobases and Schmuck's zwitterionic pyrrole, shown in Scheme 2-1b.

Table 2-1: A summary of the coupling chemistry investigated in this thesis to couple the anthraquinone moiety with a hydrogen bonding group (HB).

Linker	Coupling Reaction
propargyl	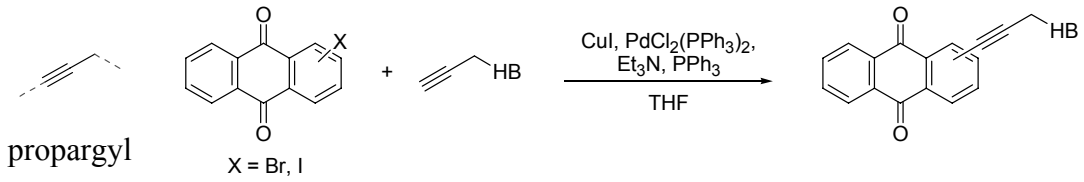 Sonogashira coupling
allyl	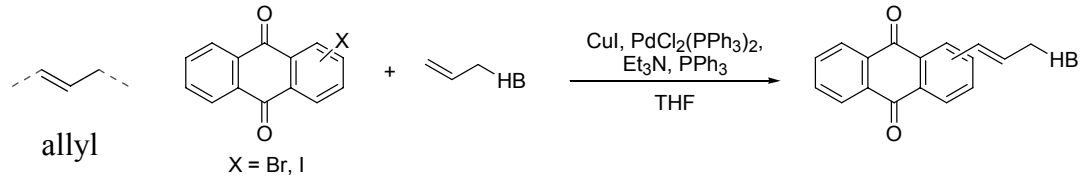 Heck coupling
ethyl ester	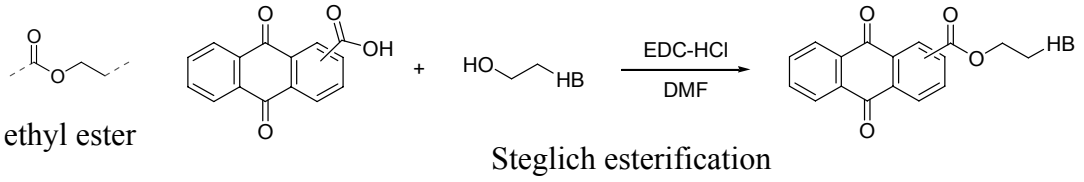 Steglich esterification
ethyl ether	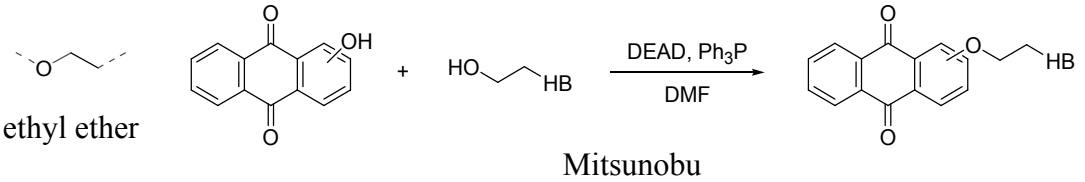 Mitsunobu

The syntheses, manipulation, HBing sites and challenges of these linkers, HBing groups, and functionalized AQs will be discussed in this chapter. In addition, there is some chemistry that does not directly belong in any of these four groups, such as the alkylation of the AQ with the intent to increase solubility of the AQ-HB system.

2.2 Overcoming the solubility challenge

2.2.1 Anthraquinone manipulations

The greatest challenge with the synthesis of the AQ systems, was overcoming the limited solubility of both the starting materials and target molecules. In the case of the target molecules, it was crucial to overcome the limited solubility due to the solution chemistry used to investigate HBing strengths and electrochemistry. This challenge was overcome by adding a saturated hydrocarbon chain to the AQ ring, and solubilising protecting groups to the HBing units which were then cleaved in the last step of the synthesis.

2.2.1.1 Nitration

To functionalize AQ 2-carboxylic acid, there are few options, based on the following electrophilic aromatic substitution reactions: nitration, sulfonation, and halogenation. Nitration,[37] shown in Scheme 2-2, appears as the simplest and most appropriate choice of these methods for future alkylation; a sulfonate functionality is too polar to increase solubility in the less polar organic solvents, while an aromatic halogen often requires a metal catalyzed reaction to functionalize, which will be discussed later.

Scheme 2-2: The electrophilic aromatic nitration of anthraquinone 2-carboxylic acid.

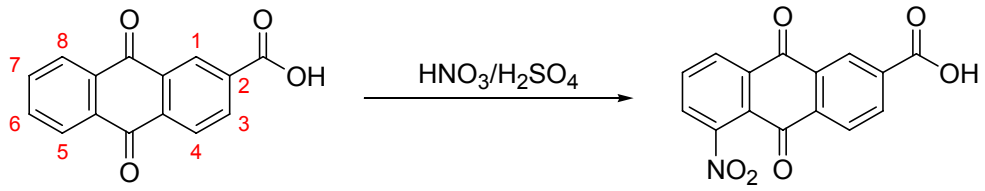

1 **2** (62%)

The nitro group adds to mainly the 5-position, but there were a great number of other nitrated by-products as was suggested by ^{1}H NMR. To isolate the desired product **2**, a hot filtration (approx. 90 °C) technique in acetic acid was employed. The ^{1}H NMR spectrum displays a downfield shift of the proton attached to C6 from 8.22 to 8.67 ppm, indicating a neighbouring electron withdrawing group. There is also a change in the integration from seven to six protons. The nitrated **2** can be reduced to an amine, which is the necessary functionality for diazonium chemistry.

2.2.1.2 Electrophilic aromatic substitution

Scheme 2-3: The attempted nitro reduction using sodium borohydride that yielded a mixture of both the phenol and amino products.

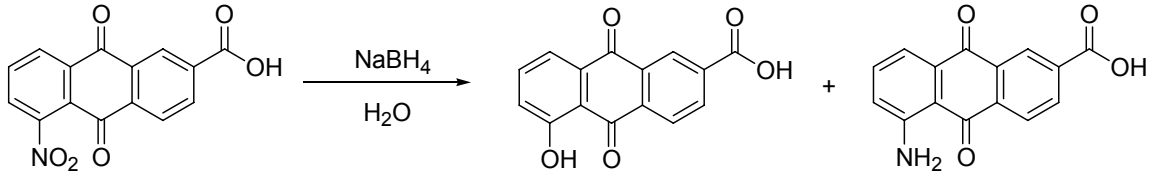

2 **3** (not isolated) **4** (not isolated)

The AQ **2** was reduced with sodium borohydride, however, the products of this reaction were a mixture of the phenol **3**, and a minimal amount of the amino product **4**, as illustrated in Scheme 2-3, which were not isolated. These two products, **3** and **4**, could be seen in the ^{1}H NMR by the addition of the exchangeable protons of the phenol at 12.26 ppm and of the amine at 10.86 ppm and 9.56 ppm. The distinction between the two amino protons is due to the HBing effects between the amino proton and the adjacent ketone. Literature precedence showed that highly electron deficient nitrated aromatics undergo a substitution with a nucleophile, as is described in Scheme 2-4.[38]

Scheme 2-4: The investigated electron deficient aromatic system and nucleophiles that were investigated by Kislyi *et al.*[38]

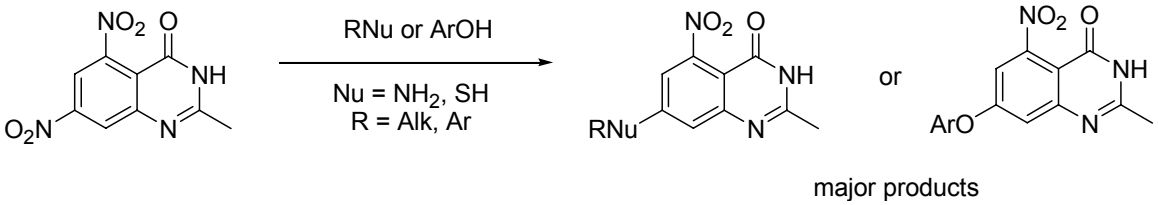

Under the basic conditions of the nitro reduction, nucleophilic hydroxide underwent substitution of the nitro group shown in Scheme 2-3. The scope of the reaction was examined with other nucleophiles including amines and phenoxides, which are discussed shortly. Unfortunately the primary amines (methylamine, neopentylamine, and n-butylamine) formed an amino-acid type zwitterionic product (Scheme 2-5) that was soluble in water.

Scheme 2-5: The zwitterionic behaviour of 5-aminoanthraquinone 2-carboxylic acid.

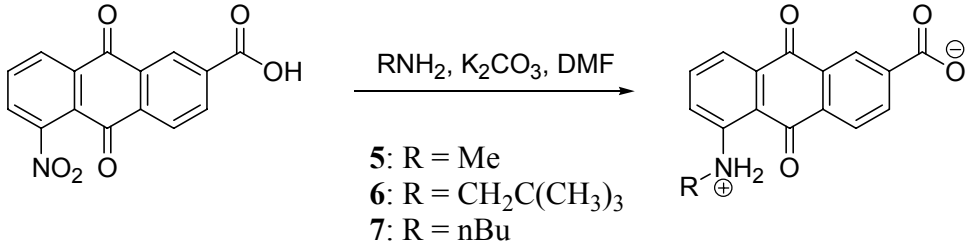

The typical purification by precipitating the products from the reaction solvent (DMF) by adding water was not possible in this case due to the zwitterionic behaviour of amino-acids. With the DMF removed *in vacuo*, the crude product was too polar and would not run on a silica column. Piperidine, a secondary amine was reacted with 5-nitroanthraquinone 2-carboxylic acid and was too bulky to undergo substitution at the nitro site. It was clear that using alkyl amines posed difficulty in purification and were not suitable targets to increase solubility of the AQ systems.

Phenols, as shown in Scheme 2-6, were then investigated as nucleophiles as the resulting ether product could not form zwitterions with the carboxylic acid functionality, as the aminoanthraquinone products do. Additionally, the nucleophilicity necessary to undergo substitution can be achieved simply by forming the phenoxide in the presence of a mild base (K_2CO_3). The starting material **2** was combined with potassium carbonate and a para-substituted phenol in DMF and heated to yield the coupled products, **8-13** shown in Scheme 2-6 with their isolated yields. The alkylated and electron-rich phenols worked the best, while the phenols with electron withdrawing substituents were not successful in this type of reaction. This reactivity pattern is attributed to the strength of the phenoxide nucleophile, which would be stronger with a richer electron donating substituent. The pentyl substituted phenol, **10**, increased the solubility in organic solvents of the AQ the greatest, and was thus selected to proceed with the coupling with the DNA bases. The other isolated phenols were still moderately solubilising, but the products were more challenging to crystallize and purify.

Scheme 2-6: The nitro substitution with different para-substituted phenols.

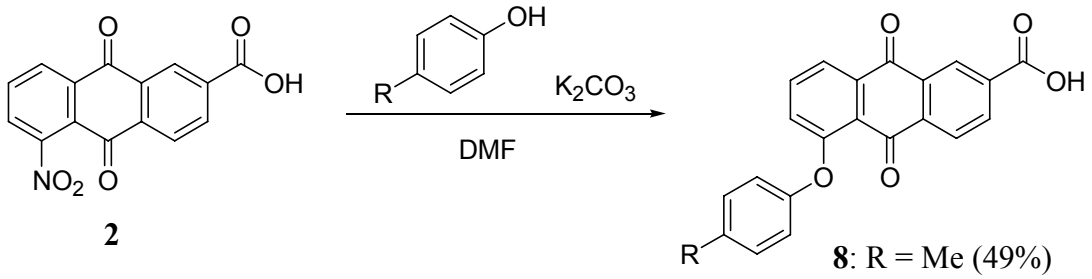

8: R = Me (49%)
9: R = OMe (50%)
10: R = C_5H_{11} (57%)
11: R = tBu (0%)
12: R = Cl (0%)
13: R = NO_2 (0%)

The hydroxyethyl functionalized adenine **14** was coupled with the pentyl derivative **10** by a Mitsunobu coupling using standard conditions, as shown in Scheme 2-7 and the mechanism is later outlined in Scheme 2-25. It was discovered that the product **15** of this reaction was not soluble enough, even in DMF at 25°C, to reach our target concentration of 10 mM for analysis by cyclic voltammetry (CV). Regardless, the polar conditions of DMF are not conducive to HBing and thus this compound is not soluble enough to be a candidate for our studies, and it is clear that a less polar target in necessary.

Scheme 2-7: The coupling of 5-(4-pentylphenoxy)anthraquinone 2-carboxylic acid and 7-(2-hydroxyethyl)adenine under Mitsunobu conditions.

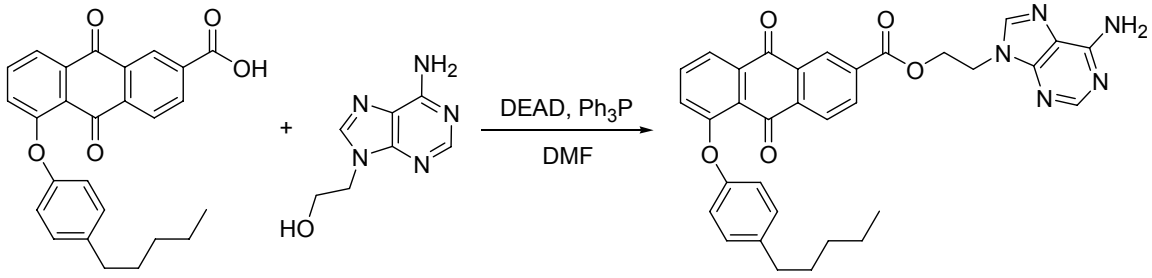

10 **14** **15** (37%)

2.2.1.3 Ether formation

To increase solubility, the phenolic substitution was replaced with an alkyl substitution, as shown in Scheme 2-8. As alcohols are not nucleophilic enough to perform the nitro substitution, and as their conjugate bases, alkoxides, are nucleophilic enough to attack the quinone ketone, a new synthetic route was investigated, namely the Williamson ether synthesis.[39] Three regioisomers of dihydroxylated AQs (1,4-; 1,5-; and 1,8-) were reacted with racemic 2-ethylhexyl bromide in the presence of potassium carbonate, to yield a mixture of alkylated products.

Scheme 2-8: The Williamson ether synthesis of 1-(2-ethylhexyloxy)-4-hydroxyanthraquinone.

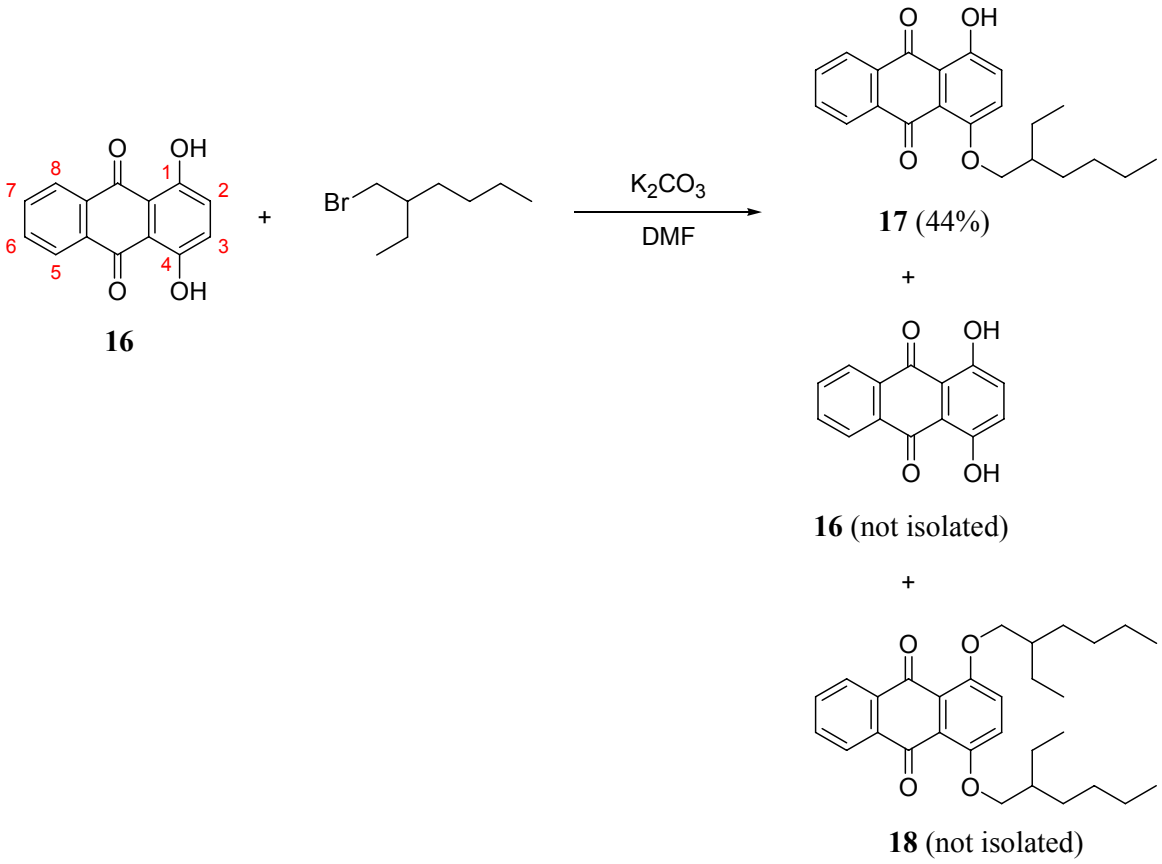

Only the 1,4-substituted system **16**, as shown in Scheme 2-8 was suitable for further manipulations due to the challenges associated with the purification of the 1,5- and 1,8-derivatives. Only the 1,4- derivatives were soluble in solvents, such as chloroform, ethyl acetate, acetone, THF and DMF, and did not streak when purified by column chromatography. This increased solubility allowed for the desired, mono-alkylated product **17** to be isolated by column chromatography (hexanes:toluene:ethyl acetate, 1:1:2, R_f = 0.05 to 0.57), and it was carried forward to the Mitsunobu coupling with the DNA bases which is discussed later in this chapter. The ^{1}H NMR spectrum shows the

loss of symmetry in the AQ, only one HBed phenolic proton at 13.05 ppm, and the addition of the ethylhexyl protons ranging between 1.91 – 0.90 ppm and at 4.03 ppm.

2.2.2 DNA/RNA nucleobase functionalization

2.2.2.1 Thymine protection

Thymine, and the RNA analogue uracil, do not selectively alkylate at either the N^1 or N^3 under most conditions. Initial attempts at alkylation at the desired N^1 with ethylene carbonate produced a mixture of products that were not distinguishable by TLC as shown in Scheme 2-9.

Scheme 2-9: The reaction of thymine/uracil with ethylene carbonate in the presence of a catalytic amount of sodium hydroxide.

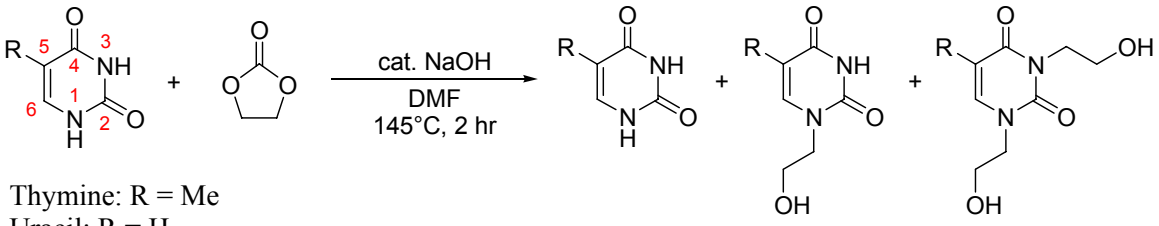

Thymine: R = Me
Uracil: R = H

19: R = Me (not isolated)
20: R = H (not isolated)

The most common protecting group in literature for these two DNA/RNA bases is the benzoyl (Bz) group[40-46] for the ease of a selective addition to either the N^1 or N^3 site, yielding the protected thymine products **21** and **24**, respectively, as shown in Scheme 2-10, and for its easy removal with base. Unlike the attempted alkylations, the N^1 site is selectively benzoylated first, as shown in Scheme 2-10a, and the N^3 second. It is likely that the NaOH deprotonation is not selective between the two NH protons while the benzoyl chloride can distinguish the N^1 and N^3 protons. To selectively protect N^3 the dibenzoylated thymine, **22**, is selectively deprotected at N^1 by exposing this compound to

an aqueous mixture of 1.0M sodium carbonate in dioxane, shown in Figure 2-10b. Once protected with the Bz group at either the N^1 or N^3 sites, thymine is more soluble in organic solvents. The N^3-protected **24** was selected to move forward in the synthesis, as N^1 site of thymine and uracil in both DNA and RNA respectively, is the one that connects to the phosphate backbone. A shortcoming of this protecting group is that it is not stable to strongly basic conditions, limiting the scope of subsequent reactions.

Scheme 2-10: The selective benzoylation of thymine and uracil in either the a) 1- or b) 3- positions.[47]

a)

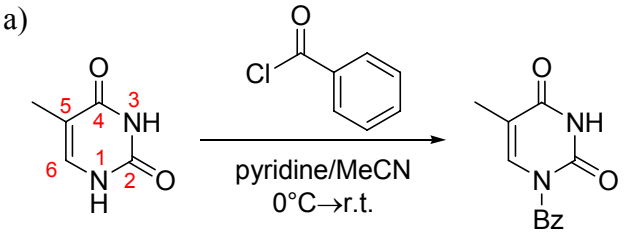

21 (74%)

b)

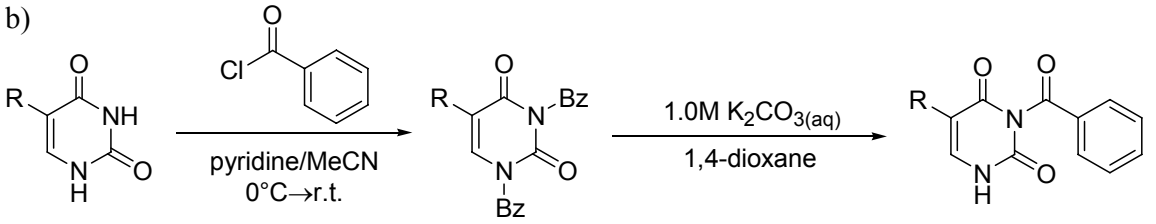

22
(not isolated)

23: R = H (64%)
24: R = Me (85%)

2.2.2.2 Guanine protection

Commercially, guanine crystals are used in cosmetics and finishes and provides a pearlescent lustre.[48] Guanine is the complementary nucleobase to cytosine, and the guanine-cytosine pair boasts

Scheme 2-11: The numbering scheme of guanine.

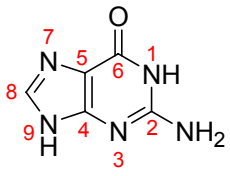

three HBs, unlike the two HBs of the thymine-adenine adduct. Each added HB increases the overall strength of the self-assembled system and is thus desirable. This nucleobase has limited solubility in both organic and aqueous solvents, and decomposes at 360°C instead of melting[49] due to its strong crystal lattice structure. The solubility is the property that prevents the DNA/RNA base guanine from being easily modified.

There are two options to overcome these solubility challenges: to work with protected versions of guanine, or to work with a more soluble precursor. Once all of the desired AQ linking synthetic steps have been undertaken, the last step is to convert the protected guanine back into guanine.

Scheme 2-12: Different amide protecting groups used at the N^2 site on guanine.

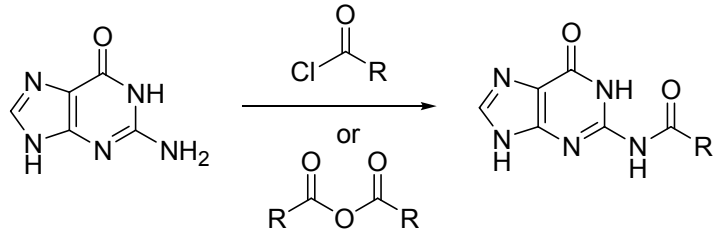

25: R = Me[50]

Pr, Bu, C_5H_{11}[51]

$C_{15}H_{31}$[52]

iPr[53,54]

tBu[55]

Common protecting groups, such as benzyl (Bn)[56] and amides,[50-55,57] are employed to aid in solubility. The methods used to form amides involve the reaction of guanine with either the respective anhydride or acyl halide shown in Scheme 2-12. The installation of the benzyl group is more involved, and starts with 2-bromohypoxanthine and benzylamine in refluxing 2-methoxyethanol[56] shown in Scheme 2-13. The addition of these amide and benzyl protecting groups was not attempted.

Scheme 2-13: The synthesis of N^2-benzylguanine.[56]

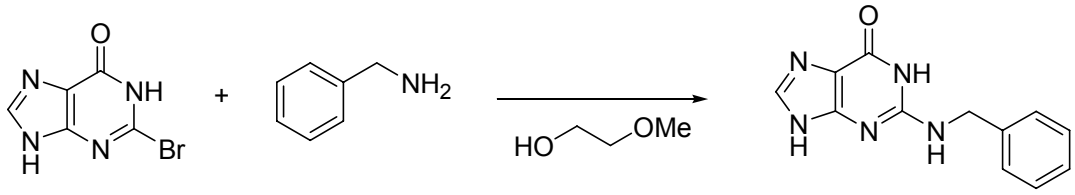

26

The other option is to work with a more soluble precursor of guanine, and then at the last step deprotect into the guanine. One common example is 6-chloroguanine, **27**, which is typically synthesized by reducing guanine with the chlorinating agent phosphorus oxychloride[58,59] shown in Scheme 2-14.

Scheme 2-14: The reduction of guanine using phosphorus oxychloride to produce 6-chloroguanine.[58,59]

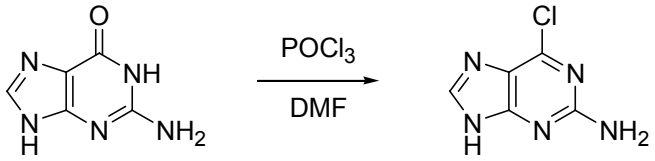

27

This chloroguanine derivative **27** is more soluble, and is easily converted back to guanine by using 2-thioethanol and sodium methoxide in methanol,[60-63] or by refluxing in a strong base[64]/acid.[65,66] The chlorination of guanine was not investigated in this thesis.

Our first approach to increase the solubility of the guanine was to form the diacetate **28** using acetic anhydride as it was the most available of all the protecting groups.[67,68] This acetylation, shown in Scheme 2-15a, called for long reaction times (18-20 hrs) and high heat (160°C), and gave a mixture of unidentified products, which did not appear to be diacetylated.

Scheme 2-15: The a) mono- and b) di-acetylation reactions of guanine.

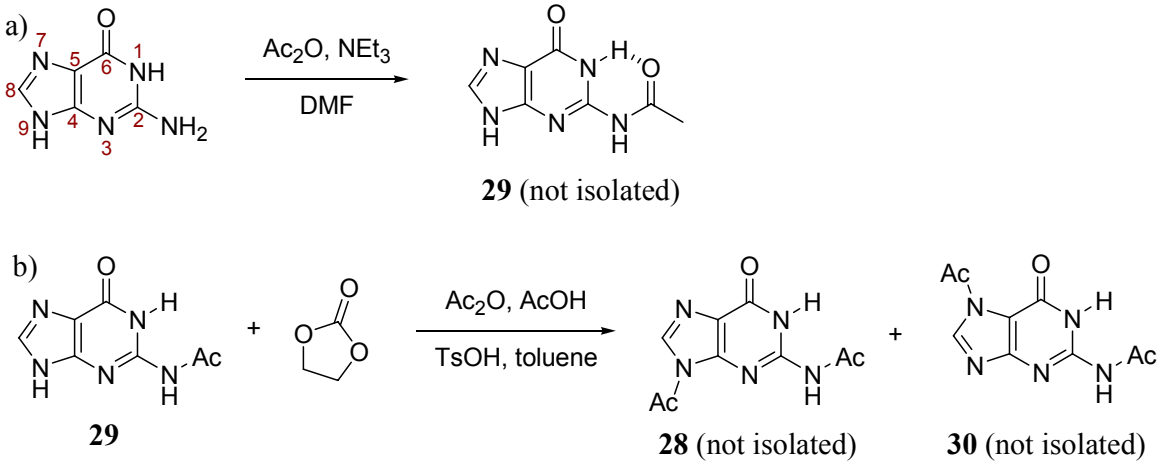

The ^{1}H NMR illustrated in Figure 2-1a, shows what appears to be two major products, and it should be noted that the peak at 3.33 ppm that integrates to three protons is not a second acetyl group, but water found in the DMSO-d_6, as dry DMSO-d_6 is expensive and saved for characterization only. For the downfield-shifted proton peaks, there are three clear pairs of peaks, which have been attributed to the HBing NH protons, but were not identified further for the proposed product **29**. The product could not be isolated by crystallization nor by column chromatography as it were too polar and insoluble in all conventional solvents. The separation of the crude mixture was abandoned with the intention to carry forward with the synthesis and purify at the next step.

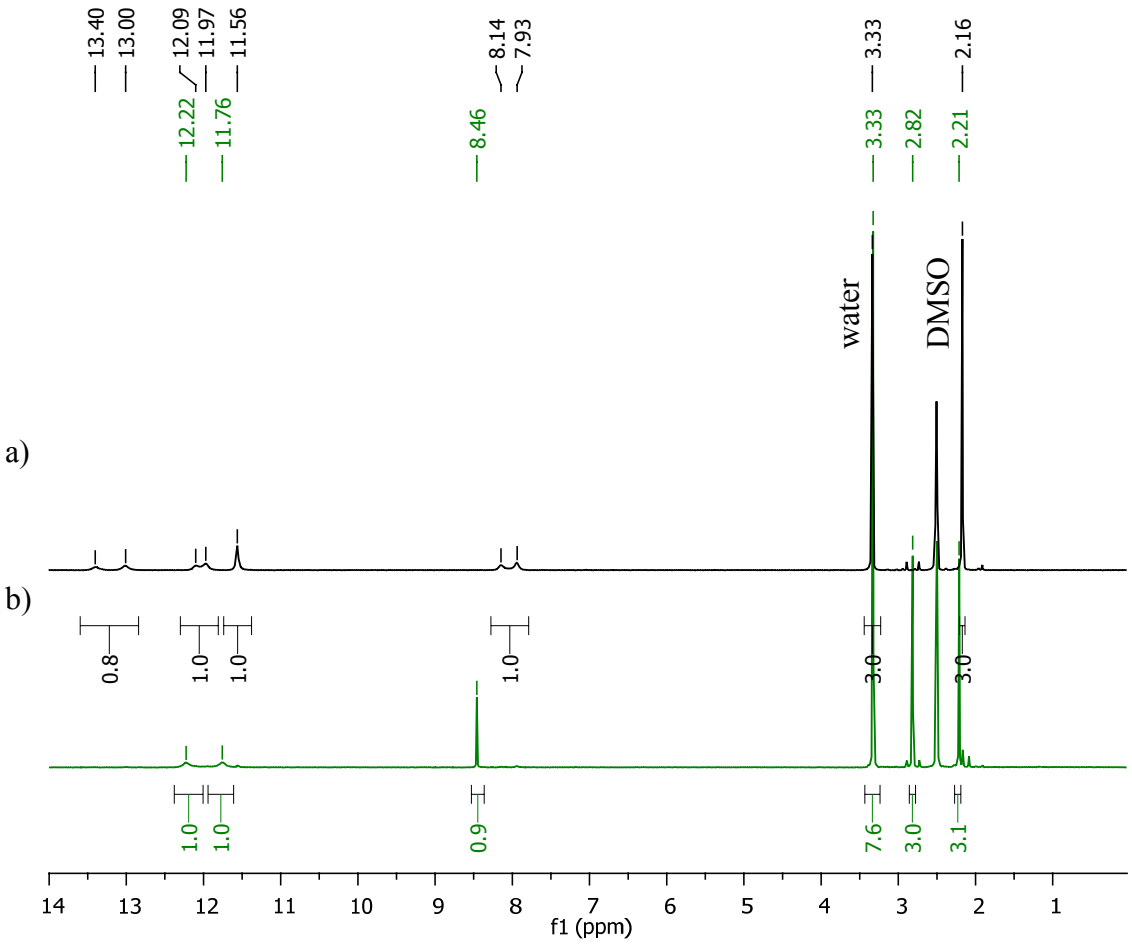

Figure 2-1: The 1H NMR spectra of the reaction products of the a) mono-acetylated 29 and b) di-acetylated guanine 28.

Literature reports the alkylation at the N^7 site of 2-acetylguanine using ethylene carbonate under acidic conditions, as shown in Scheme 2-16.[69,70] One of the solvents to this reaction was acetic anhydride, and instead of the expected product 9-(2-acetyloxyethyl)-2-acetylguanine, the ^{1}H NMR shown in Scheme 2-15b suggests that the diacetylated product was isolated. The acetylation sites were not determined, but literature precedence suggests to be a mixture of the 2- and 9- sites, and 2- and 7- sites.[69,70] As neither of the products of these two reactions were purified, no percent yields were calculated. The most interesting difference between the two spectra shown in Figure 2-1 is the proton

peak of C^8 at 11.56 ppm and at 8.46 ppm. It was at first postulated as residual acetic acid, but the methyl group of the acetate falls at 1.91 ppm in DMSO,[71] which is absent.

Scheme 2-16: The selective deprotection of N^7/N^9 and N^2–acetylated guanine using sodium hydroxide.

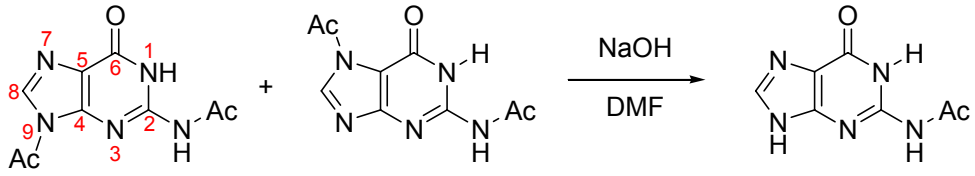

28 **30** **29**

The crude diacetylated guanine mixture of **28** and **30** was then reacted with sodium hydroxide in DMF and selectively cleaved what was attributed to the N^7/N^9 acyl group, shown in Scheme 2-16. Further reaction of the clean acetylated **29** with ethylene carbonate in the presence of DMAP in DMF yields a mixture of products that gave no indication of the desired product, **31**, shown in Scheme 2-17a). Finally, two other bases, including potassium carbonate and sodium hydroxide, were used and neither yielded the desired product.

Scheme 2-17: The attempted N^7 alkylation of 2-acetylguanine using a) ethylene carbonate and b) Mitsunobu conditions.

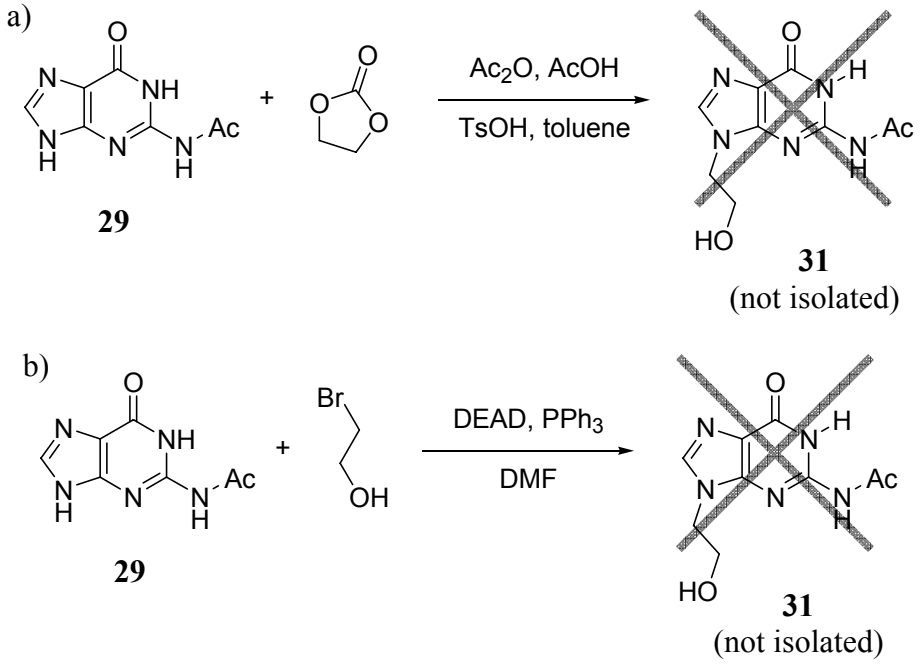

The final method attempted with the protected **29** was using the Mitsunobu conditions that worked well for the thymine alkylation as shown in Scheme 2-17b). When the reaction had been worked up, the only compound confirmed by ^{1}H NMR was the starting material **29**, as this alkylation route was not suitable for the precursor **29**.

2.2.3 Schmuck's hydrogen-bonding unit

2.2.3.1 Schmuck's work

An alternative HBing system is the guanidiniocarbonyl pyrrole carboxylate zwitterion[72] used by Schmuck's group, shown in Scheme 2-18. Because it is zwitterionic, it has ionic interactions in addition to HBing holding the

Scheme 2-18: Schmuck's zwitterionic hydrogen bonded dimer.

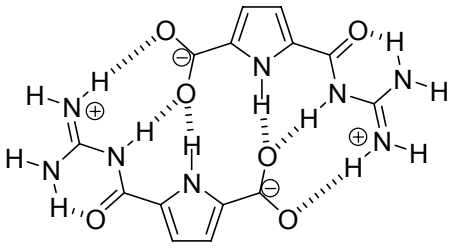

dimer together, which gives association constants (K_a) of 170 M^{-1} in water and 10^{10} M^{-1} in DMSO. The zwitterion is formed in the last step of the synthesis by a simple deprotection step to prevent solubility complications during earlier steps.

The synthetic route begins with the starting material, ethyl 3,4-dimethylpyrrole-5-carboxylate 2-carboxylic acid, **37**, which is created from the precursors 2,4-pentadione and diethyl malonate, shown in Scheme 2-19, following literature procedures.[73-79]

Scheme 2-19: The synthesis of the Schmuck's precursor, ethyl 3,4-dimethylpyrrole-5-carboxylate 2-carboxylic acid.[73-79]

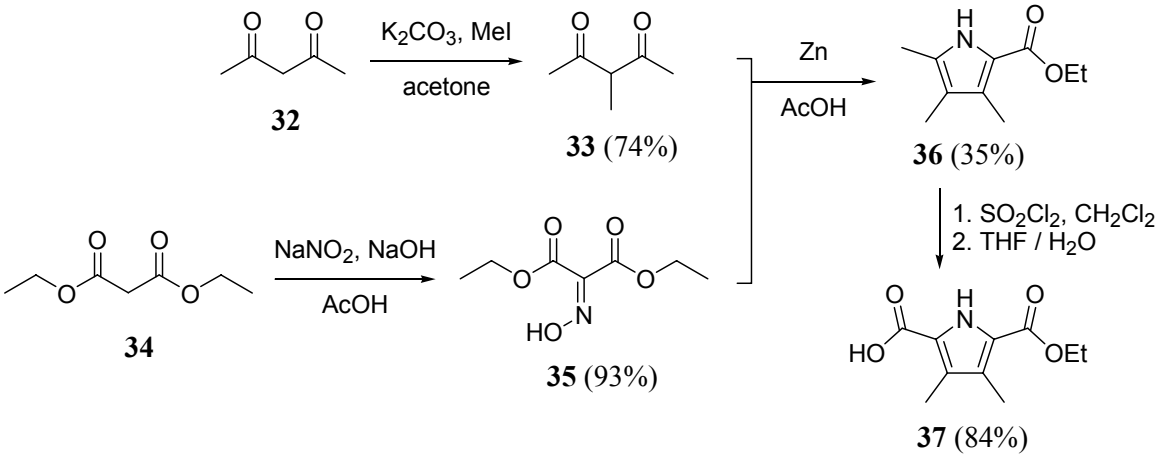

Acetylacetone, **32**, was methylated using methyl iodide in the presence of potassium carbonate to give **33**,[79] and diethyl malonate, **34**, was converted to the oxime **35** using sodium nitrite.[76] These two products were then converted into the pyrrole **36** via the Knorr synthesis.[76,78] The Zn in acetic acid reduces the oxime functionality to an amine, which then is able to undergo two condensation reactions with the methylated **33** to yield the pyrrole **36**. The methyl of the 5- position of **36** was successfully converted into the carboxylic acid **37** in a two-step reaction: the first step was the radical chlorination of the methyl group, followed by the hydrolysis of the chlorides with water in THF.[76] This

transformation was confirmed by the appearance of the carboxylic acid ^{1}H NMR signal at 12.70 ppm, and the lack of one of the methyl signals, as supported by literature reports.[76]

Scheme 2-20: Schmuck's synthesis to the water soluble zwitterionic hydrogen bonded dimer.[72]

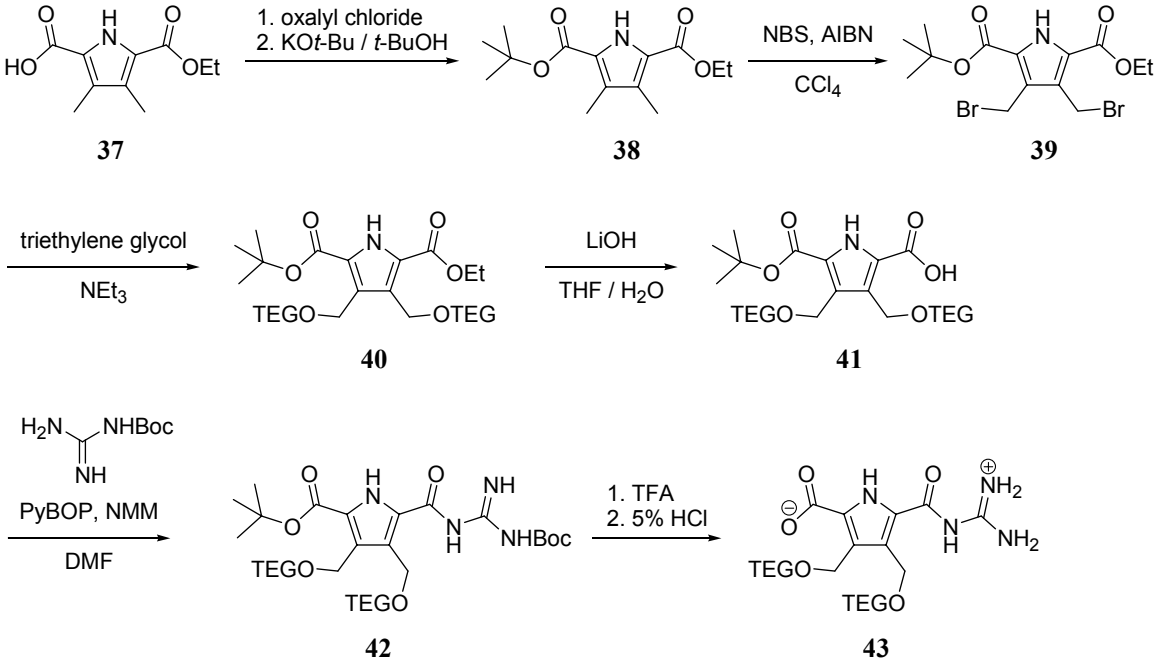

The acid **37** is then converted to the *t*-butyl ester **38** via an acyl chloride intermediate. This protection differentiates the *t*Bu ester from the ethyl ester in later steps. The 3- and 4-position methyl groups of **38** are then radically brominated using *N*-bromosuccinimide (NBS) to give **39**, allowing triethylene glycol (TEG) to substitute in the next step giving **40** which increases the solubility of the monomer in water. Lithium hydroxide is used to selectively deprotect the ethyl ester of **40** to produce **41**. A Boc-protected guanidine is then added to the carboxylic acid to yield **42**. In the last step the Boc group and *t*Bu ester are deprotected with TFA leaving Schmuck's zwitterionic pyrrole, **43**.

The challenge in using Schmuck's pyrrole is in functionalizing it with AQ, and having the target compound soluble in organic solvents, not water. To do this, some changes

need to be made to the synthesis outline in Scheme 2-20. It is desirable to install the AQ moiety to either the 3- or 4- position of the pyrrole, and to neglect the addition of the TEG groups. The solubilising groups would instead be added directly to the AQ unit.

With the acid-ester-pyrrole **37** in hand, the next step of creating the *t*-butyl ester **38** gave poor yields in the range of 10-20%. The following step was to brominate the two methyl groups at the 3- and 4 sites with NBS, as shown in Scheme 2-20, for a subsequent substitution. With poor yields at the *t*Bu esterification step, and a potential for a variety of alkylation products at the 3- and/or 4- sites, this synthesis did not promise a direct and efficient route to the desired zwitterionic product.

2.2.3.2 Alternate route to 3,4- differentiation

A new synthetic route, shown in Scheme 2-21, was constructed to replace one of the methyl groups on the 3,4-positions of the pyrrole precursor **37** with another handle. This alternative avoids the mixture of products from an alkylation via the brominated species, **39**. To begin the new synthesis, acetylacetone, **32**, was alkylated with TBDMS-protected **44** to give the functionalized dione **45** as in Scheme 2-21. This product **45** was then reacted with the oxime **35** and reduced to the pyrrole product **46** in 43% yield, as shown in Scheme 2-21. Unfortunately, the subsequent chlorination with sulfuryl chloride and substitution with water to convert the methyl in the 2- position into an acid yielded a variety of inseparable products.

Scheme 2-21: The synthesis of the TBDMS protected 2-(ethoxycarbonyl)- 4-[2-(*t*-butyldimethylsilanyloxy)ethyl]-3,5-trimethylpyrrole, 46.

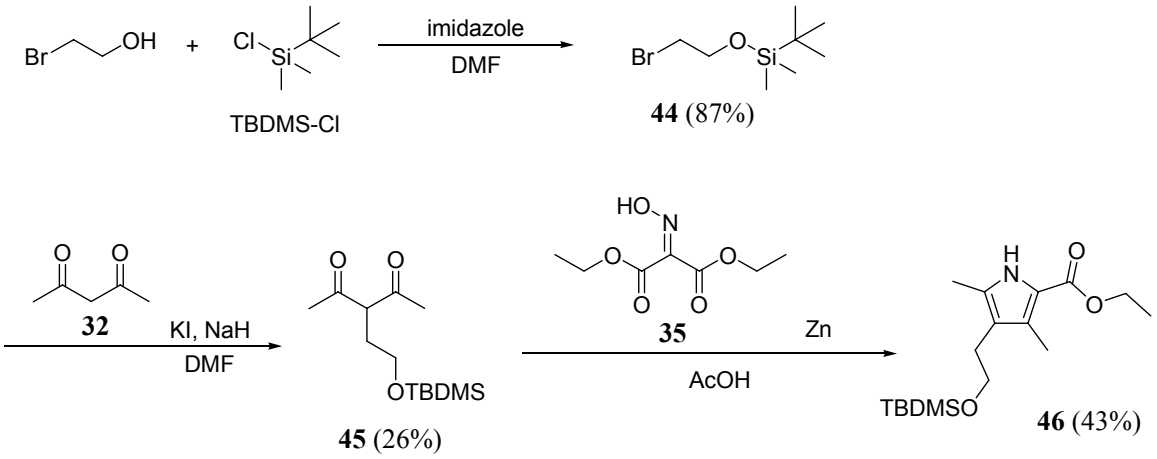

2.3 DNA nucleobase and linker chemistry

It is important to note that the DNA nucleobases are simply the HBing components of DNA; there are no sugars or phosphates involved in this chemistry. Additionally, the nucleobases are modified at the site that is typically bonded to the sugar, which was illustrated earlier as the N highlighted in green in Scheme 2-1. This requirement for this specific N-selectivity is two-fold: 1. to avoid crowding of the HBing face, and 2. to mimic the conditions of these nucleobases in nature.

Ideally, the DNA nucleobases are functionalized with the "linker" first, and then this moiety is connected with the AQ in the last step. This order was preferred as the chemistry of the nucleobases was limited by their lack of solubility, and by adding the "linker", the solubility of these starting materials in organic solvents was increased.

2.3.1 Ethylene carbonate

Many chemists use ethylene carbonate to deliver a hydroxyethyl group to nucleobases,[44,80-82] but this method is selective only for adenine and cytosine, shown in Scheme 2-22. The reason for this selectivity is the increased s character of the aromatic, or sp^2 hybridized NH, which increases the acidity. that is deprotonated is already donating its lone pair into the cyclic structure to satisfy the aromatic requirements.[83] This donation increases the stability of the deprotonated adenine or cytosine as the resonance of the aromatic core is able to delocalize the negative charge.[83] Thus, under the ethylene carbonate alkylating conditions, neither adenine nor cytosine needs a protecting group to produce the desired products **14** and **47** respectively, as shown in Scheme 2-22. In addition, these compounds are soluble in refluxing DMF, and the addition of the hydroxyethyl functionality improves solubility. ^{1}H NMR confirms this transformation by the addition of two methylene signals between 3.5-4.5 ppm, and the addition of an broad peak correlating to the alcohol proton. To purify the products, crystallization in hot ethanol was used yielding between 62-64%.

Scheme 2-22: The selective hydroxyalkylation of adenine and cytosine with ethylene carbonate.

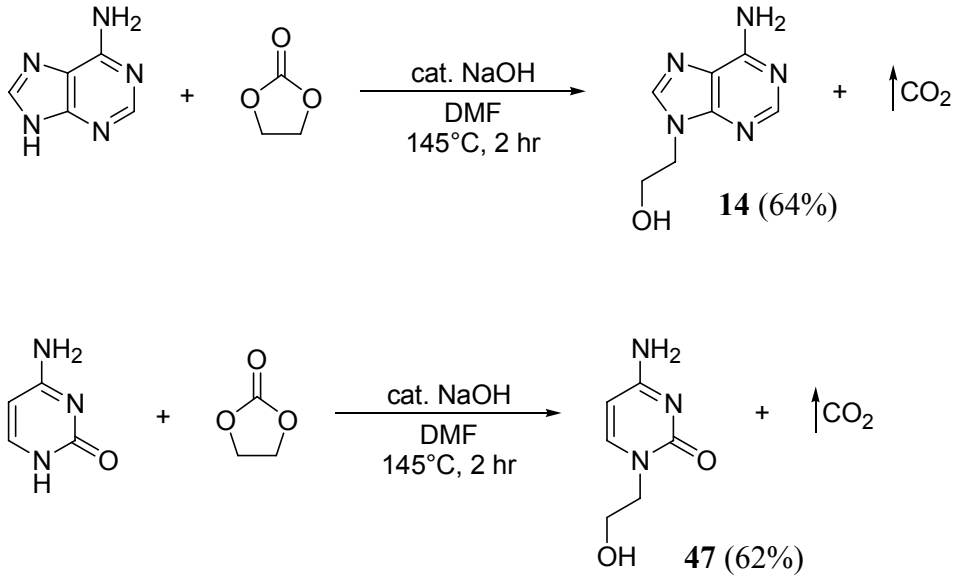

Thymine and uracil gave a mixture of products when reacted with ethylene carbonate in the presence of catalytic amounts of NaOH in DMF. Alkylation occurred at the 1- and/or 3- positions, as earlier shown in Scheme 2-9. However, by reacting the benzoyl-protected **24** under the same alkylation conditions, only deprotection of the benzoyl functionality was observed. Further discussion on the alkylation of the protected **24** will follow in the next section 2.3.2. The limited solubility of guanine prevents the ethylene carbonate alkylation under these conditions.

2.3.2 Protected thymine substitution with propargyl bromide and allyl bromide

It should be noted that thymine was investigated primarily over uracil, because the additional methyl group increases solubility and hence reactivity in the solution-based reactions.

The first N-alkylation attempts involved functionalizing thymine with propargyl (**48**) and allyl (**49**) functionalities, shown in Scheme 2-23, to utilize these compounds in the Sonogashira and Heck reactions, respectively. Both the Pd catalyzed coupling reaction precursors, **48** and **49**, were both synthesized as shown in Scheme 2-23. The N^1H was deprotonated with the DBU, allowing the anionic form of **24** to react with the activated alkyl bromide. The ^1H NMR suggests alkylation occurred due to the loss of the N^1 proton, and the inclusion of the appropriate alkyl peaks at 5.86, 5.28, and 4.35 ppm, which correlate to H_d, H_e, and H_f. The propargyl group shows at 4.49 and 3.37 ppm which correlate to the two methylene H_a and the $\equiv CH_b$ groups respectively.

Scheme 2-23: The alkylation conditions of 3-benzoylthymine with propargyl bromide and allyl bromide.

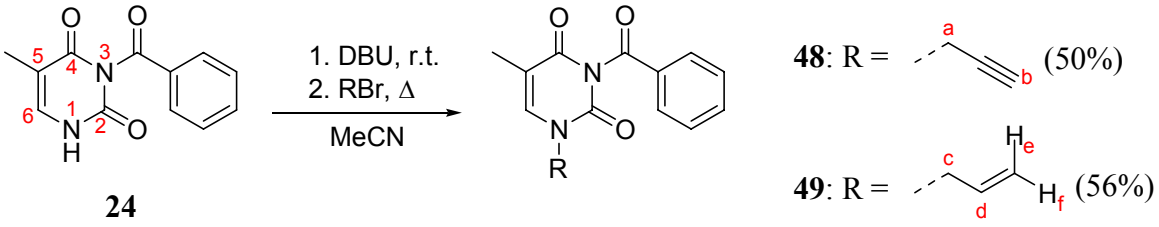

24

Further reaction of **48** and **49** with 2-iodoanthraquinone, **55**, in the presence Pd catalysts leads to a mixture of undesired products that were not further investigated. The Sonogashira and Heck reactions are later discussed in the section *2.4.1: Pd catalyzed coupling*.

2.3.3 2-Hydroxyethyl-thymine synthesis

Mitsunobu coupling conditions were then used successfully with the protected thymine **24** and 2-bromoethanol, as shown in Scheme 2-24, to yield the alkyl bromide **50**. The bromide functionality was reacted with $AgNO_3$ with the intention to convert the bromide

to the alcohol **52**. However the major product at 50% was the nitro-ester **51**. The ^{1}H NMR of the nitro-ester **52** showed a CH_2 group shift downfield from 3.68 to 4.75 ppm, and no alcohol proton, consistent with the nitro-ester. Evidence that further supports nitro-ester was the molecular ion (M^+) at 319.08 *m/z* and the appearance of the NO_3 peaks in the IR at 1643 and 1280 cm^{-1}. This product was then transformed into the alcohol **51** by reducing the nitro-ester with zinc in acetic acid,[84] producing a precursor for the Mitsunobu reaction with the appropriate hydroxyanthraquinone.

Scheme 2-24: The synthesis of 3-benzoyl-1(2-hydroxyethyl)thymine from thymine.

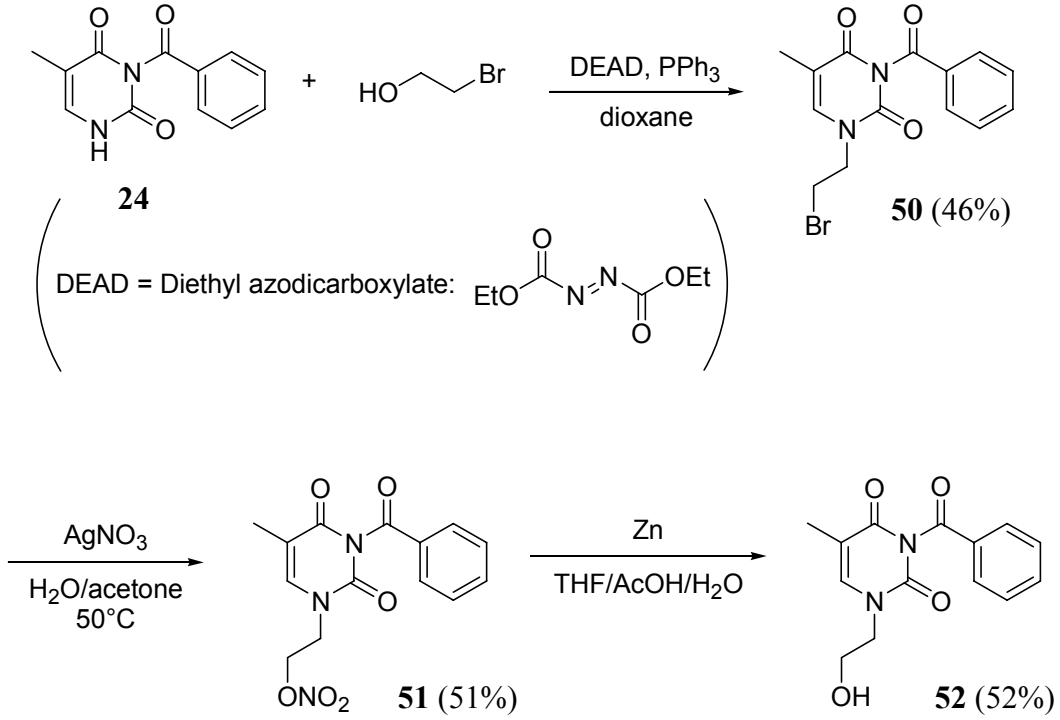

A successful Mitsunobu coupling between thymine and 2-bromoethanol requires the protection of thymine at the N^3 site as the Mitsunobu coupling is not selective to the N^1-site.[44] The Mitsunobu reaction involves the dehydrating agent diethyl azodicarboxylate (DEAD) and triphenylphosphine. These two reactants create a phosphonium ion, which is

an excellent leaving group. This condition is what drives the reaction to couple the alcohol and acid to form an ether, as shown by the mechanism in Scheme 2-25.

Scheme 2-25: The mechanism of the Mitsunobu coupling between an alcohol and a DNA nucleobase.

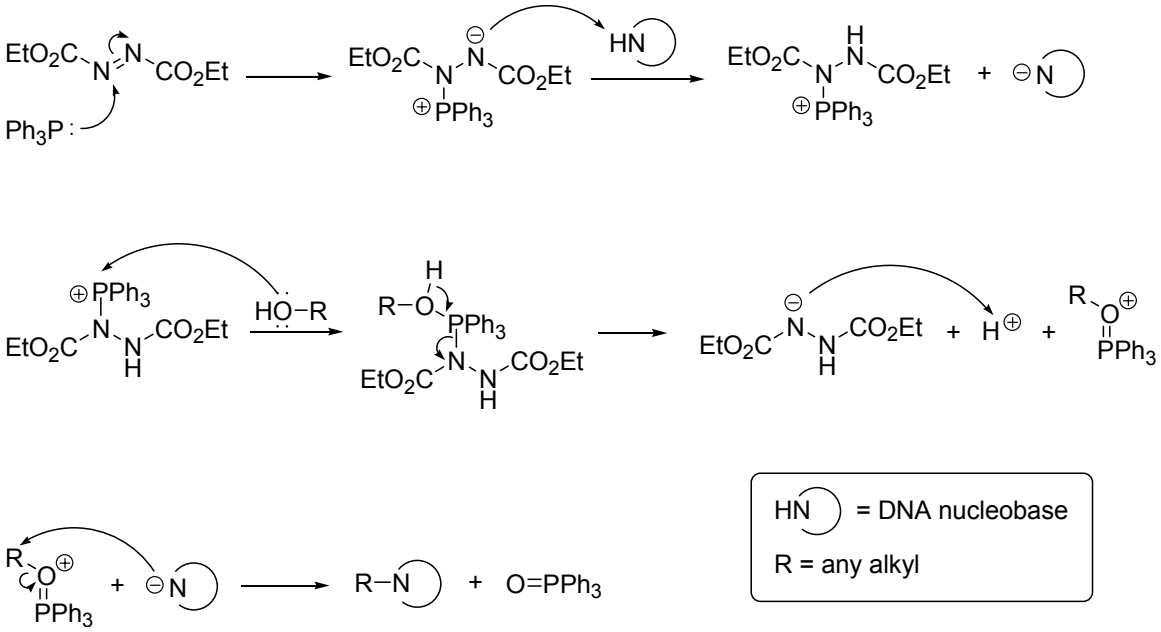

2.4 Connecting the hydrogen bonding moiety to anthraquinone

2.4.1 Pd catalyzed coupling

2.4.1.1 Aryl-halide formation

To form the aryl halides necessary for the catalyzed Pd coupling reactions investigated, such as Sonogashira and Heck, 2-aminoanthraquinone, **53**, underwent diazotization and substitution to form 2-iodoanthraquinone, **55**, and 2-bromoanthraquinone, **54**, using the efficient, one-pot synthesis shown in Scheme 2-26.[85] Commercially available 2-chloroanthraquinone was not considered as aryl chlorides are much less reactive in Sonogashira reactions.[86]

Scheme 2-26: The one-pot synthesis of 2-haloanthraquinone using hydrobromic or hydroiodic acid, and $NaNO_2$ in DMSO.[85]

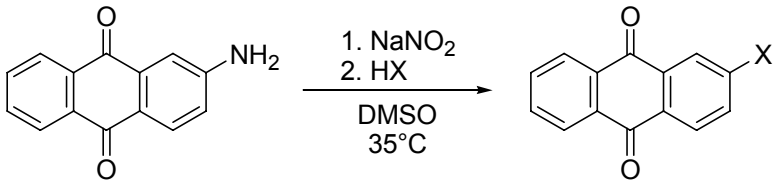

53

54: X = Br (73%)
55: X = I (69%)

2.4.1.2 Suzuki-Miyaura

Scheme 2-27: A simple Suzuki-Miyaura coupling between a generic aryl bromide and aryl organoboronic acid.[87-96]

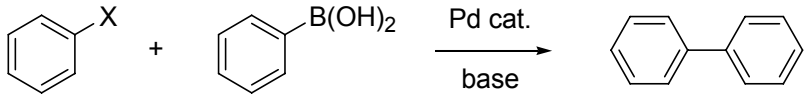

X = Br, I

The first reaction that was briefly investigated was the Suzuki coupling, shown in Scheme 2-27, where an aryl halide and an aryl organoboronic acid are combined in the presence of a Pd^0 catalyst, such as $Pd(OAc)_2$ and base. By changing the catalyst ligands[87-92] and/or the organoboronic acid,[93-96] alkynyl, alkenyl, and alkyl groups may also be used in this reaction.

After a preliminary reaction, it was clear that AQs are not suitable for the lithium-halogen exchange necessary to form the boronic acid/ester. The carbonyl groups in the AQs are not stable in the presence of butyl lithium; however, the DNA nucleobases also contain carbonyl functionalities and so were not used to form an organoboronic acid either.

2.4.1.3 Sonogashira

Scheme 2-28: The Sonogashira reaction between a generic aryl bromide and an alkyne, and two products of the Sonogashira reaction.

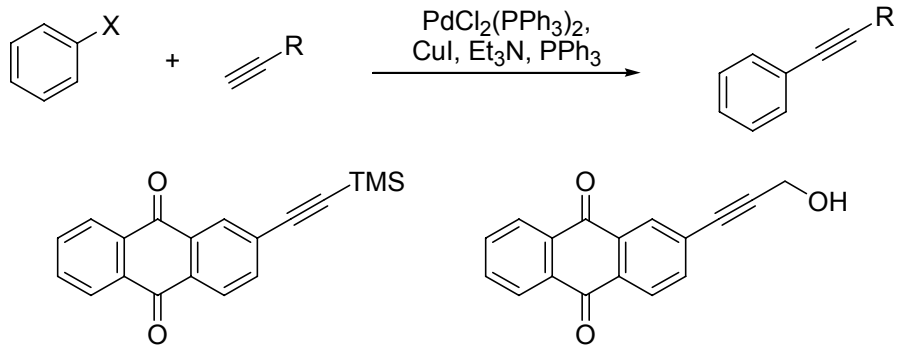

56 **57**

The second palladium catalyzed reaction investigated was the Sonogashira coupling shown in Scheme 2-28. This reaction held promise as trimethylsilylethynyl (TMS) protected AQ, **56**, and the AQ substituted propargyl alcohol, **57**, shown in Scheme 2-28, were both successfully synthesized. Literature precedence[97] confirmed the successful addition of the TMS group by the appearance of the following peaks: ^{1}H NMR at 0.30 ppm, and ^{13}C NMR at -0.0 ppm. The triple bond appeared in the ^{13}C NMR at 113.4 and 100.4 ppm. The addition of the propargyl alcohol was suggested by the appearance of the following peaks in the ^{1}H NMR: the methylene protons appeared adjacent to the alkyne functionality appeared at 4.58 ppm, the alcohol at 1.81 ppm, and the disappearance of the CH proton from the propargyl alcohol precursor. Additionally, both the bromo (**54**) and iodo (**55**) functionalized AQs gave the desired products in this reaction. The TMS-protected-AQ **56** was deprotected using potassium fluoride shown in Scheme 2-29.

Scheme 2-29: The deprotection of 2-trimethylsilanylethynyl-anthraquinone

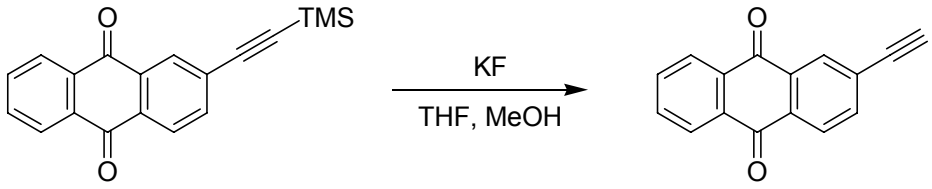

56 **58** (99%)

The alkyne **58** was combined with 2-iodoanthraquinone, **55**, under typical Sonogashira conditions (Scheme 2-30) in the attempt to create a coupled AQ-AQ system. This di-AQ product could then be studied to see how covalently coupled AQs compare to HBed AQ systems. However, the result of this Sonogashira reaction was not the desired AQ-≡-AQ, but instead the insoluble product was suspected to be the homo-coupled product, shown as **60**, based on the molecular ion found by mass spectroscopy. This product was not purified by chromatography nor characterized by standard methods due to its limited solubility in conventional organic solvents, such as hexane, toluene, methylene chloride, or DMSO. Sublimation was also unsuccessful as a purification method as the product decomposed before subliming under heat and vacuum.

Scheme 2-30: The reaction of 2-ethynyl-anthraquinone, 58, and 2-iodoanthraquinone, 55, and the expected and crudely assigned product.

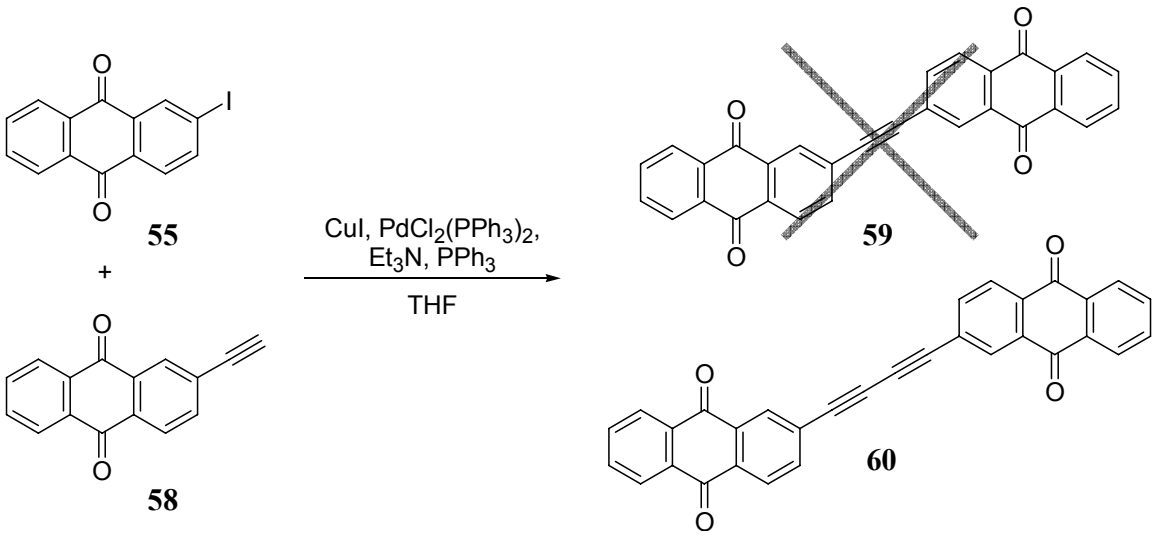

It has been shown that in the presence of I_2, the preferred route is the homocoupled alkyne, instead of the Sonogashira product,[98] and as the CuI in the Sonogashira reactions was not washed prior to use, it is the likely source of I_2, as shown by the equation 2-1.[99] As the Mitsunobu coupling method had proved successful upon discovery of this side reaction, the Sonogashira reaction was not further investigated with purified CuI.

$$2CuI \rightleftharpoons 2Cu + I_2 \qquad \text{(eq. 2-1)}$$

Scheme 2-31: The synthesis of 2-(3-hydroxyprop-1-ynyl)anthraquinone and the tosylated product from 2-iodoanthraquinone and propargyl alcohol

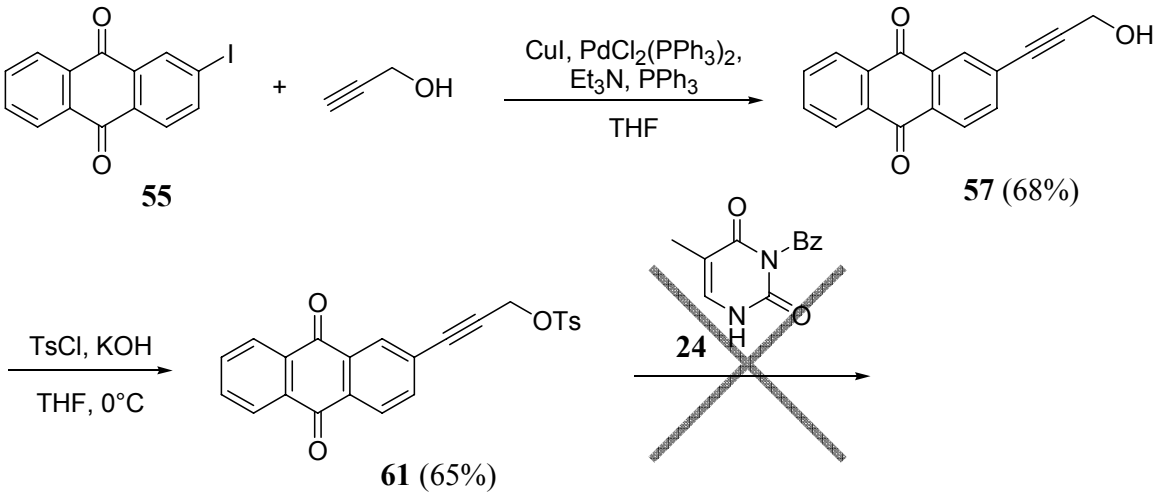

The propargyl alcohol did not require any protection as the alcohol functionality did not interfere with the palladium centre in the catalysis. The alcohol **57** was then tosylated, and the product **61** was reacted with the benzoyl-protected thymine **24**, and yielded no desired products as illustrated in Scheme 2-31.The crude reaction mixture showed mostly starting material when examined. It is possible that the N1 lone pair of thymine is not nucleophilic enough because of the π electron resonance requirements. Deprotonating the thymine with a non-nucleophilic base such as DBU, and then adding the tosylated **61**

may work, but was not attempted as it was clear a more soluble AQ system was necessary.

Scheme 2-32: The attempted reaction to connect 3-benzoylthymine and 2-iodoanthraquinone with a propargyl linker through Sonogashira conditions.

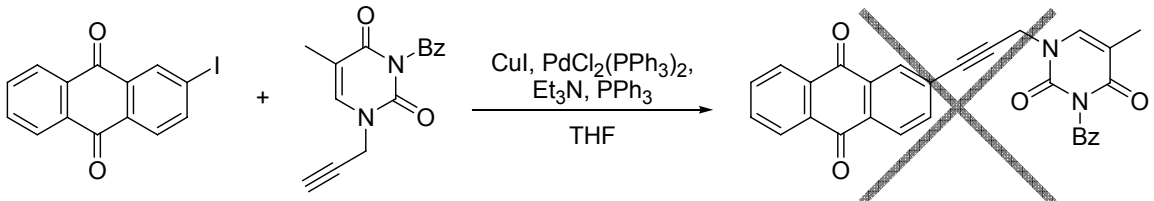

55 **48** **62** (not isolated)

The third strategy used the N-propargylated DNA bases that were prepared by the reaction between the protected thymine **24** and propargyl bromide in the presence of DBU, as previously depicted in Scheme 2-23. These propargylated DNA precursors, thymine shown in Scheme 2-32, adenine and uracil, were reacted with 2-iodo or 2-bromoanthraquinone, **55** or **54** respectively, under Sonogashira conditions, as described in Table 2-2. Both hot plate and microwave methods were investigated, but under all of the attempted conditions, none of the desired products were isolated, but instead a mixture of compounds that were not identified. The conditions presented in Table 2-2 became harsher with increasing trials. As no products were found in the reaction mixtures, one explanation is the possibility of the nucleobases were forming coordination complexes with the Pd catalyst, thus deactivating it. Additionally, electron rich alkynes, such as propargyl amines, and electron poor aryl halides, such as iodo- and bromo-anthraquinone, lower the catalyst turnover rate.[86]

Table 2-2: The Sonogashira conditions attempted between 2-bromoanthraquinone and 3-benzoyl-1-propargylthymine.

Trial	Catalyst	CuI equiv.	PPh_3 equiv.	Base	Solvent ([ArX])	Temperature
1	$PdCl_2(PPh_3)_2$ (0.2 equiv.)	0.2	0.02	Et_3N	THF (0.30 M)	r.t. – 40°C
2	$PdCl_2(PPh_3)_2$ (0.1 equiv.)	0.1	0.01	Et_3N	THF (0.36 M)	r.t. – 60°C
3	$PdCl_2(PPh_3)_2$ (0.1 equiv.)	0.1	0.01	Et_3N	THF (0.10 M)	r.t. – 80°C
4	$PdCl_2(PPh_3)_2$ (0.1 equiv.)	0.1	0.01	Et_3N	THF (0.25 M)	150°C (microwave)

2.4.1.4 Heck

Unfortunately, the Sonogashira reactions proved to be unsuccessful in coupling DNA nucleobases to AQ, so a Heck reaction was employed. This reaction is very similar to the Sonogashira reaction, where the main differences are that no copper co-catalyst is used, and the alkyne is replaced with an alkene. The Heck reaction is quite selective for the trans- product, but it can also give a variety of by-products (Scheme 2-33). The standard Heck reaction is shown in Scheme 2-33.

Scheme 2-33: The Heck coupling between an aryl halide and an alkene, and the potential products.

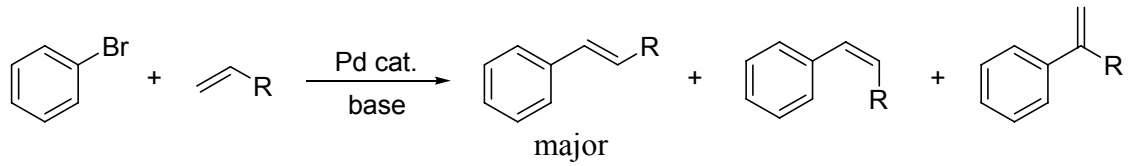

It should be noted that the alkene shown in Scheme 2-33 needs to be activated by an electron withdrawing group[100] to favour the trans-product. Electron neutral and electron

donating groups encourage side reactions and yield higher cis and vinyl isomers.[101] Unfortunately, the allyl group substituted to 3-benzoylthymine at the 1- position falls into this latter set of alkenes, which is why, the desired product was not found in the reaction mixture.

2.4.2 Steglich esterification

2.4.2.1 Formation of carboxylic acid

With the lack of success with the palladium catalyzed reactions, the next path investigated the synthesis of the carboxylic acid **1** to create an ester linkage between the nucleobase and AQ moieties, as the hydroxyethyl functionalized nucleobases had already been synthesized. The acid **1** was easily made as per literature precedence by oxidizing the methyl precursor **63** with chromium(VI) oxide in 80.5% yield.[102] The oxidation was confirmed by the following ^{1}H NMR peaks: the methyl singlet disappeared and gave rise to the appearance of the carboxylic acid proton at 13.70 ppm, which was also confirmed by literature.[102]

Scheme 2-34: The oxidation of 2-methylanthraquinone to anthraquinone 2-carboxylic acid.

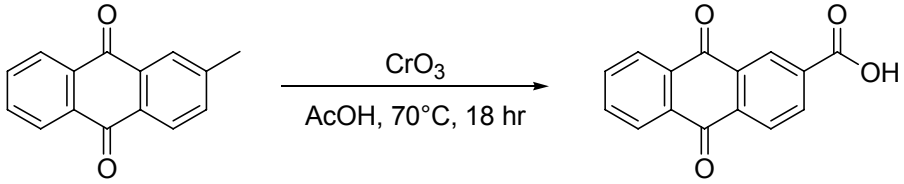

63 **1** (81%)

2.4.2.2 EDC·HCl as a coupling agent

The Steglich esterification (Scheme 2-35) traditionally uses dicyclohexylcarbodiimide (DCC), but the easier removal of the urea byproduct of 1-ethyl-3-(3-dimethylaminopropyl) carbodiimide hydrochloride (EDC·HCl), due to its increased solubility in water, makes this coupling agent preferable.

In the first step of the mechanism found in Scheme 2-35, the acidic proton protonates one of the nitrogens of the carbodiimide functionality, N=C=N, which increases the electrophilicity of the central carbon. The conjugate base of the carboxylic acid then attacks this electrophilic carbon to give the intermediate **I1** that then undergoes protonation at the second nitrogen of the original carbodiimide, leaving the central carbon again electrophilic which is satiated by the addition of the alcohol. This intermediate **I2** rearranges to give the consumed EDC·HCl as a urea derivative and **I3**. After a deprotonation of **I3**, the ester product **P1** is formed.

Scheme 2-35: The mechanism of the Steglich esterification using EDC·HCl as the dehydrating agent.

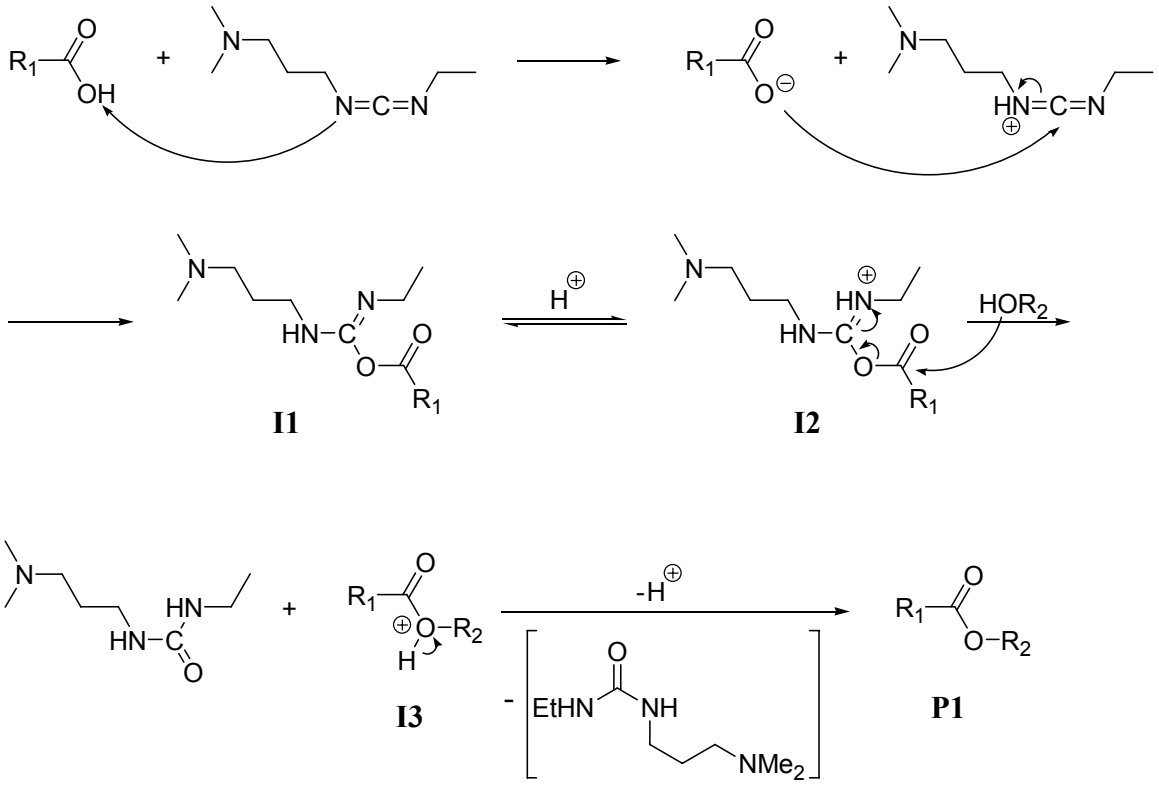

Both **14** and **47** were coupled with **1** using EDC·HCl to give the products **64** and **65**, respectively, as shown in Scheme 2-36. These insoluble products were confirmed by ^{1}H NMR in DMSO-d_6 by all of the appropriate peaks from the nucleobase and the AQ, with the exception of the carboxylic acid proton and the alcohol proton, as shown in Figure 2-2 for the product **64**. Additionally, the amino protons can be seen at 7.20ppm, which confirms that a deuterium exchange has not taken place, which is unlikely in DMSO-d_6 as it an aprotic solvent.

Scheme 2-36: The coupling of hydroxyl-ethyl functionalized adenine and cytosine with anthraquinone 2-carboxylic acid under modified Steglich conditions.

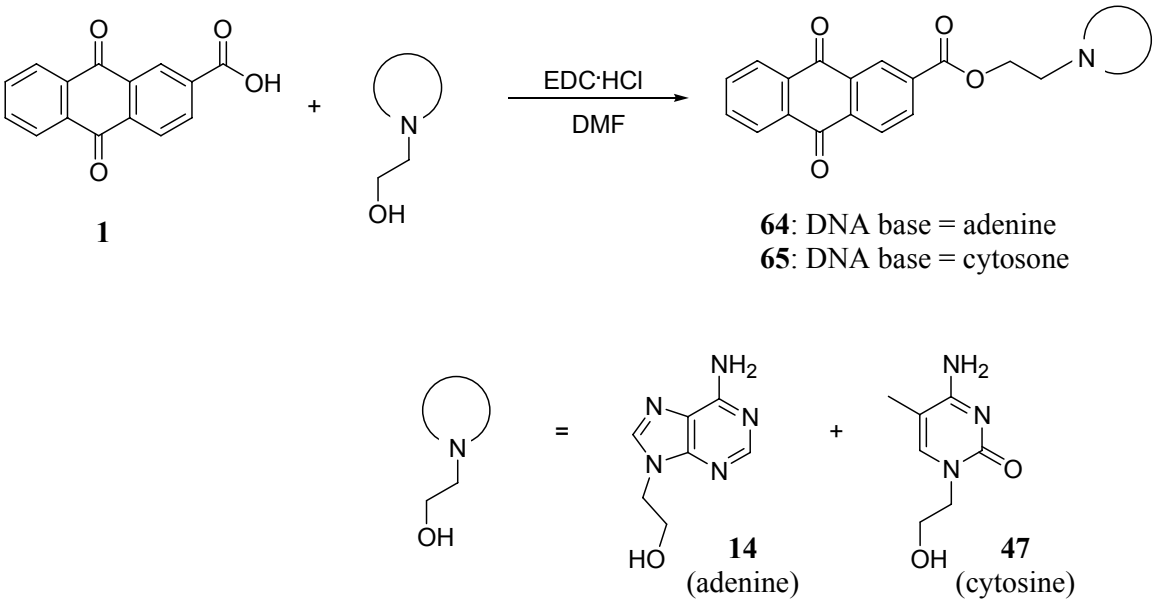

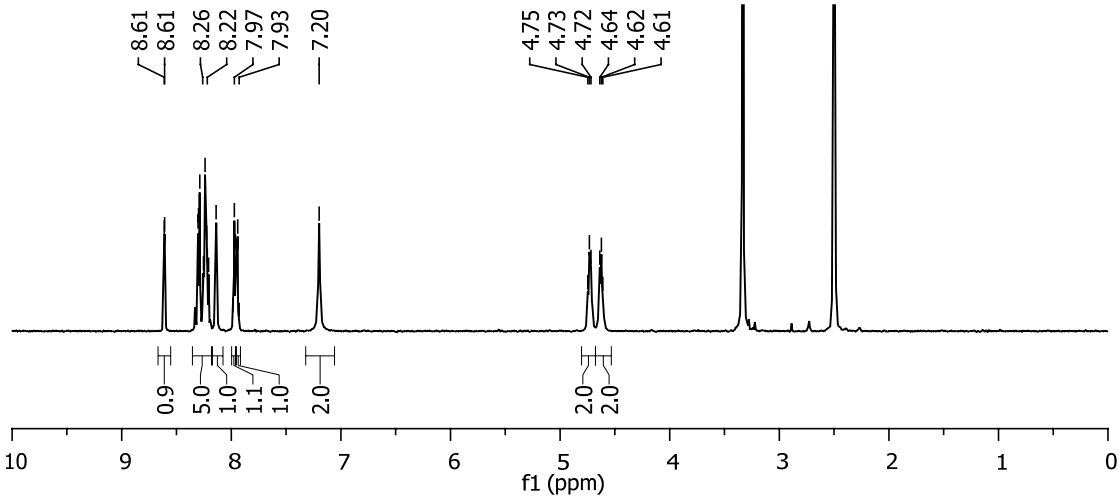

Figure 2-2: The ^{1}H NMR of the coupled product of the adenine functionalized anthraquinone 64 in DMSO-d_6 under Steglich esterification conditions.

Unfortunately, due to the limited solubility of the products **64** and **65**, they were not purified and were not carried on to the physical properties investigation. It was concluded that EDC·HCl was a suitable coupling agent, but that the AQ would have to be

functionalized with solubilising alkyl groups. This solubility challenge, in addition to potential ester hydrolysis, suggested for different, less polar, linkage chemistry to be investigated.

2.4.3 Mitsunobu Coupling

The Mitsunobu coupling, shown in Scheme 2-37, offered an easy alternative to couple the AQ and DNA nucleobases that offered linkage chemistry that was less polar than the Steglich esterification. Additionally, this reaction does not depend on an electron rich aromatic system, such as the Pd catalyzed systems. Typically, the Mitsunobu coupling involves an alcohol and a carboxylic acid, but literature revealed that phenols are acidic enough to take part in the Mitsunobu reaction, and thus hydroxy-substituted AQs are ideal candidates to employ.[103,104]

Scheme 2-37: The coupling of hydroxyl-ethyl functionalized adenine and thymine with 1-(2-ethylhexyloxy)-4-hydroxyanthraquinone under Mitsunobu conditions.

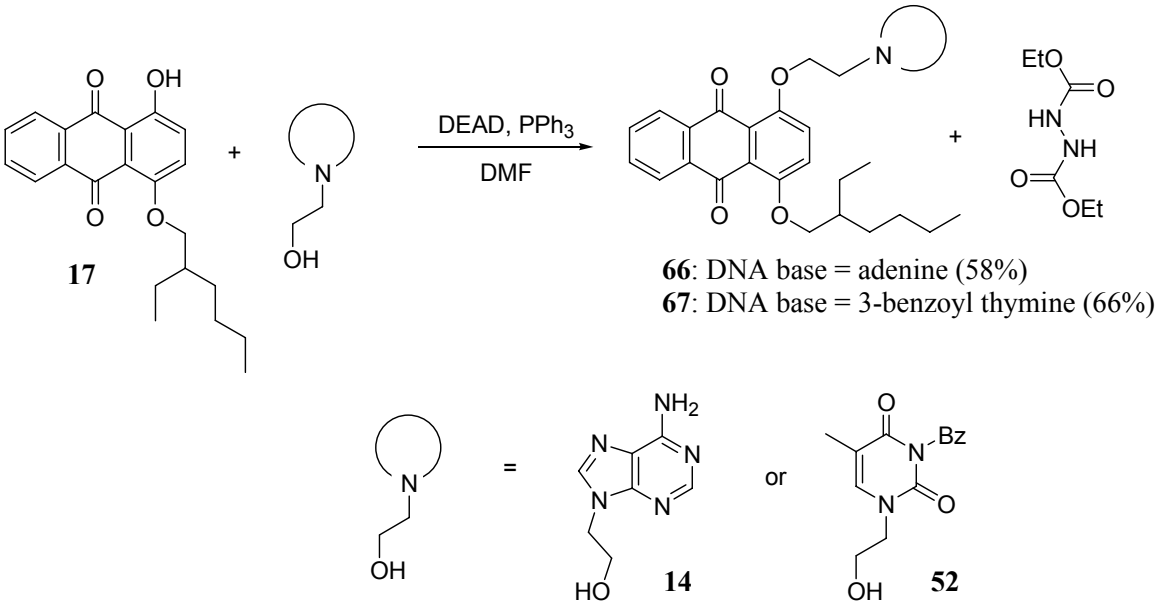

Both the adenine and 3-benzoyl thymine derivatives were successfully coupled with 1-(2-ethylhydroxy)-4-anthraquinone resulting in compounds **66** and **67** under the standard Mitsunobu conditions, as shown in Scheme 2-37. Removing the reduced DEAD, 1,2-diethyl (1,2-hydrazine)dicarboxylate, from the purified reaction products was performed by stirring the products in water and acetic acid at 70°C, and the mixture was filtered while still hot. The products **66** and **67** were then simply left in the Buchner funnel with vacuum to dry, before being placed in a dessicator to dry completely. The benzoyl functionality was removed producing **68** in 87.4% yield as shown in Scheme 2-38, only after the Mitsunobu reaction because it increased solubility of the thymine derivative during the synthesis.

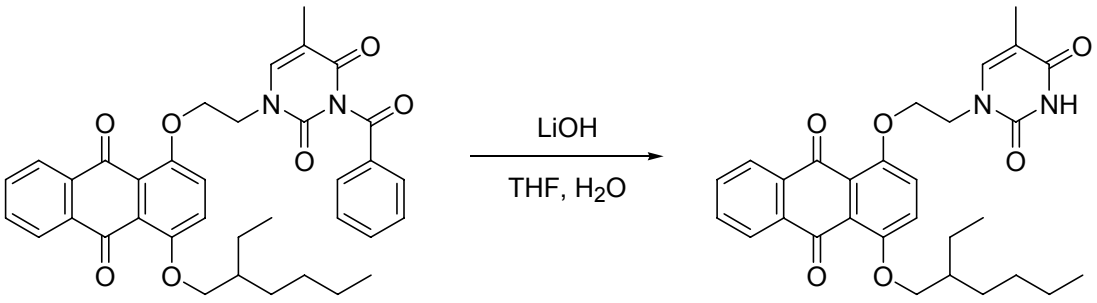

67 **68** (87%)

Scheme 2-38: The deprotection of the 3-benzoylthymine anthraquinone derivative.

2.5 Experimental

All purchased chemicals were used as received. Flash column chromatography was performed on silica gel 60 (60–200 μm, Silicycle, Ontario). ^{1}H- and ^{13}C NMR spectra were carried out at room temperature, and recorded on a Bruker DMX-300 or a Bruker DRX-400 spectrometer. Elemental analyses were performed at the University of Calgary, Department of Chemistry. Mass spectrometry was carried out using a Finigan SSQ700

spectrometer. Infrared spectra were measured with a Varian FTS-7000 FT-IR spectrometer in a KBr suspension operating in diffuse reflectance mode at room temperature. UV-vis spectra were recorded in dry THF (inhibitor free) solutions in a 1cm quartz cell on a Cary5000 spectrometer. CVs were performed on a commercial potentiostat (Autolab PGSTAT 302 Electrochemical Workstation) and data acquisition was controlled through software interface (GPES 4.9). All experiments were performed in a THF solution of 0.1 M tetrabutylammonium hexafluorophosphate (TBAHFP) at 25°C. Three-electrode experiments were performed using a commercial Ag|AgCl|KCl_{3M} reference electrode (Bioanalytical Systems, Inc.); and a Pt wire working electrode, and a Pt mesh counter electrode that were both flame annealed prior to each experiment. Solutions were purged with argon prior to each experiment.

Synthesis of: anthraquinone-2-carboxylic acid, ***1***[102]

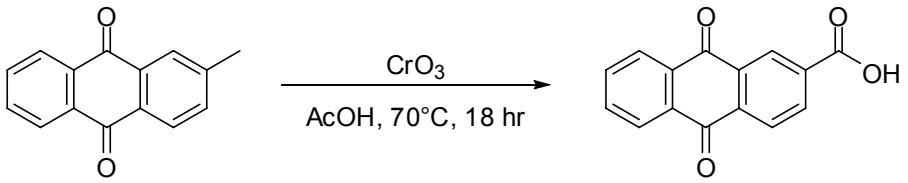

Chromium(VI) oxide (3.54g, 35.4 mmol) was added to 2-methylanthraquinone (1.016g, 4.57 mmol) in AcOH (50mL) and stirred for 18 hrs at 70°C. The black mixture was allowed to cool to room temperature before being poured into water (400 mL). The precipitate was collected by vacuum filtration and rinsed with water until the filtrate became colorless. Yield: 0.929g (80.5%). ^{1}H NMR (300MHz, DMSO-d_6) δ 13.70 (s, 1H), 8.64 (s, 1H), 8.38 (d, *J* = 8.1, 1H), 8.29 (d, *J* = 8.0, 1H), 8.26 – 8.17 (m, 2H), 7.95 (dd, *J*

= 3.4, 5.5, 2H), 3.33 (s, 2H). ^{13}C NMR (75 MHz, DMSO-d_6) δ 181.93, 181.77, 165.87, 135.62, 135.47, 134.69, 134.35, 133.07, 132.92, 127.32, 127.27, 126.80.

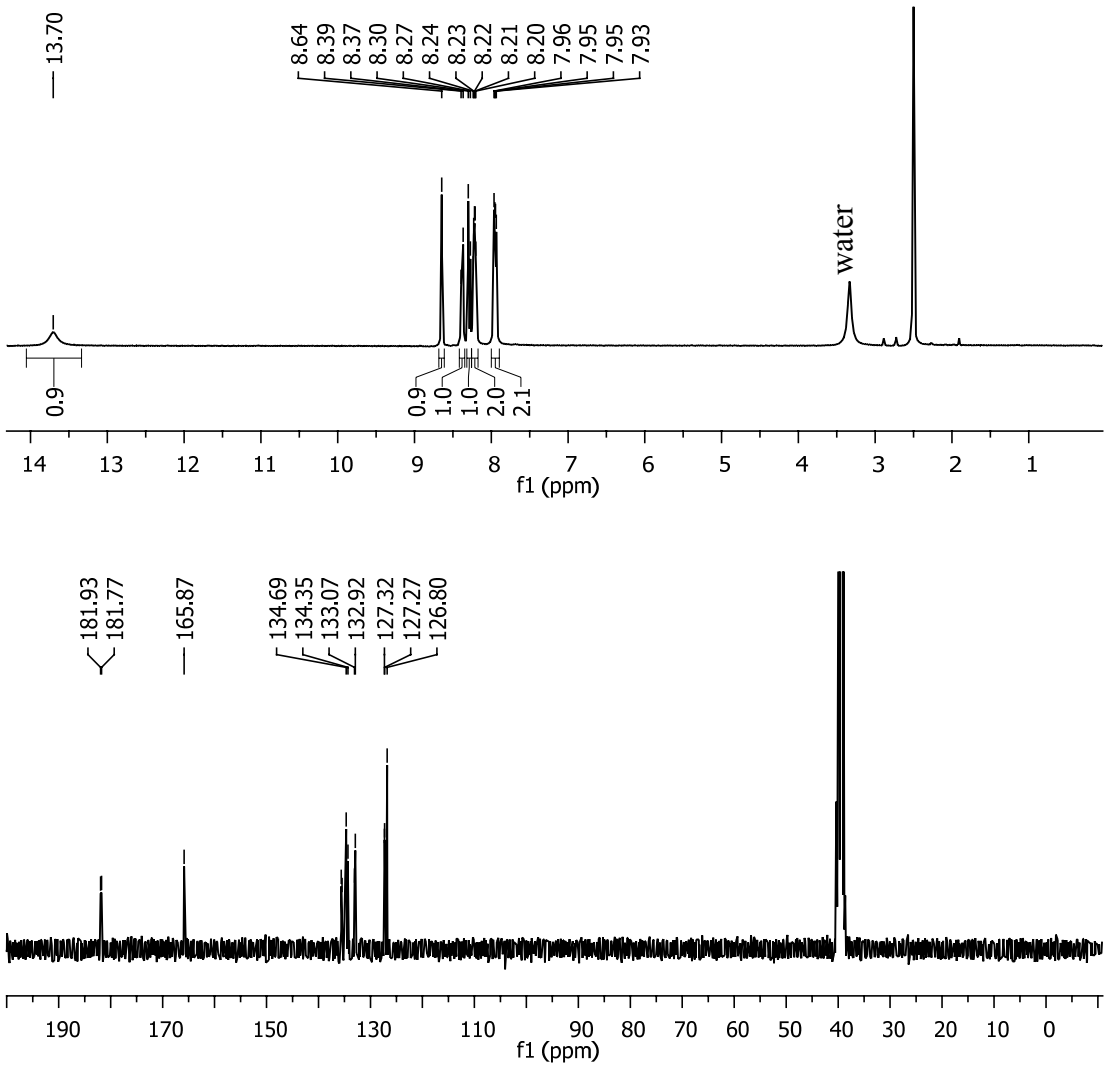

Synthesis of: 5-(4-pentylphenoxy)-anthraquinone-2-carboxylic acid, ***10***[38]

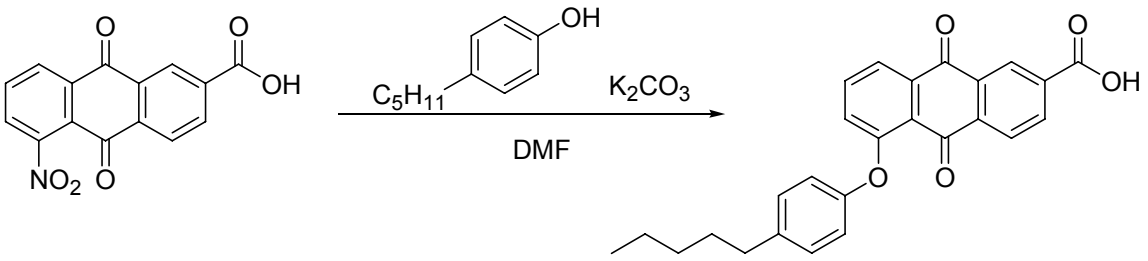

5-nitroanthraquinone-2-carboxylic acid (0.188g, 0.634 mmol), 4-pentylphenol (0.109g, 0.662 mmol), and potassium carbonate (0.290g, 2.10 mmol) were dissolved in DMF (4.0mL) and stirred at 80°C for 30 hrs. 3M HCl was slowly added to the red solution until the solution was acidic. The bright yellow precipitate was collected by vacuum filtration, rinsed with cold water (15mL), and crystallized in hot acetic acid and toluene. Yield: 0.148g (56.7%). Melting point: 202-205°C. Anal. calcd for $C_{26}H_{22}O_5$, %: C, 75.4; H, 5.4. Found, %: C, 75.1; H, 5.4. ^{1}H NMR (300 MHz, DMSO-d_6) δ 13.57 (s, 1H), 8.54 (d, *J* = 1.5, 1H), 8.32 (dd, *J* = 1.6, 8.1, 1H), 8.22 (d, *J* = 8.0, 1H), 7.99 (d, *J* = 7.6, 1H), 7.83 (t, *J* = 8.0, 1H), 7.32 (d, *J* = 8.2, 1H), 7.20 (d, *J* = 8.5, 2H), 6.94 (d, *J* = 8.5, 2H), 2.59 – 2.52 (m, 2H), 1.59 – 1.52 (m, 2H), 1.33 – 1.22 (m, 4H), 0.85 (t, *J* = 6.8, 3H). ^{13}C NMR (75 MHz, DMSO-d_6) δ 181.92, 180.15, 165.95, 156.85, 154.23, 137.78, 135.78, 135.66, 135.21, 134.69, 134.33, 133.76, 129.75, 127.38, 126.91, 126.41, 123.39, 122.43, 118.35, 34.34, 30.87, 30.74, 21.95, 13.91. IR (KBr), υ_{max}/cm^{-1}: 1703 (conj. C=O), 1676 (conj. C=O), 1298 (aryl C-O), 1254 (aryl C-O), 1213 (aryl C-O).

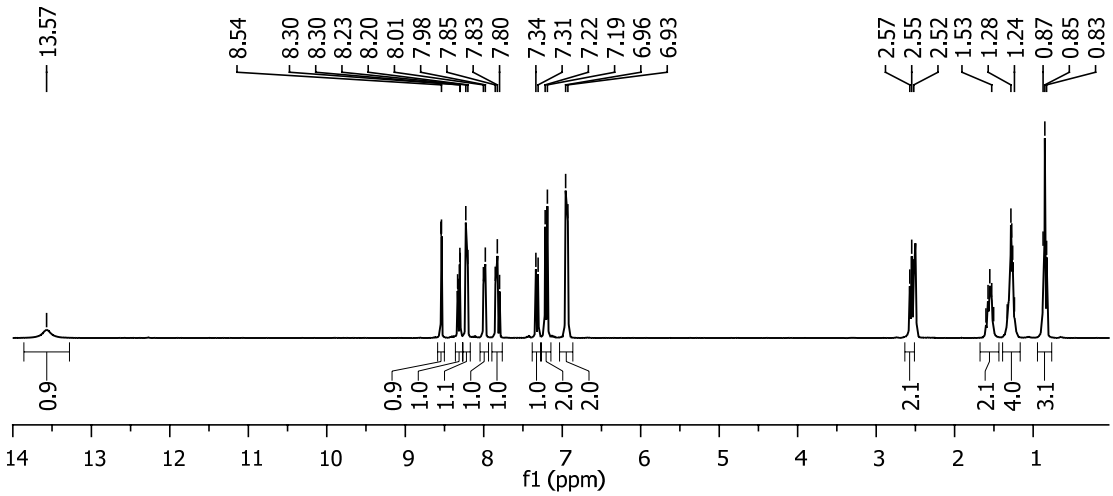
13.57
8.54
8.30
8.30
8.23
8.20
8.01
7.98
7.85
7.83
7.80
7.34
7.31
7.22
7.19
6.96
6.93
2.57
2.55
2.52
1.53
1.28
1.24
0.87
0.85
0.83
0.9
0.9
1.0
1.1
1.0
1.0
1.0
2.0
2.0
2.1
2.1
4.0
3.1
14
13
12
11
10
9
8
7
6
5
4
3
2
1
f1 (ppm)

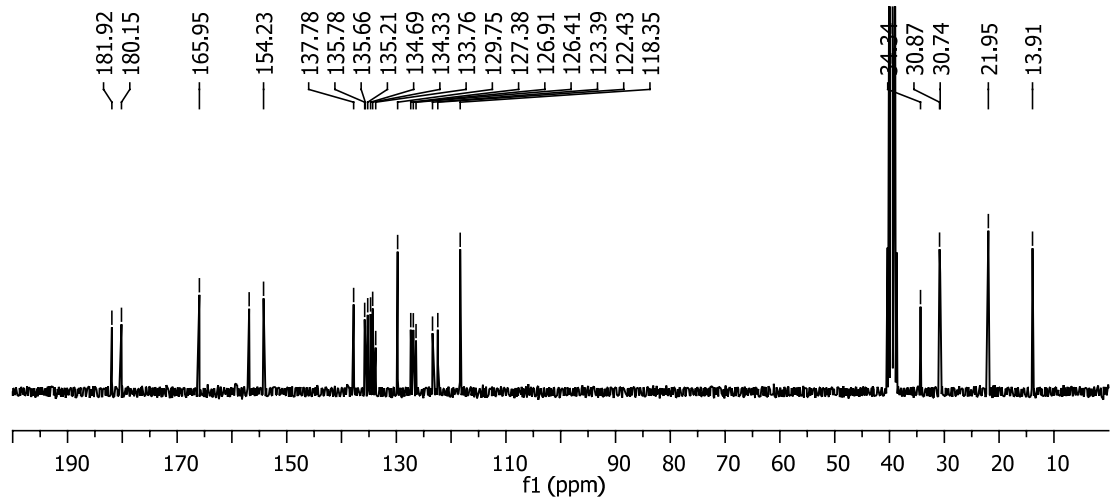
181.92
180.15
165.95
154.23
137.78
135.78
135.66
135.21
134.69
134.33
133.76
129.75
127.38
126.91
126.41
123.39
122.43
118.35
34.24
30.87
30.74
21.95
13.91
190
170
150
130
110
90
80
70
60
50
40
30
20
10
f1 (ppm)

Synthesis of: 5-(4-methoxyphenoxy)-anthraquinone-2-carboxylic acid, ***9***[38]

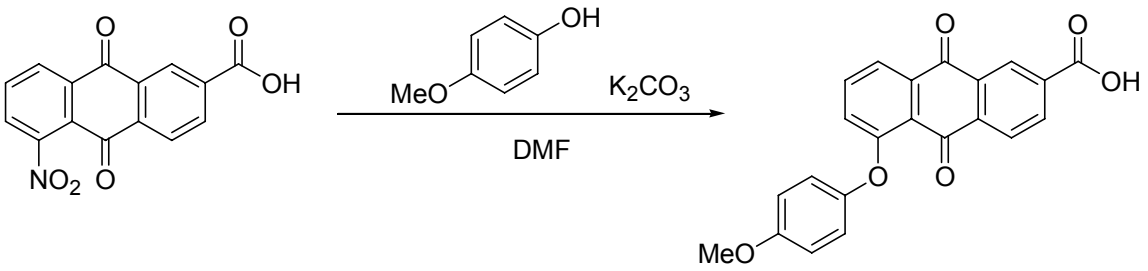

5-nitroanthraquinone-2-carboxylic acid (0.581g, 1.95 mmol), 4-methoxyphenol (0.258g, 2.08 mmol), and potassium carbonate (0.90g, 6.51 mmol) were dissolved in DMF (12.5mL) and stirred at 80°C for 30 hrs. 3M HCl was slowly added to the red solution until the solution was acidic. The bright yellow precipitate was collected by vacuum filtration, rinsed with cold water (50mL), and crystallized in hot acetic acid and toluene. Yield: 0.368g (50.4%). Melting point: 240-244°C. ^{1}H NMR (300 MHz, DMSO-d_6) δ 8.58 (s, 1H), 8.33 (d, *J* = 8.0, 1H), 8.23 (d, *J* = 8.0, 1H), 7.96 (d, *J* = 7.5, 1H), 7.79 (t, *J* = 8.0, 1H), 7.23 (d, *J* = 8.3, 1H), 6.99 (q, *J* = 9.2, 4H), 3.74 (s, 3H). ^{13}C NMR (100 MHz, DMSO-d_6) δ 182.05, 180.27, 165.98, 157.94, 155.84, 149.16, 135.79, 135.59, 135.22, 134.74, 134.48, 133.72, 127.38, 126.92, 125.05, 122.75, 121.80, 120.39, 115.20, 55.43. IR (KBr), υ_{max}/cm^{-1}: 3069, 3015, 2902, 2838, 2053, 1994, 1884, 1699, 1676, 1606, 1583, 1504, 1460, 1440, 1324, 1299, 1270, 1244, 1205, 1123, 1103, 1086, 1036, 1021. HRMS (EI, 70 eV) *m/z*: M^+ calcd for $C_{22}H_{14}O_6$, 374.0790; found 374.0793.

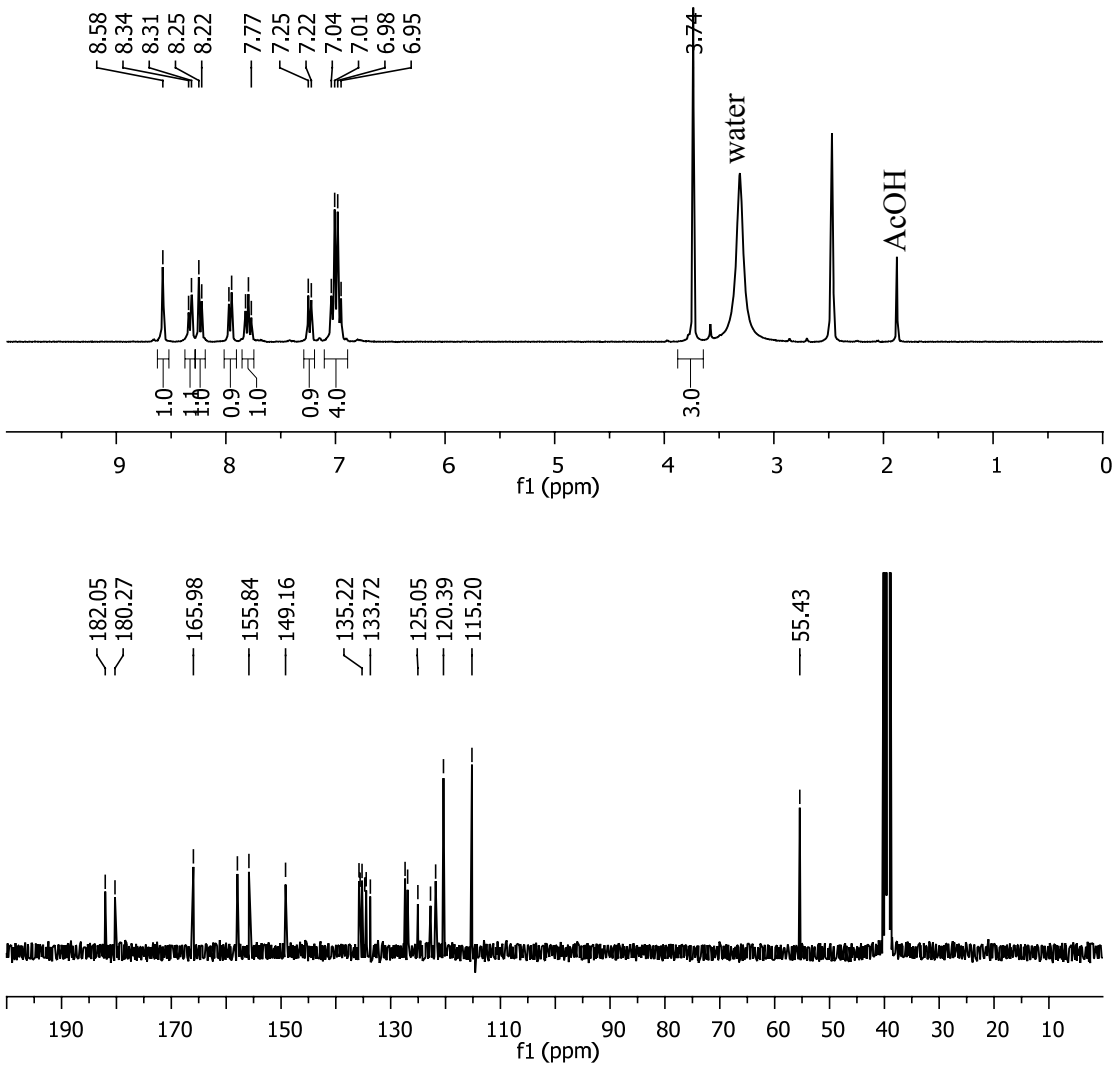

Synthesis of: 2-iodoanthraquinone, ***55***[85]

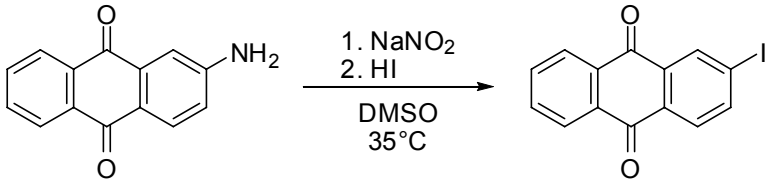

2-aminoanthraquinone (3.441g, 15.4 mmol) was added to a solution of $NaNO_2$ (4.265g, 61.6 mmol) in DMSO (125mL) at 35°C. An aqueous solution of 57% HI (8.13mL, 36.2

mmol) was slowly added to the 2-aminoanthraquinone mixture over the course of one hour, and then stirred for an additional hour. An aqueous solution of 1M Na_2CO_3 (80 mL) was then added, and the solution formed a white suspension. The crude mixture was extracted with methylene chloride (3 x 80mL) which formed a thick emulsion. This emulsion was removed by passing both the organic and aqueous layers through a paper filter *in vacuo*. The combined organic extracts were dried over $MgSO_4$ and reduced *in vacuo*, and the residue was purified by column chromatography on silica (hexanes:ethyl acetate, 5:1, R_f = 0.43). Yield: 3.57g (69.4%). ^{1}H NMR (300 MHz, $CDCl_3$) δ 8.63 (d, *J* = 1.7 Hz, 1H), 8.28 (m, 2H), 8.14 (dd, *J* = 8.2 Hz, 1.8 Hz, 1H), 7.98 (d, *J* = 8.2 Hz, 1H), 7.81 (m, 2H). ^{13}C NMR (75 MHz, $CDCl_3$) δ 182.81, 182.11, 143.29, 136.45, 134.62, 134.53, 134.24, 133.50, 133.24, 132.76, 128.84, 127.55, 127.49, 102.44.

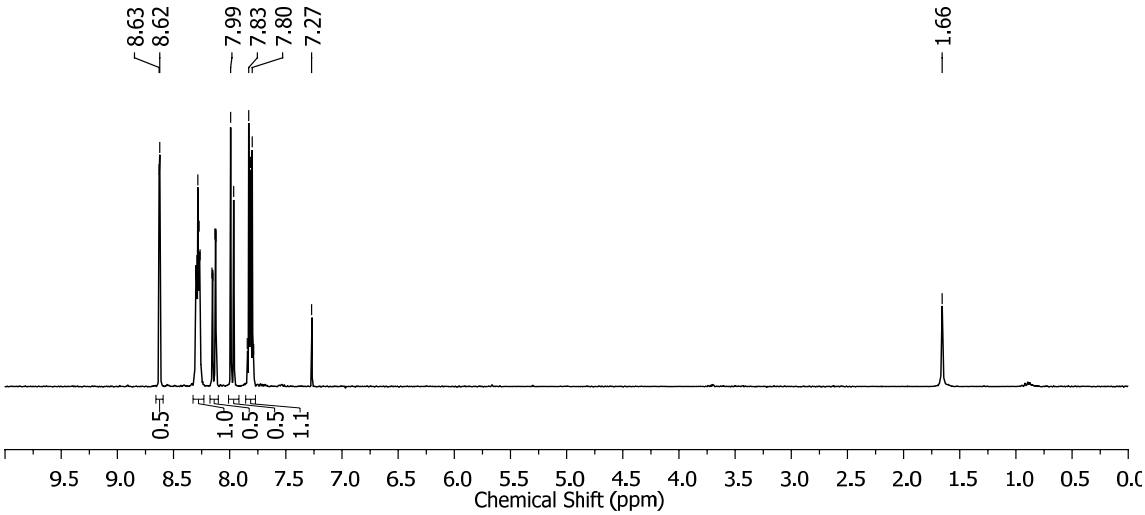

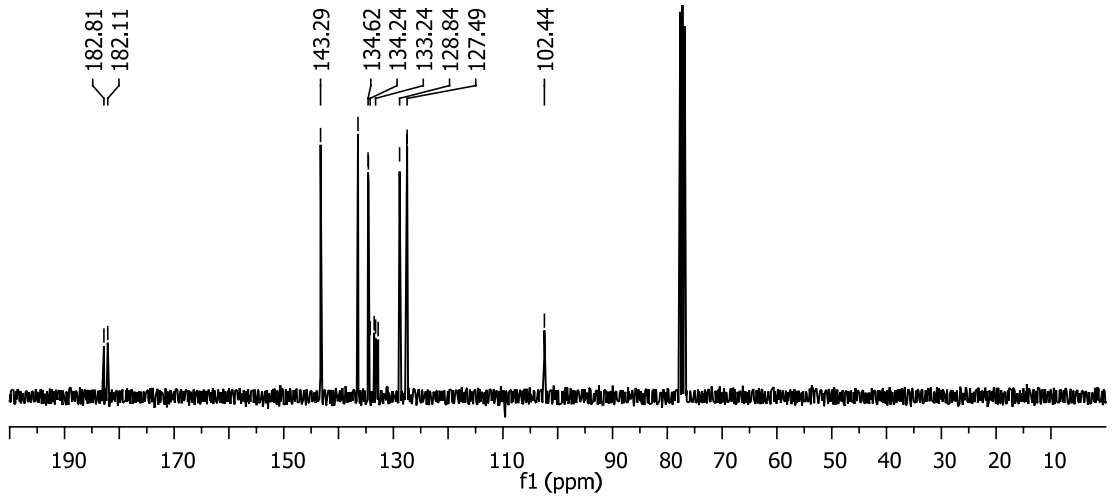

Synthesis of: 2-trimethylsilanylethynyl-anthraquinone, ***56***[97]

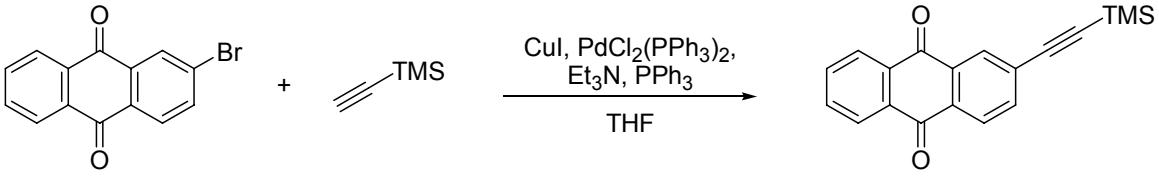

$PdCl_2(PPh_3)_2$ (29mg, 0.041 mmol), PPh_3 (~10mg), CuI (22mg, 0.116 mmol), 2-bromoanthraquinone (0.116g, 0.405 mmol), THF (2mL), Et_3N (0.26mL), and ethynyltrimethylsilane (0.06mL, 0.446 mmol) were all combined in a flask and stirred for 2 hrs. A TLC showed unreacted 2-bromoanthraquinone (hexanes: ethyl acetate, 2:1, R_f = 0.78), so additional ethynyltrimethylsilane (0.03mL, 0.223 mmol) was then added and stirred for 18 hrs. The mixture was quenched with water (1.0mL) and extracted with ethyl acetate (3 x 5mL). The combined organic extracts were dried with $MgSO_4$ and then brought to dryness *in vacuo*. The crude product was purified by column chromatography on silica (hexanes:ethyl acetate, 2:1, R_f = 0.78). Yield: 94mg (75.8%). ^{1}H NMR (300 MHz, $CDCl_3$) δ 8.38 (d, *J* = 1.5, 1H), 8.33 (ddd, *J* = 1.5, 3.8, 5.2, 2H), 8.26 (d, *J* = 8.0,

1H), 7.87 – 7.77 (m, 3H), 0.30 (s, 9H). ^{13}C NMR (75 MHz, $CDCl_3$) δ 182.69, 137.04, 134.47, 134.39, 133.83, 133.71, 132.80, 130.90, 129.66, 127.53, 127.47, 113.89, 100.38, -0.02.

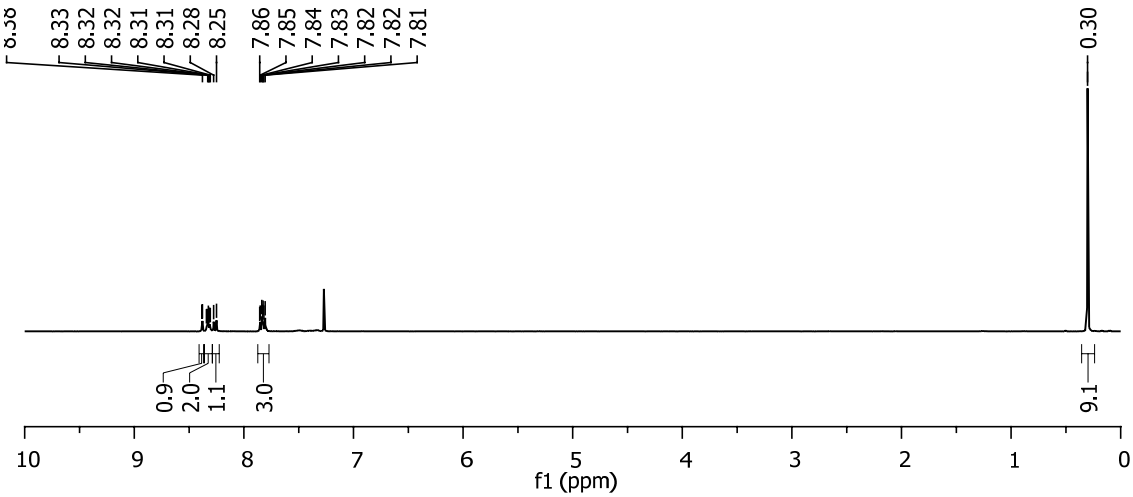

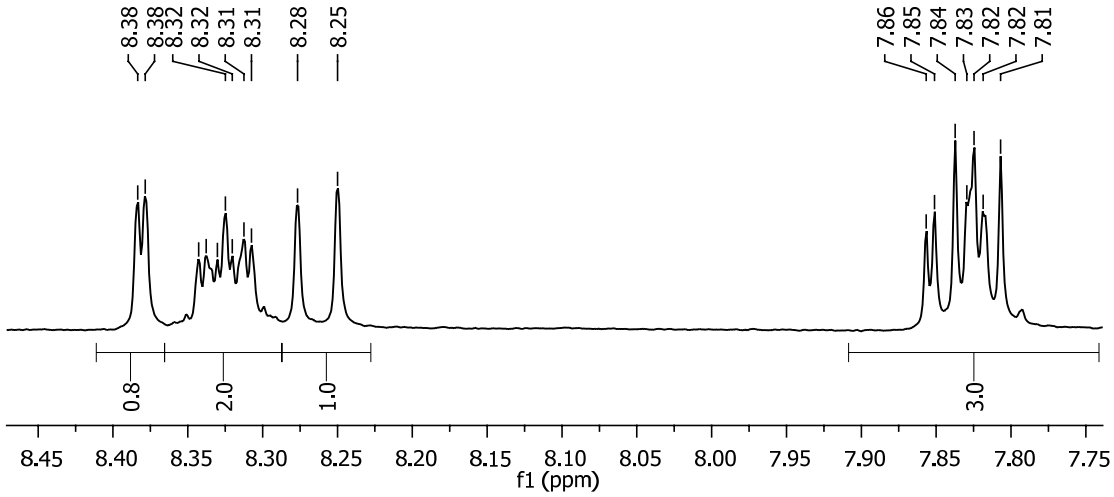

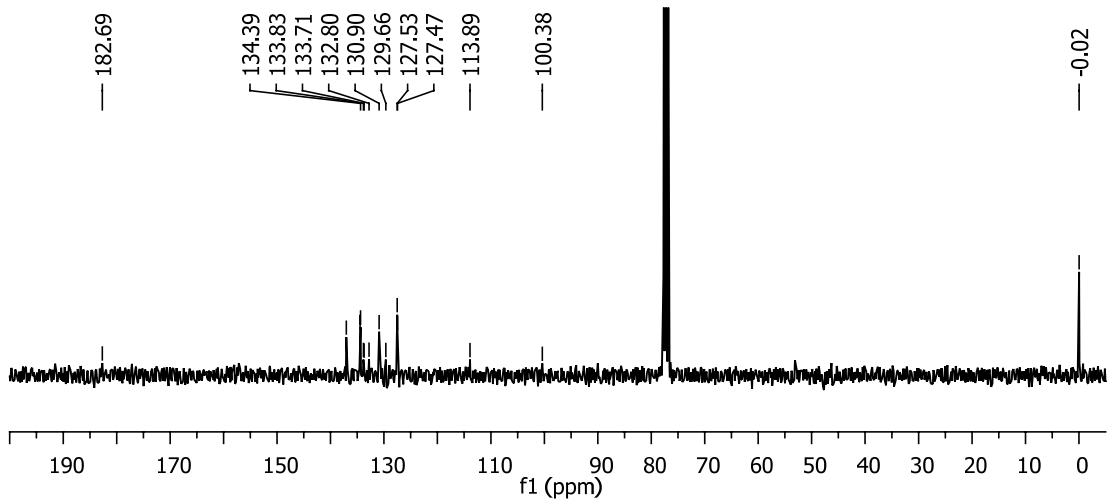

Synthesis of: 1-(2-ethylhexyloxy)-4-hydroxyanthraquinone, ***17***

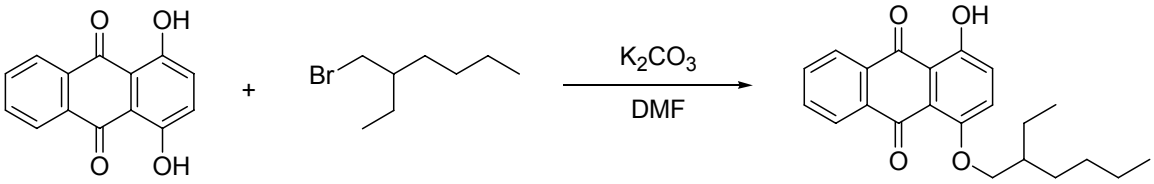

1,4-dihydroxyanthraquinone (3.48g, 14.5 mmol) and potassium carbonate (2.1g, 15.2 mmol) were dissolved in DMF (50mL) and heated to 130°C for 20 min. Racemic 2-ethylhexyl bromide (2.71mL, 15.2 mmol) was added to the hot solution and stirred for 24hrs. Water (20mL) and 3M HCl was added until acidic, and the resultant precipitate was collected by vacuum filtration. The crude product was purified by column chromatography on silica (toluene:hexanes:ethyl acetate, 1:1:0 to 1:1:0.05, R_f = 0.05 to 0.57). Yield: 2.26g (44.2%). Melting point: 54-58°C. Anal. calcd for $C_{22}H_{24}O_4$, %: C, 74.9; H, 6.9. Found, %: C, 75.1; H, 6.8. ^{1}H NMR (300 MHz, $CDCl_3$) δ 13.05 (s, 1H), 8.30 (td, *J* = 1.6, 7.6, 2H), 7.81 – 7.73 (m, 2H), 7.41 (d, *J* = 9.4, 1H), 7.33 – 7.28 (m, 1H), 4.12 – 3.94 (m, 2H), 1.98 – 1.80 (m, 1H), 1.72 – 1.49 (m, 5H), 1.44 – 1.28 (m, 5H), 1.05

– 0.83 (m, 7H). ^{13}C NMR (300 MHz, $CDCl_3$) δ 189.58, 181.13, 155.33, 154.10, 153.59, 135.36, 135.05, 134.56, 133.42, 133.19, 132.80, 132.51, 127.60, 126.98, 126.67, 126.56, 123.48, 121.79, 119.74, 116.60, 72.94, 39.70, 39.66, 30.49, 30.45, 29.26, 23.88, 23.26, 14.34, 11.27. IR (KBr), υ_{max}/cm^{-1}: 1669 (conj. C=O), 1642 (conj. C=O), 1265 (aryl C-O), 1237 (aryl C-O), 1010 (alkyl C-O).

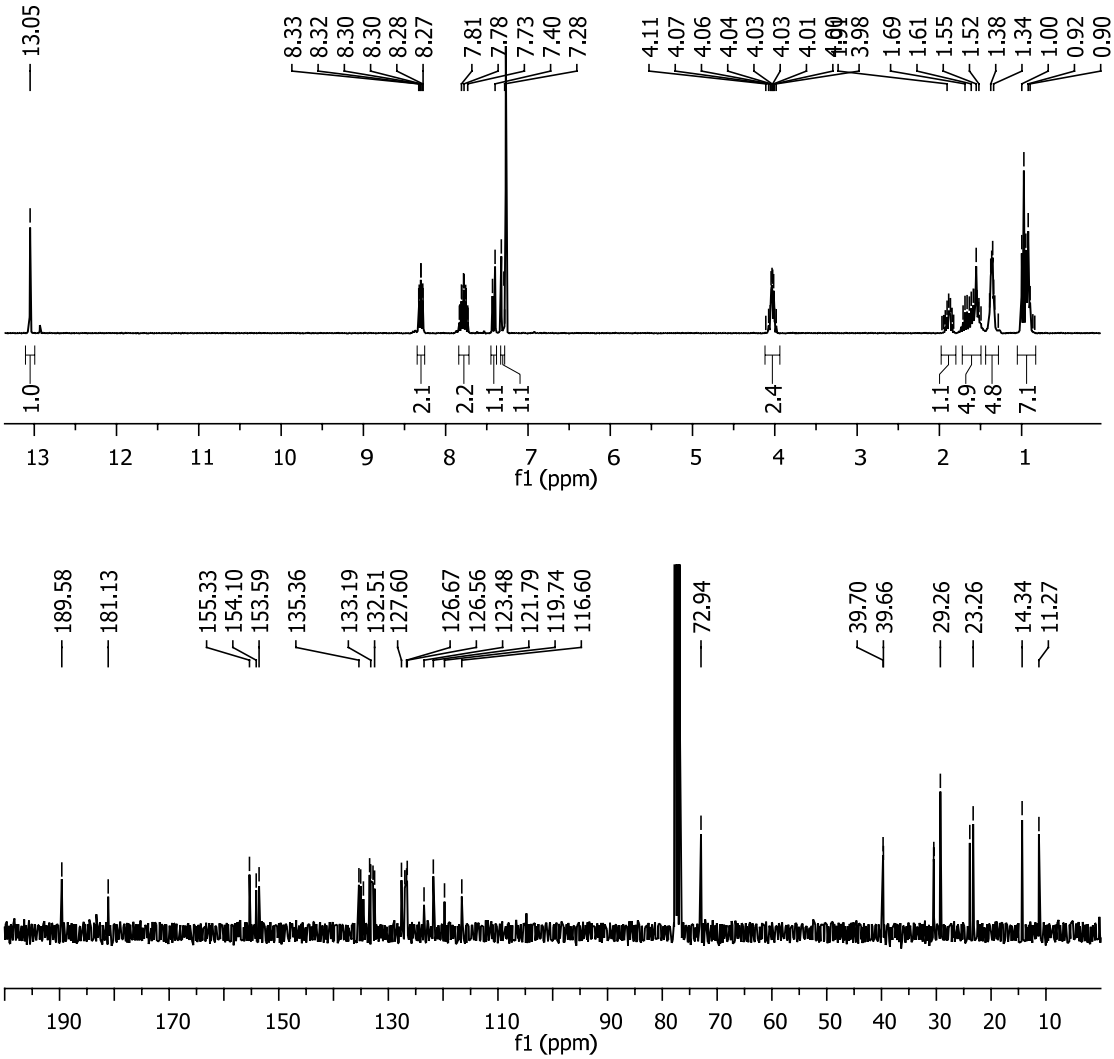

Synthesis of: 9-(2-hydroxyethyl)adenine, ***14***[44,80-82]

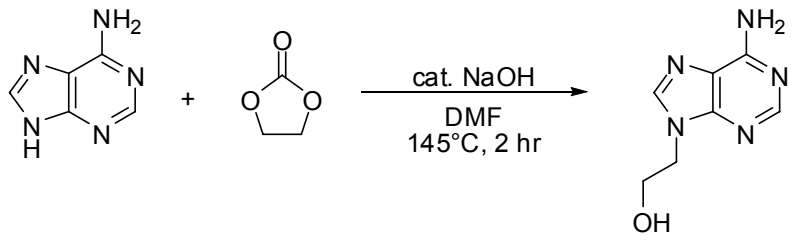

Adenine (0.504g, 3.73 mmol) and ethylene carbonate (0.332g, 3.76 mmol) in DMF (10mL) was brought to reflux (145°C) before adding NaOH (~10mg). After the mixture stirred for 2 hrs, the solvent was removed *in vacuo* and the crude product was taken up in 95% ethanol. The mixture was filtered through Celite, and the solution volume was reduced to 15mL and crystallized at -30°C. Yield: 0.45g (67.3%). ^{1}H NMR (300 MHz, DMSO-d_6) δ 8.13 (s, 1H), 8.07 (s, 1H), 7.17 (s, 2H), 5.02 (s, 1H), 4.18 (t, J = 5.4, 2H), 3.73 (t, J = 5.3, 2H). ^{13}C NMR (100 MHz, D_2O) δ 154.6, 151.6, 148.0, 142.2, 117.6, 59.4, 45.9.

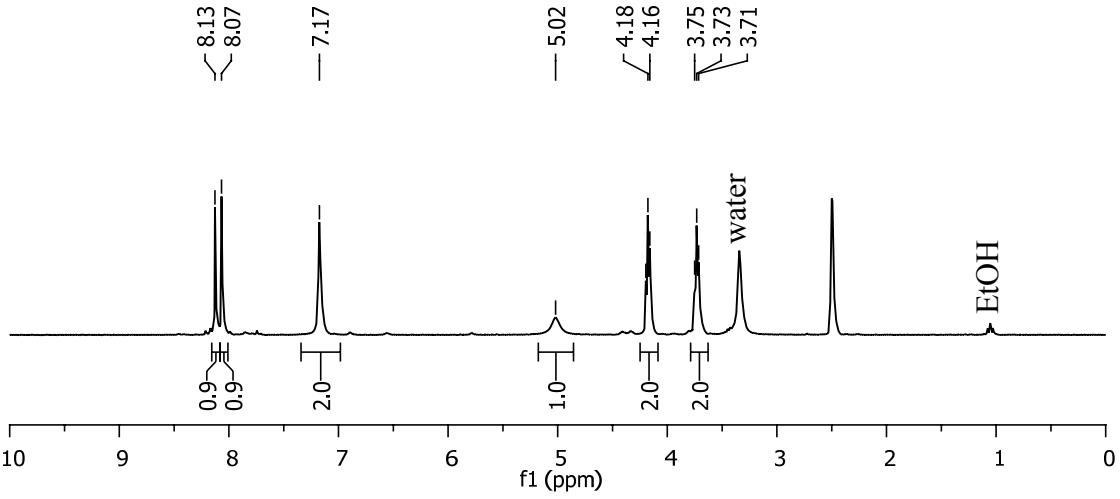

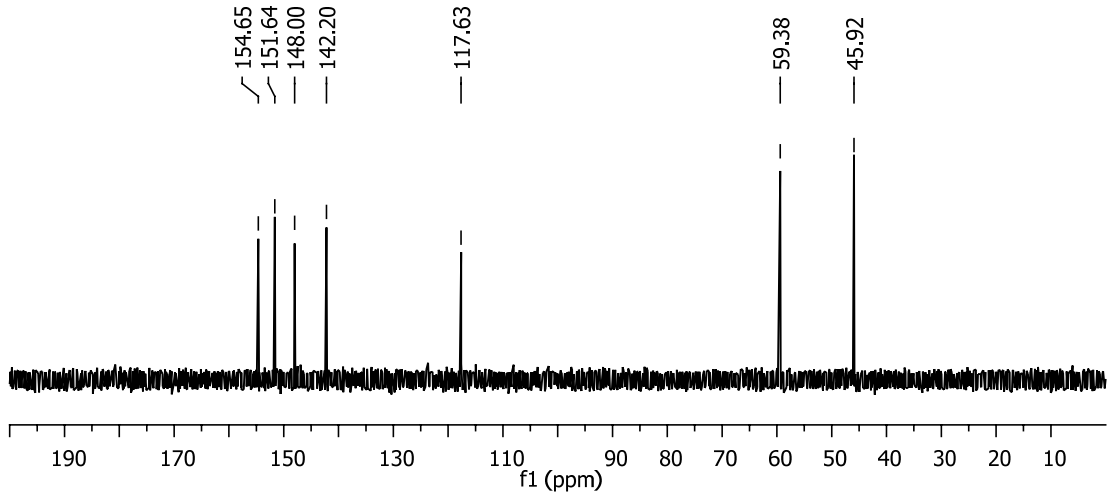

Synthesis of: 1-(2-hydroxyethyl)cytosine, ***47***[44,80-82]

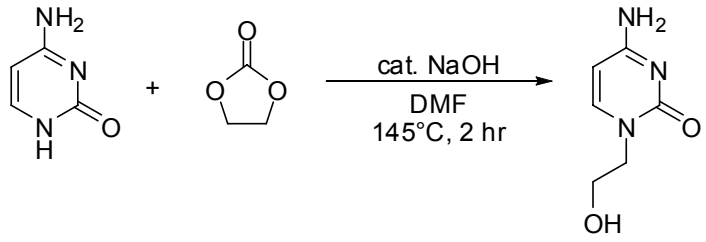

Cytosine (0.403g, 3.26 mmol) and ethylene carbonate (0.585g, 6.64 mmol) in DMF (50mL) were brought to reflux (145°C) before adding NaOH (~10mg). After the mixture stirred for 2 hrs, the solvent was removed *in vacuo* and the crude product was taken up in 95% ethanol. The mixture was filtered through Celite, and the solution volume was reduced to 15mL and crystallized at -30°C. Yield: 0.314g (62.1%). ^{1}H NMR (300 MHz, DMSO-d_6) δ 7.47 (d, J = 6.5, 1H), 6.93 (s, 2H), 5.60 (d, J = 7.1, 1H), 4.80 (t, J = 4.7, 1H), 3.67 (t, J = 5.0, 2H), 3.53 (dd, J = 5.0, 10.1, 2H).^{13}C NMR (100 MHz, DMSO-d_6) δ 166.01, 155.87, 146.94, 92.50, 58.91, 51.35.

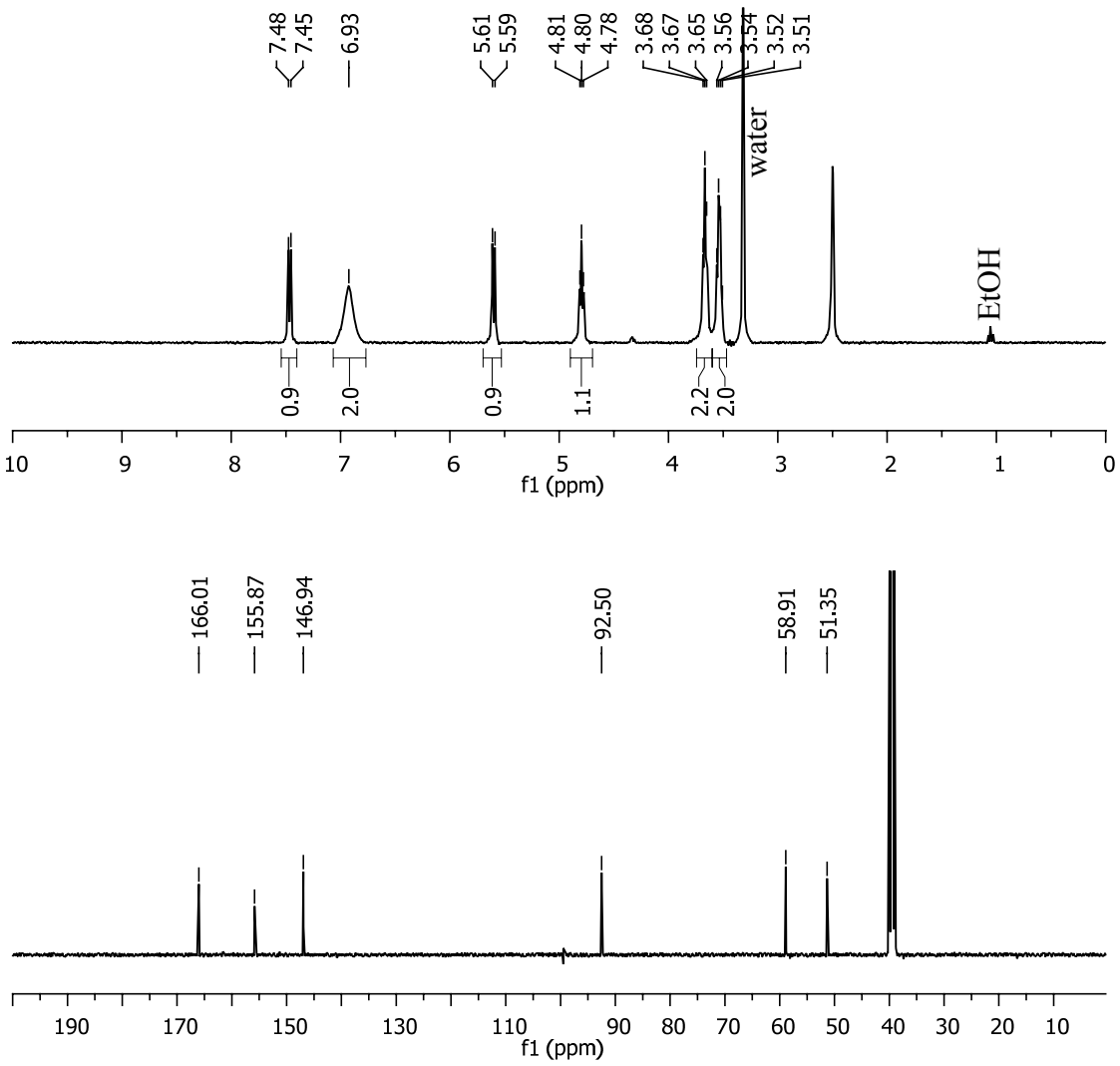

Synthesis of: 3-benzoylthymine, ***24***[46,47]

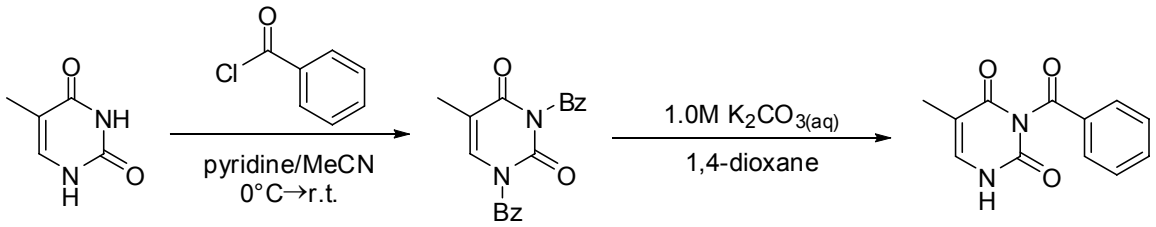

To a slurry of thymine (1.147g, 9.10 mmol) in pyridine (6.5mL) and MeCN (15.5mL) at 0°C was slowly added benzoyl chloride (2.32mL, 20.0mL) and stirred for 24 hr. The solvent was removed *in vacuo*, and the crude solid was taken up in methylene chloride (100mL) which was then washed with water (100mL). The solvent was removed *in vacuo*, and to the crude solid was added 1.0M K_2CO_3 (80mL) and 1,4-dioxane (80mL). The two-phase mixture was stirred for 18 hr, and AcOH was then added until acidic. The solvent of the organic layer was removed *in vacuo*, and the crude solid was crystallized in acetone to yield colorless crystalline needles. Yield: 1.750g (7.60 mmol, 83.5%). ^{1}H NMR (300 MHz, $CDCl_3$) δ 7.95 (dd, *J* = 8.3, 1.2 Hz, 2H), 7.69 (tt, *J* = 7.4, 1.2 Hz, 1H), 7.53 (t, *J* = 7.7 Hz, 2H), 7.05 (d, *J* = 1.2 Hz, 1H), 1.93 (d, *J* = 1.1 Hz, 3H). ^{13}C NMR (75 MHz, $CDCl_3$) δ 169.05, 163.48, 151.89, 136.47, 135.47, 131.64, 130.72, 129.46, 111.16, 12.50.

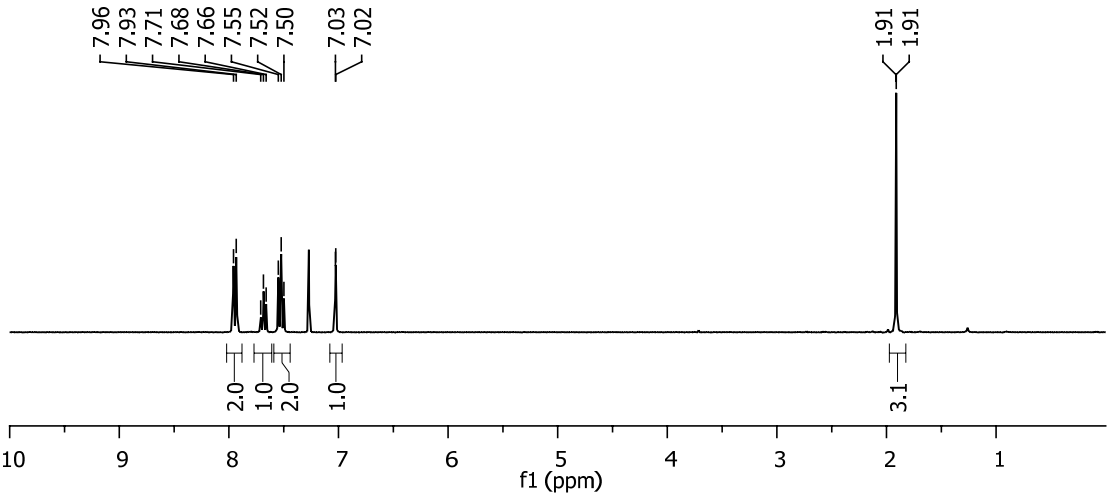

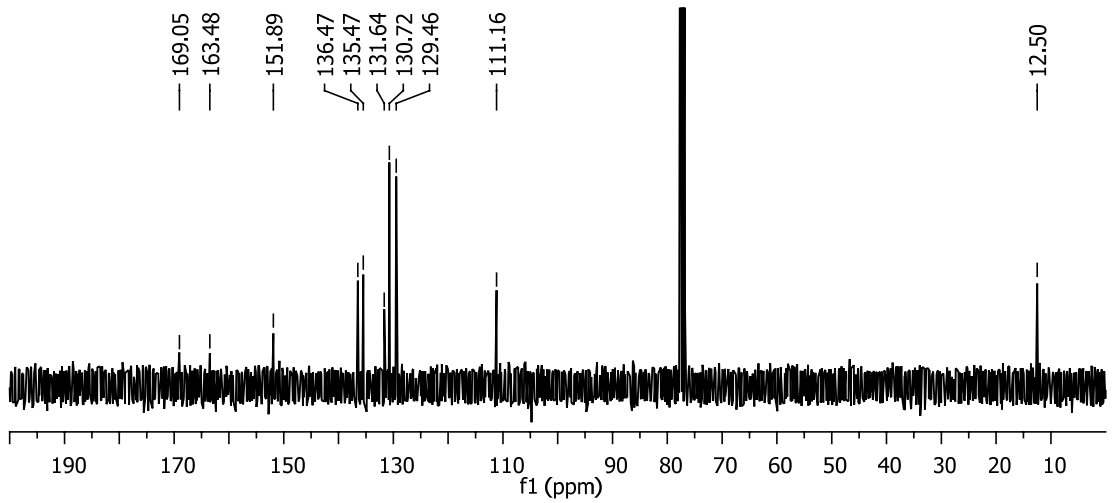

Synthesis of: 3-benzoyl-1-(2-bromoethyl)thymine, ***50***[44]

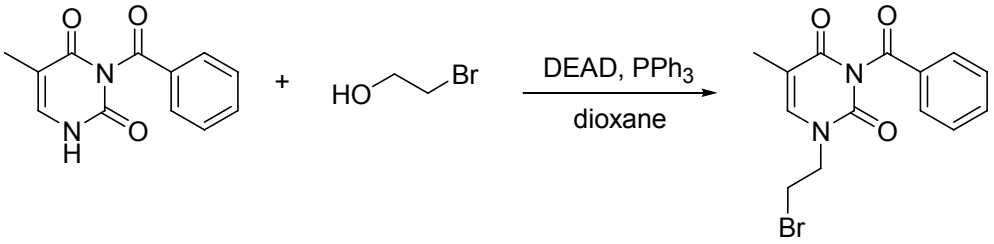

3-benzoylthymine (2.01g, 8.73 mmol), 2-bromoethanol (0.68mL, 9.60 mmol), and triphenylphosphine (2.52g, 9.60 mmol) were dissolved in dioxane (90 mL). Diethyl azodicarboxylate (1.51mL, 9.60 mmol) was slowly added to the solution and was stirred for 18 hrs. The dioxane was removed *in vacuo* and the residue was taken up in toluene (30mL). This organic solution was washed with saturated sodium bicarbonate (2 x 20mL) and water (20mL). The organic layer was dried over $MgSO_4$ and evaporated *in vacuo*. The crude product was purified by column chromatography on silica (toluene:ethyl acetate, 1:1, $R_f = 0.53$). Yield: 1.35g (45.9%). ^{1}H NMR (300 MHz, $CDCl_3$) δ 7.93 (d, J = 7.2, 2H), 7.67 (t, J = 7.4, 1H), 7.51 (t, J = 7.7, 2H), 7.17 (d, J = 1.2, 1H), 4.13 (t, J = 5.8,

2H), 3.68 (t, J = 5.8, 2H), 1.99 (t, J = 1.0, 3H). ^{13}C NMR (75 MHz, $CDCl_3$) δ 168.95, 163.26, 149.84, 140.94, 135.31, 131.67, 130.64, 129.40, 110.65, 51.03, 29.55, 12.60.

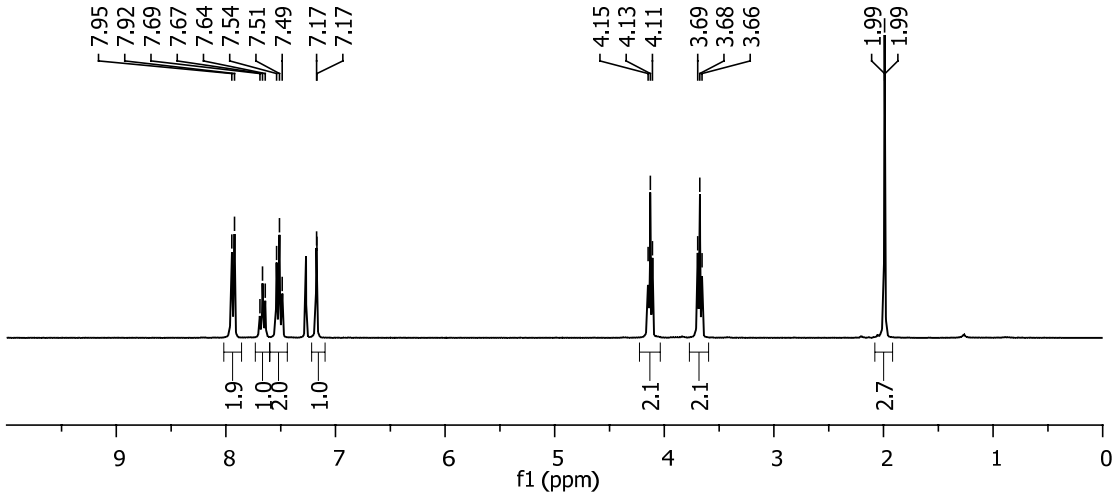

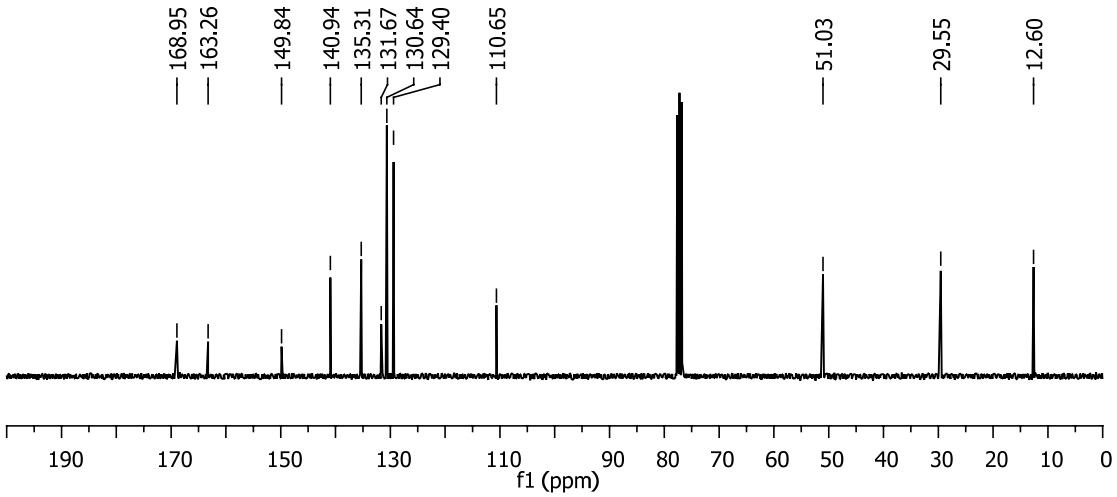

Synthesis of: 3-benzoyl-1-(2-(nitrooxy)ethyl)thymine, ***51***[84]

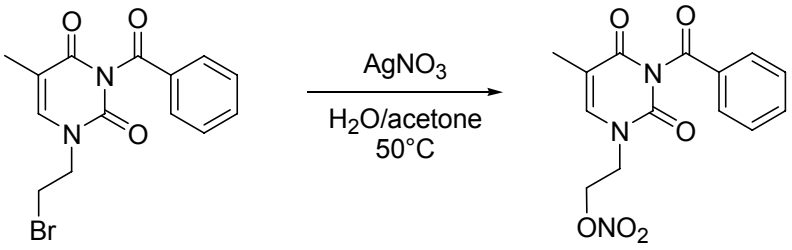

3-benzoyl-1-(2-bromoethyl)thymine (1.30g, 3.86mmol) and silver nitrate (1.10g, 6.50mmol) were dissolved in acetone (10.5mL) and water (2.5mL). The solution was heated to 50°C and stirred for 18 hrs. The reaction was quenched with 10% sodium chloride (5.0mL), and all precipitate was removed by vacuum filtration through celite and rinsed with acetone (10.0mL). The solvent volume was reduced to approximately 80% *in vacuo*, and ethyl acetate (20mL) and saturated sodium bicarbonate (20mL) were added to the remaining solvent mixture. The organic layer was then separated and dried *in vacuo*, and purified by column chromatography on silica (hexanes:ethyl acetate, 1:2, $R_f = 0.63$) to yield a viscous, golden oil that solidified upon standing for 18 hrs. Yield: 0.622g (1.95 mmol, 50.5%). Melting point: 98-107°C. ^{1}H NMR (300 MHz, $CDCl_3$) δ 7.94 (d, $J = 7.4$, 2H), 7.67 (t, $J = 7.4$, 1H), 7.52 (t, $J = 7.8$, 2H), 7.08 (d, $J = 1.1$, 1H), 4.84 – 4.65 (m, 2H), 4.16 – 4.00 (m, 2H), 1.98 (d, $J = 0.9$, 3H). ^{13}C NMR (75 MHz, $CDCl_3$) δ 168.79, 163.08, 149.98, 139.99, 135.41, 131.60, 130.70, 129.43, 111.78, 70.11, 46.83, 12.64. IR (KBr), υ_{max}/cm^{-1}: 3073 (C=C), 1752 (C=O), 1687 (C=O), 1643 (NO_3), 1377 (C-N), 1356 (C-N), 1280 (NO_3). HRMS (EI, 70 eV) *m/z*: M^+ calcd for $C_{14}H_{13}N_3O_6$, 319.0804; found 319.0806.

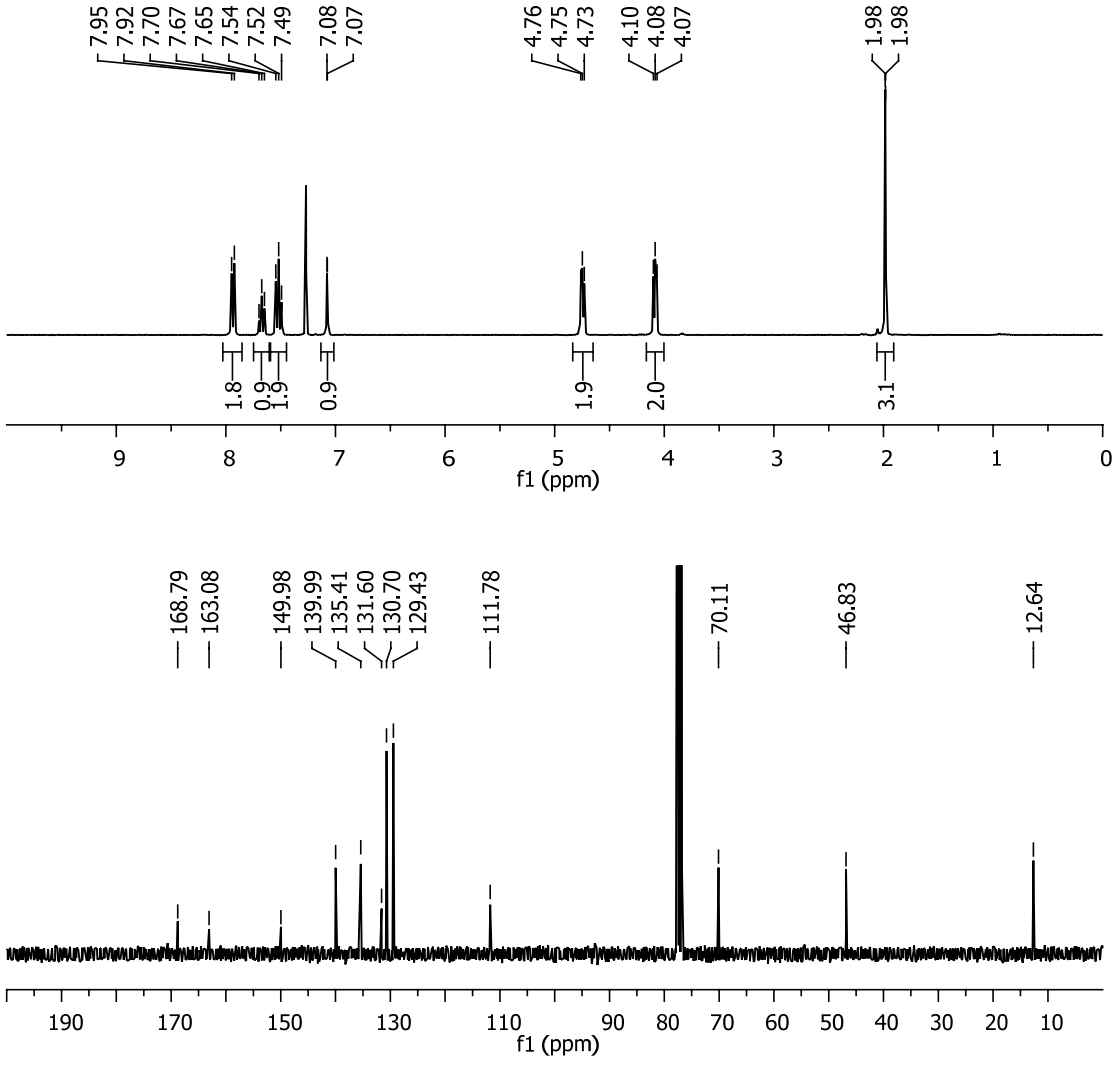

Synthesis of: 3-benzoyl-1-(2-hydroxyethyl)thymine, ***52***

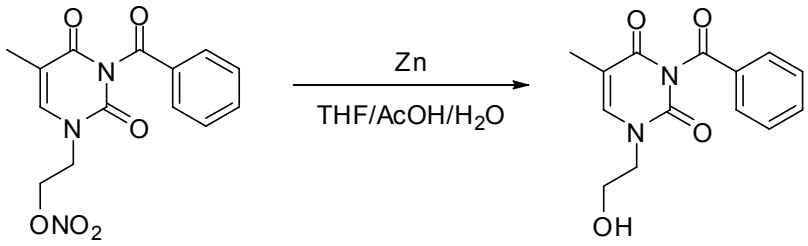

Zinc (0.407g, 6.23 mmol) was added in portions to a solution of 3-benzoyl-1-(2-(nitrooxy)ethyl)thymine (0.497g, 1.58 mmol) in THF (27mL), acetic acid (5.4mL) and

water (1.1mL) over 2 hrs. The resultant zinc salts were removed by vacuum filtration, which were then rinsed with chloroform (20mL). The volume of the filtrate was reduced *in vacuo* (10mL) and taken up in chloroform (20mL). This organic layer was washed with water (2 x 20mL), saturated sodium bicarbonate (20mL) and water (20mL), and then dried over $MgSO_4$ and the solvent was removed *in vacuo*. The crude product was crystallized in hot ethyl acetate. Yield: 0.224g (51.6%). Melting point: 157-159°C. Anal. calcd for $C_{14}H_{14}N_2O_4$, %: C, 61.3; H, 5.1; N, 10.2. Found, %: C, 61.3; H, 5.3; N, 10.1. ^{1}H NMR (300 MHz, $CDCl_3$) δ 7.94 (d, *J* = 7.3, 2H), 7.66 (t, *J* = 7.4, 1H), 7.50 (t, *J* = 7.7, 2H), 7.23 (d, *J* = 1.0, 1H), 3.92 (d, *J* = 2.4, 4H), 1.97 (s, 4H). ^{13}C NMR (100 MHz, $CDCl_3$) δ 169.24, 163.43, 150.50, 141.57, 135.22, 131.86, 130.68, 129.36, 110.51, 61.20, 51.21, 12.59. IR (KBr), υ_{max}/cm^{-1}: 3487 (O-H), 3089 (C=C), 1741 (C=O), 1685 (C=O), 1653 (C=O), 1636 (C=O), 1358 (C-N), 1349 (C-N).

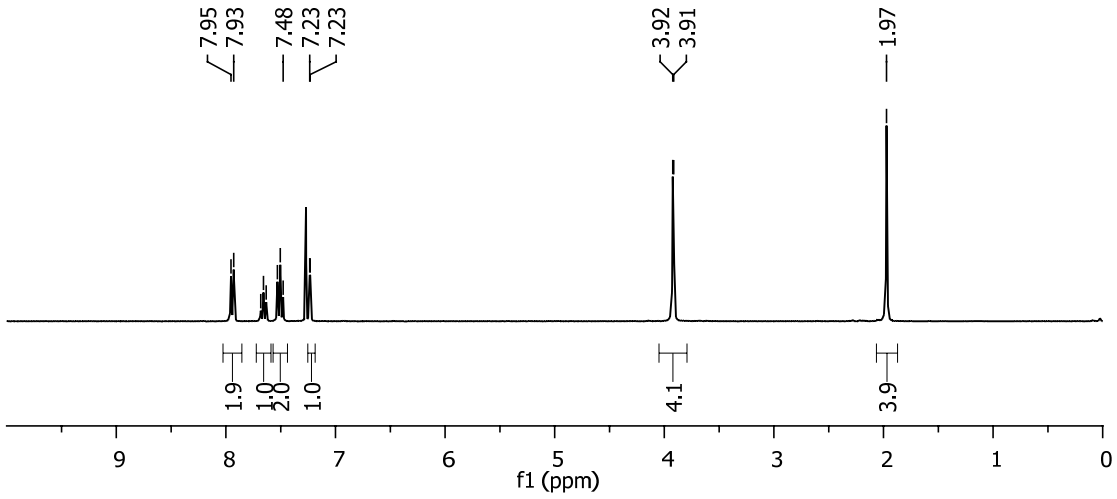

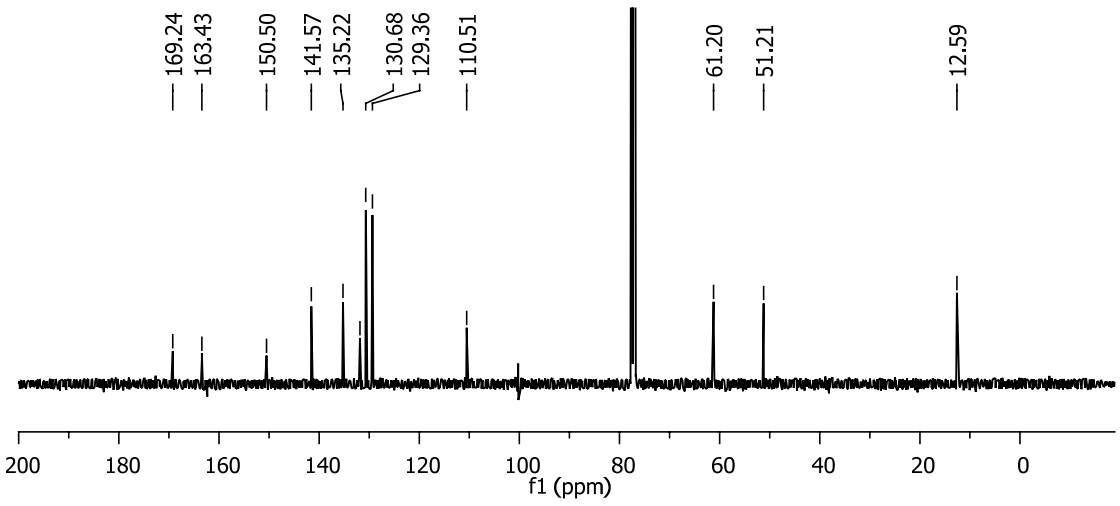

Synthesis of: 5-(ethoxycarbonyl)-3,4-dimethylpyrrole-2-carboxylic acid, ***37***[76]

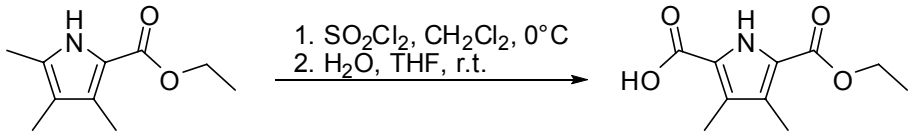

Ethyl 3,4,5-trimethylpyrrole-2-carboxylate (3.58g, 19.8 mmol) was dissolved in diethyl ether (250mL) at 0°C. Sulfuryl chloride (4.80mL, 59.3 mmol) was added dropwise and stirred for 30 min. at 0°C before removing the ice bath. The mixture was then stirred for an additional 5 hrs at room temperature. The solvent was removed *in vacuo*, and the oily residue was taken up in THF (125mL) and water (85mL). The solution was allowed to react for 18 hrs. To this mixture was added ethyl acetate (150mL) and 10% NaCl (100mL). The organic layer was separated and was then reduced *in vacuo*, leaving a small amount of water and the crude product. This mixture was taken up in acetone (30 mL) to make a uniform solution. Water (100mL) was then slowly added to precipitate the product, which was then collected by vacuum filtration. Yield: 3.500g (83.7%).[1]H NMR (300 MHz, DMSO-d_6) δ 12.70 (s, 1H), 11.25 (s, 1H), 4.23 (q, J = 7.1, 2H), 2.17 (s, 7H),

1.29 (t, J = 7.1, 3H). ^{13}C NMR (300 MHz, DMSO-d_6) δ 161.98, 160.42, 125.82, 125.48, 122.50, 121.25, 59.71, 14.14, 9.83, 9.81.

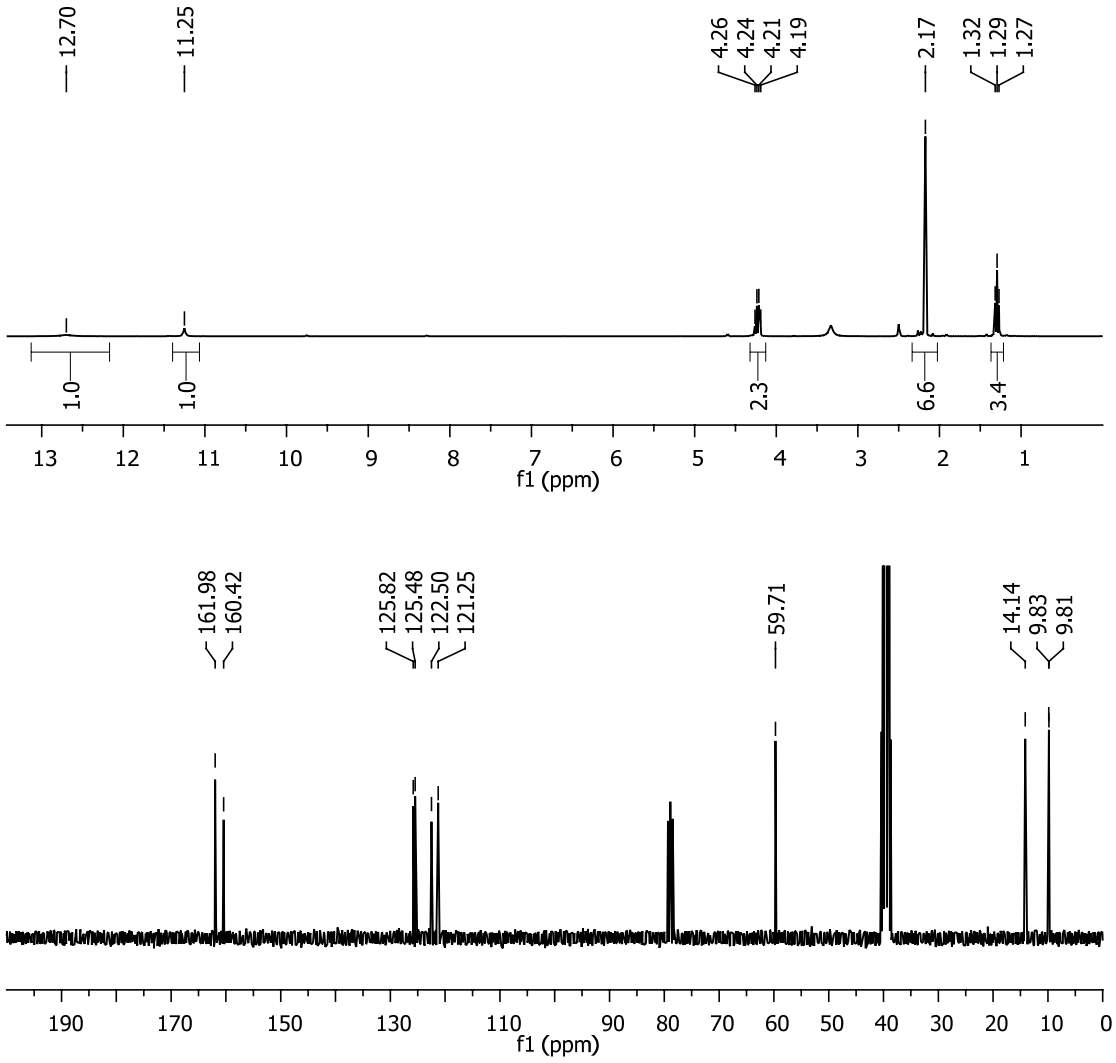

Synthesis of: 1-(2-(adenine-9-yl)ethoxy)-4-(2-ethylhexyloxy)anthraquinone, ***66***

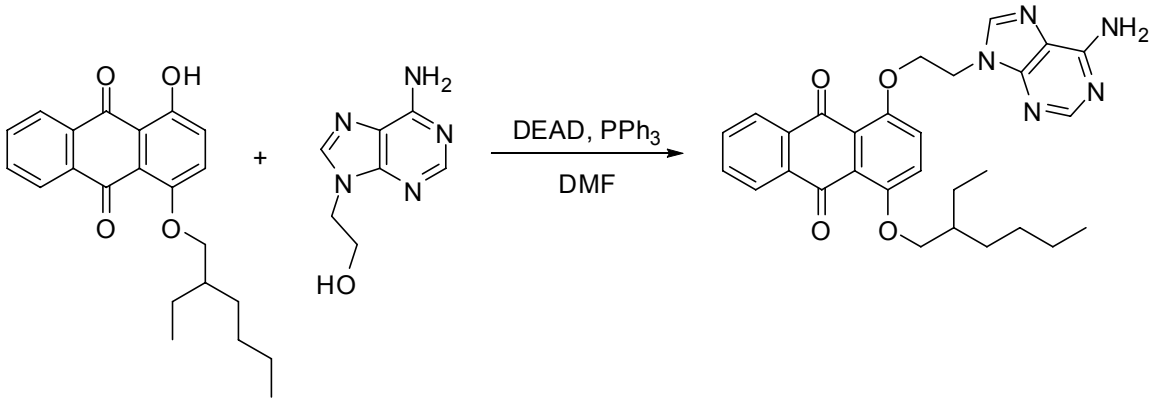

Diethyl azodicarboxylate (87µL, 0.55 mmol) was added to a solution of triphenylphosphine (0.144g, 0.553 mmol) and 9-(2-hydroxyethyl)adenine (99mg, 0.553 mmol) in DMF (4.0mL). To this mixture, a solution of 1-(2-ethylhexyloxy)-4-hydroxyanthraquinone (0.177g, 0.503 mmol) in DMF (2.0mL) was added slowly and allowed to stir for 18 hrs. The volume of the mixture was reduced *in vacuo*, and then purified by column chromatography on silica (toluene:acetone:methanol, 20:20:1, R_f = 0.24). Yield: 0.149g (57.9%). Melting point: 238-243°C. Anal. calcd for $C_{29}H_{31}N_5O_4$, %: C, 67.8; H, 6.1; N, 13.6. Found, %: C, 67.5; H, 6.3; N, 13.3. ^{1}H NMR (300 MHz, $CDCl_3$) δ 8.66 (s, 1H), 8.37 (s, 1H) 8.22-8.15 (m, 2H), 7.75-7.69 (m, 2H), 7.27 (d, *J* = 9.4, 1H), 7.15 (d, *J* = 9.4, 1H), 5.62 (s, 2H), 4.77 (t, *J* = 4.6, 2H), 4.38 (t, *J* = 4.7, 2H), 3.99-3.92 (m, 2H), 1.86 (p, *J* = 6.0, 1H), 1.72-1.45 (m, 4H), 1.35-1.26 (m, 4H), 0.97-0.88 (m, 6H). ^{13}C NMR (100 MHz, $CDCl_3$) δ 183.45, 182.80, 155.59, 154.96, 153.03, 152.24, 150.13, 143.39, 134.49,134.19, 133.61, 133.37, 126.70, 126.62, 123.68, 123.42, 121.54, 121.47, 119.64, 77.43, 72.83, 68.57, 43.26, 39.59, 30.45, 29.22, 23.86, 23.22, 14.31, 11.23. IR (KBr), υ_{max}/cm^{-1}: 3293 (N-H), 3122 (N-H), 1669 (C=O), 1320 (C-N), 1270 (C-N), 1244 (C-N).

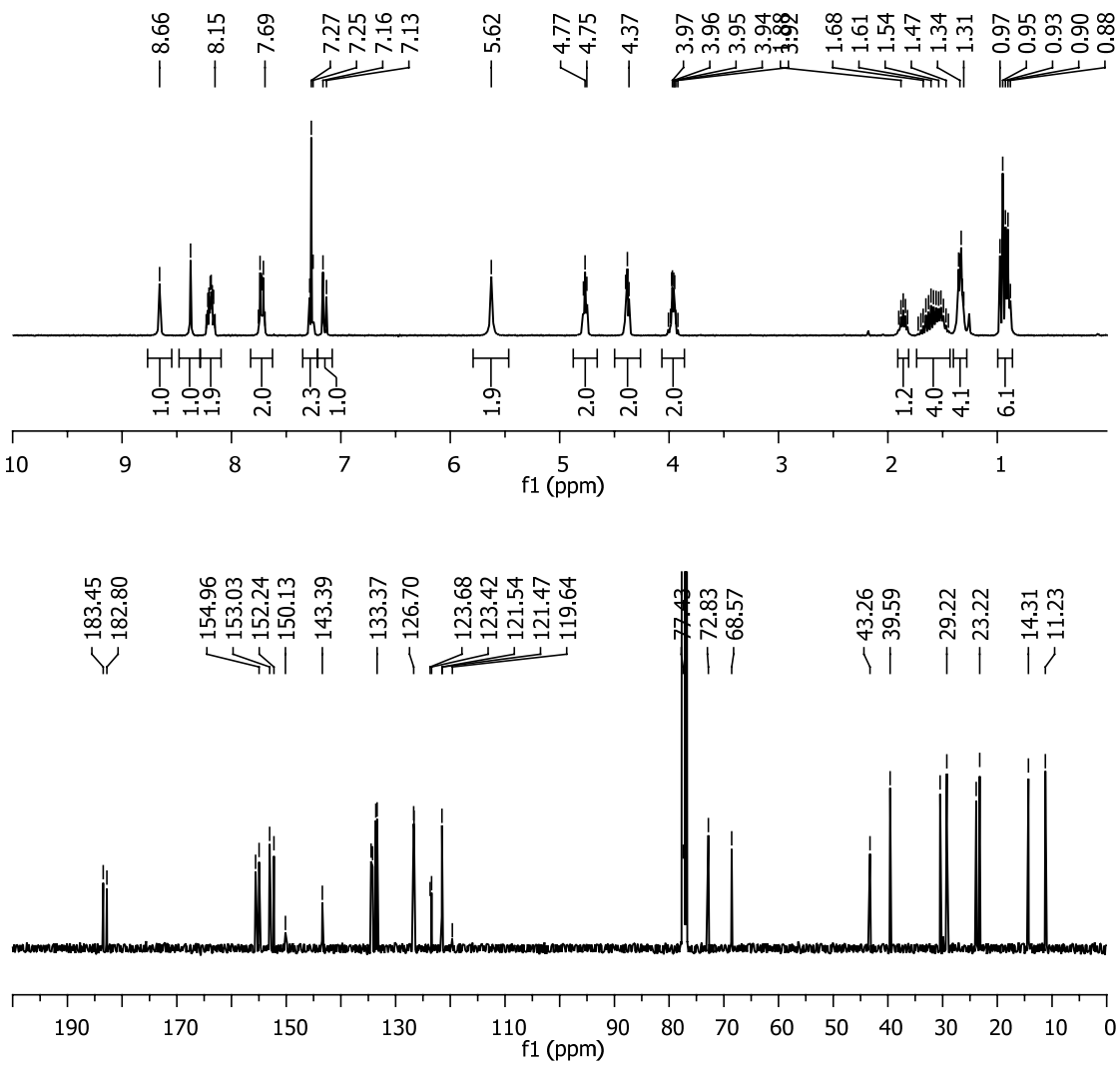
8.66
8.15
7.69
7.27
7.25
7.16
7.13
5.62
4.77
4.75
4.37
3.97
3.96
3.95
3.94
1.68
1.61
1.54
1.47
1.34
1.31
0.97
0.95
0.93
0.90
0.88
1.0
1.0
1.9
2.0
2.3
1.0
1.9
2.0
2.0
2.0
1.2
4.0
4.1
6.1
10
9
8
7
6
5
4
3
2
1
f1 (ppm)
183.45
182.80
154.96
153.03
152.24
150.13
143.39
133.37
126.70
123.68
123.42
121.54
121.47
119.64
77.43
72.83
68.57
43.26
39.59
29.22
23.22
14.31
11.23
190
170
150
130
110
90
80
70
60
50
40
30
20
10
0
f1 (ppm)

Synthesis of: 1-(2-(3-benzoylthymine-1-yl)ethoxy)-4-(2-ethylhexyloxy)anthraquinone, ***67***

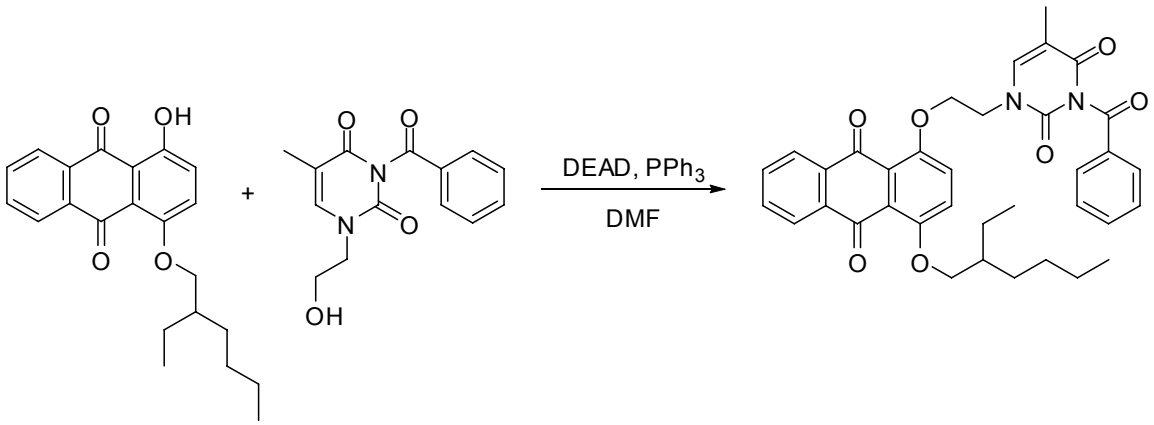

Diethyl azodicarboxylate (0.11mL, 0.682 mmol) was slowly added to a solution of triphenylphosphine (0.179g, 0.682 mmol), 1-(2-ethylhexyloxy)-4-hydroxyanthraquinone (0.219g, 0.620 mmol), and 3-benzoyl-1-(2-hydroxyethyl)thymine (0.170, 0.620 mmol) in THF (6.2mL), and allowed to stir for 18 hrs at room temperature. Brine (20mL) was added to the mixture and the crude product was extracted with methylene chloride (2 x 25mL). The organic layers were then dried over $MgSO_4$ and the solvents were removed *in vacuo*. The remaining residue was purified by column chromatography on silica (toluene:hexanes:ethyl acetate, 1:1:2, R_f = 0.56). Yield: 0.248g (65.8%). Melting point: 170-175°C. ^{1}H NMR (300 MHz, $CDCl_3$) δ 8.25 – 8.18 (m, 1H), 8.15 (d, *J* = 5.5, 2H), 7.97 (d, *J* = 7.3, 2H), 7.78 – 7.69 (m, 2H), 7.63 (t, *J* = 7.5, 1H), 7.46 (t, *J* = 7.8, 2H), 7.35 (d, *J* = 9.4, 1H), 7.24 (d, *J* = 9.4, 1H), 4.31 (s, 4H), 4.01 (dd, *J* = 2.3, 5.7, 2H), 2.06 (s, 3H), 1.97 – 1.81 (m, 1H), 1.77 – 1.44 (m, 4H), 1.44 – 1.26 (m, 4H), 0.96 (dd, *J* = 8.0, 15.5, 6H). ^{13}C NMR (101 MHz, $CDCl_3$) δ 183.53, 182.79, 169.50, 163.70, 154.92, 152.19, 150.36, 143.44, 135.12, 134.54, 134.20, 133.70, 133.42, 131.95, 130.72, 129.29, 126.82, 126.27, 123.40, 123.38, 121.74, 121.04, 110.09, 72.86, 68.19, 47.94, 39.59, 30.45, 29.23, 23.86, 23.24, 14.33, 12.49, 11.24. IR (KBr), υ_{max}/cm^{-1}: 3075 (C=C), 1746

(C=O), 1701 (C=O), 1668 (C=O), 1650 (C=O), 1348 (C-N), 1325 (C-N), 1262 (C-O), 1247 (C-O), 1008 (C-O), 981 (C-O). HRMS (EI, 70 eV) *m/z*: M^+ calcd for $C_{36}H_{36}N_2O_7$, 608.2523; found 608.2512.

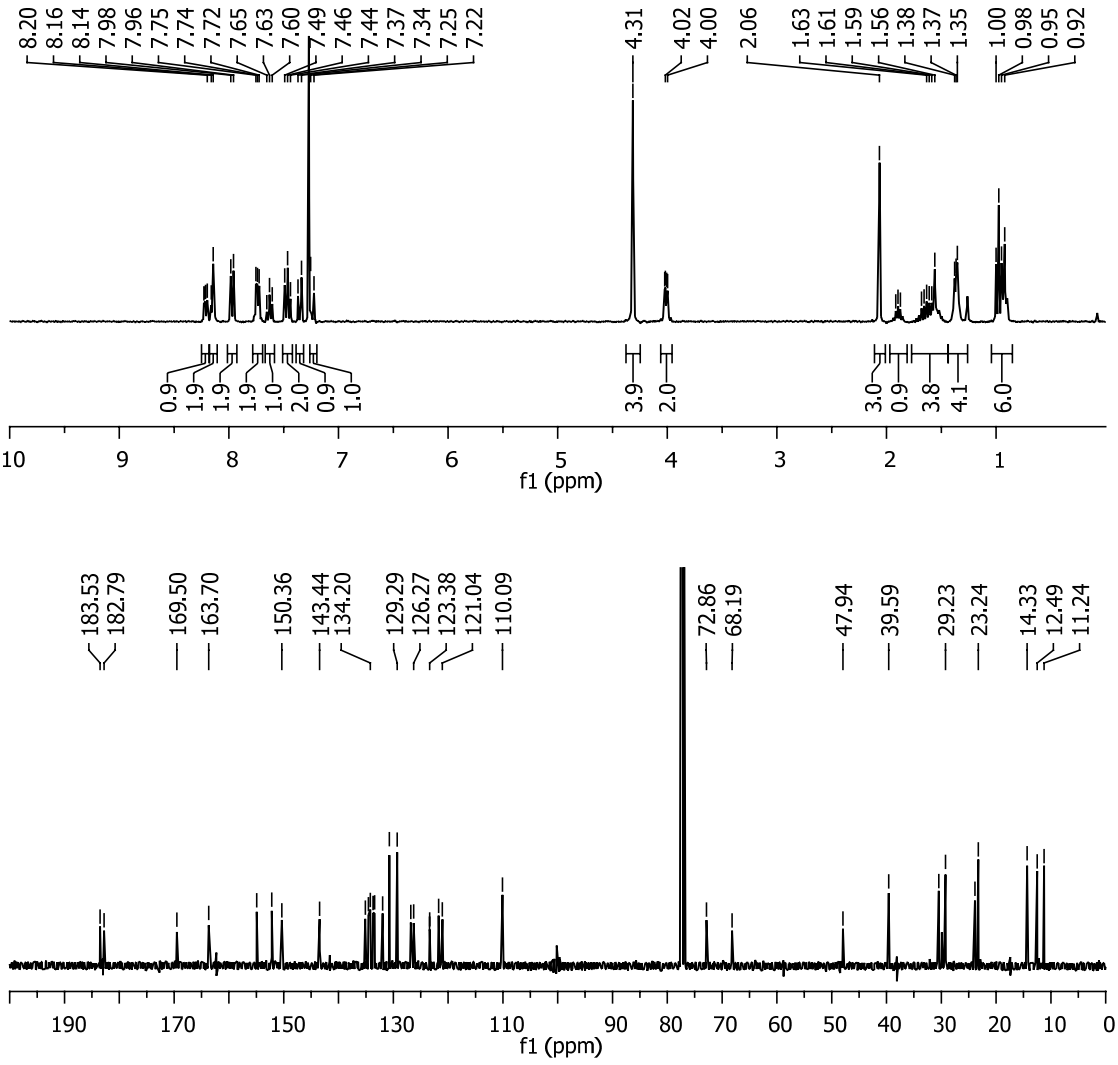

Synthesis of: 1-(2-(thymine-1-yl)ethoxy)-4-(2-ethylhexyloxy)anthraquinone, ***68***

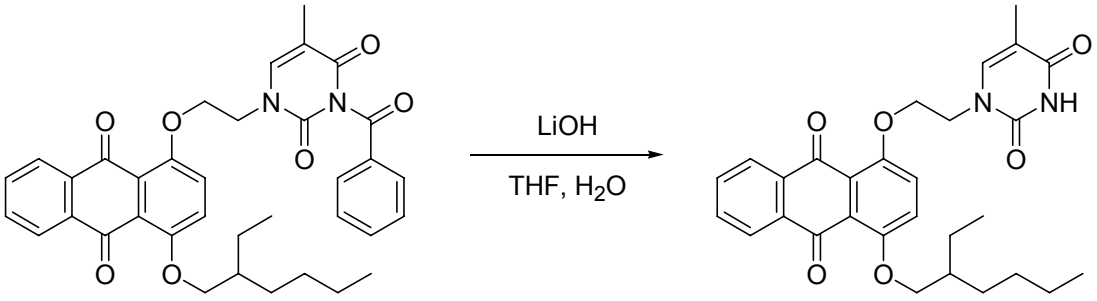

1-(2-(3-benzoylthymine-1-yl)ethoxy)-4-(2-ethylhexyloxy)anthraquinone (0.204g, 0.335 mmol) and LiOH (0.091 g, 0.368 mmol) were dissolved in THF (50mL) and water (20mL) and stirred for 8 hrs at 50°C. 5% NH_4Cl was added to the solution until a neutral pH was reached. The crude product was extracted with methylene chloride (3 x 50mL), and the combined organic extracts were washed with 1M $NaHCO_3$ (50mL) and 1M Na_2CO_3 (50mL). Yield: 0.148g (87.4%). Melting point: 227-231°C. ^{1}H NMR (400 MHz, $CDCl_3$) δ 8.57 (s, 1H), 8.19 (dd, J = 6.1, 3.0 Hz, 1H), 8.12 (dd, J = 6.1, 3.0 Hz, 1H), 8.02 (d, J = 1.1 Hz, 1H), 7.72 (dd, J = 5.3, 3.8 Hz, 2H), 7.33 (d, J = 9.4 Hz, 1H), 7.21 (d, J = 9.4 Hz, 1H), 4.28 (s, 4H), 4.06 – 3.93 (m, 2H), 2.02 (d, J = 0.9 Hz, 3H), 1.88 (m, 1H), 1.66 – 1.52 (m, 6H), 1.39 – 1.32 (m, 4H), 0.94 (m, 6H). ^{13}C NMR (101 MHz, $CDCl_3$) δ 183.42, 182.79, 164.47, 154.81, 152.31, 151.25, 143.69, 134.55, 134.24, 133.63, 133.39, 126.79, 126.28, 123.49, 123.28, 121.78, 120.68, 110.05, 77.43, 72.93, 68.17, 47.69, 39.63, 30.48, 29.24, 23.89, 23.24, 14.31, 12.39, 11.24. IR (KBr), υ_{max}/cm^{-1}: 3165 (N-H), 1689 (C=O), 1670 (C=O), 1651 (C=O), 1346 (C-N), 1316 (C-N), 1266 (C-O), 1240 (C-O), 1046 (C-O), 1023 (C-O). HRMS (EI, 70 eV) *m/z*: M^+ calcd for $C_{29}H_{32}N_2O_6$, 504.2260; found 504.2251.

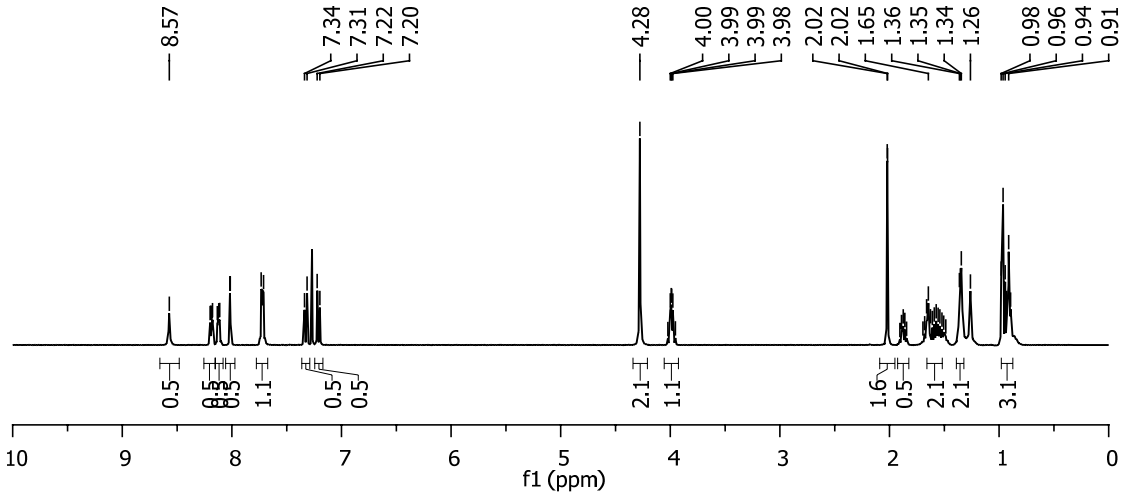
8.57
7.34
7.31
7.22
7.20
4.28
4.00
3.99
3.99
3.98
2.02
2.02
1.65
1.36
1.35
1.34
1.26
0.98
0.96
0.94
0.91
0.5
0.5
0.5
1.1
0.5
0.5
2.1
1.1
1.6
0.5
2.1
2.1
3.1
10
9
8
7
6
5
4
3
2
1
0
f1 (ppm)

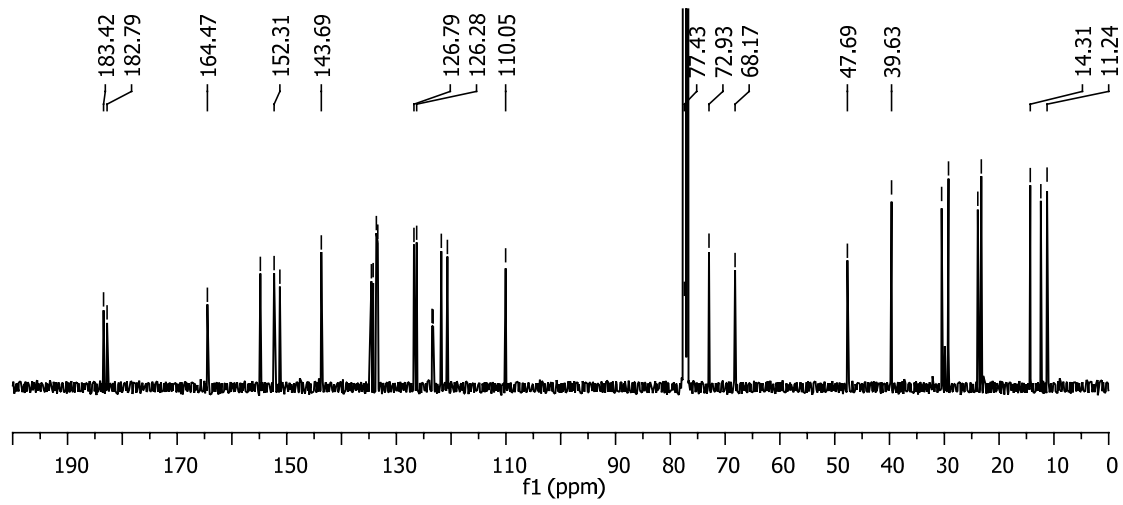
183.42
182.79
164.47
152.31
143.69
126.79
126.28
110.05
77.43
72.93
68.17
47.69
39.63
14.31
11.24
190
170
150
130
110
90
80
70
60
50
40
30
20
10
0
f1 (ppm)

Chapter Three: **Physical Properties**

3.1 Chapter goals

The purpose of this chapter is to describe the physical properties that were investigated of the functionalized AQ series. These experiments looked into the ability of the target molecules to HB, and their electrochemical properties. Recognition studies were performed using adenine-anthraquinone adduct **54** and thymine in THF. Cyclic voltammetry (CV) was also used to determine diffusion coefficients, and the rate of charge transfer.

3.2 Preliminary binding studies

3.2.1 Instrumentation

UV-vis spectra were measured from 300-800 nm in dry THF (inhibitor free) solutions in a 0.1cm quartz cell on a Cary5000 spectrometer.

3.2.2 Analysis

To investigate the binding capability of the adenine-thymine (A-T) pair, a preliminary study was performed with **54** and thymine which were dissolved in THF at varying concentrations. In theory, by the increasing concentration of thymine, there will be an increasing number of bound **54**·T species present. The bound species would have a

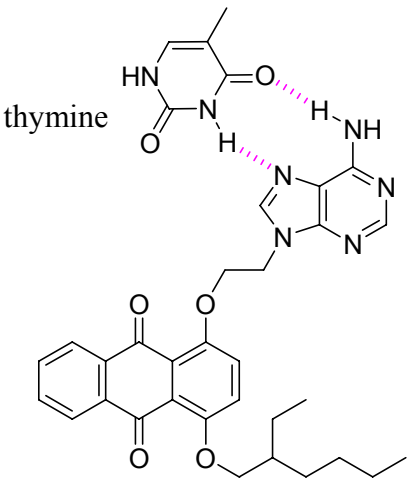

54

Scheme 3-1: The Watson-Crick binding between thymine and the adenine functionalized anthraquinone.

different absorbance profile than the unbound AQ derivative, such as the absorbance peak or the molar absorbtivity. With some manipulation by equations 3.1-3.5, this change allows for the binding constant to be evaluated.

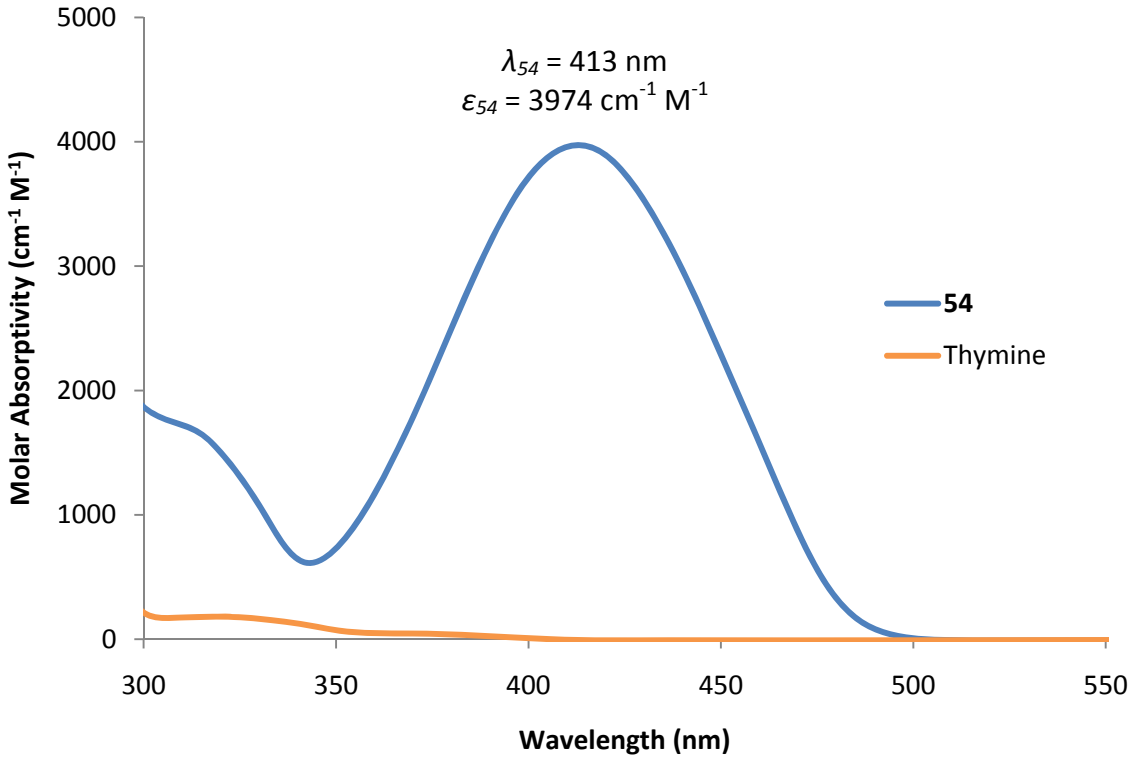

Figure 3-1: The visible spectra for a 0.128 mM solution of 54, and a 1.17 mM solution of thymine in THF.

The molar absorbtivity, ε_{54}, is determined using Beer's Law (equation 3.1),

$$A = \varepsilon \ell c \qquad (3.1)$$

Where A is absorption, ℓ is path length (cm), and c is sample concentration (M). The path length in this case is equal to 0.1cm. From equation 3.1, the molar absorbtivity of **54** at 413 nm (ε_{54}) is 3974 M^{-1} cm^{-1}. The molar extinction coefficient for adenine in water is 13 400 M^{-1}cm^{-1} at 261 nm, and the nucleobase does not absorb in the visible range.[105] Therefore the absorption from the compound 54 is due to the AQ moiety.

A number of solutions were prepared with a constant concentration of **54** and varying concentrations of thymine. The bound species, **54**·T, will have a different molar absorbtivity than **54** due to the altered electronic environment after HBing. The total absorption, A_t, is a sum of the absorption of all anthraquinone species present, **54** and **54**·T shown by equation 3.2.

$$\begin{aligned} A_t &= A_{54} + A_{54\cdot T} \\ A_t &= \varepsilon_{54} c_{54} \ell + \varepsilon_{54\cdot T} c_{54\cdot T} \ell \end{aligned} \tag{3.2}$$

Where A_{54} is the absorption resulting from the unbound anthraquinone species **54**, $A_{54\cdot T}$ is the absorption resulting from the HBed anthraquinone species **54** with thymine, c_{54} is the concentration of the unbound anthraquinone species **54**, $c_{54\cdot T}$ is the concentration of the HBed anthraquinone species **54** with thymine, and $\varepsilon_{54\cdot T}$ is the molar absorbtivity of the HBed anthraquinone species **54** with thymine.

The variable c_{54} is substituted using the following equation,

$$c_{54_0} = c_{54} + c_{54\cdot T} \tag{3.3}$$

Where c_{54o} is the initial concentration of the anthraquinone **54**. This equation is then rearranged to:

$$A_t = \varepsilon_{54} c_{54_0} \ell + (\varepsilon_{54\cdot T} - \varepsilon_{54}) c_{54\cdot T} \ell \tag{3.4}$$

The variable c_{54} from eq. 3.3 is also substituted into eq. 3.5, and is then rearranged to yield eq. 3.6.

$$K_a = \frac{c_{54\cdot T}}{c_{54} c_T} \tag{3.5}$$

Where K_a is the coefficient of absorption. Eq. 3.6 is solved using the quadratic formula (eq. 3.7).

$$0 = (c_{54\cdot T})^2 - \left(c_{54_0} + c_{T_0} + \frac{1}{K_a} \right) c_{54\cdot T} + c_{54_0} c_{T_0} \tag{3.6}$$

$$x = \frac{-b \pm \sqrt{b^2 - 4ac}}{2a} \tag{3.7}$$

In the current case, the ± operator in eq. 3.7, the minus sign must be chosen, otherwise $c_{54\cdot T}$, is greater than c_{54_o} which is impossible. The solved $c_{54\cdot T}$ is then substituted into eq. 3.4, and by iterating K_a, and ε_{54}, the total absorbance is calculated and fitted to the actual absorbance, as shown in Figure 3-2. This figure illustrates the difference between theory and observation.

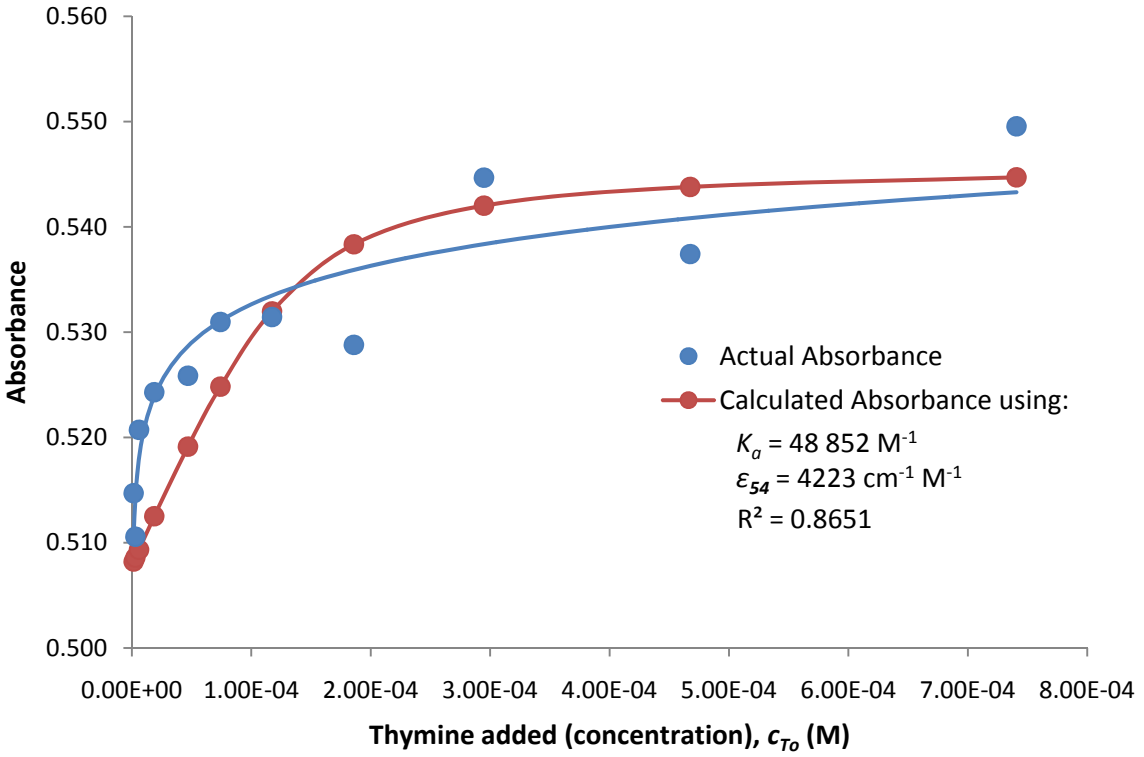

Figure 3-2: The closest fit for the actual and calculated absorbance measurements for the binding study of 54 and thymine in THF at 413 nm.

As can be seen in Figure 3-2, the calculated values were not able to be fitted to the actual values, indicating that the binding study of the two species is inconclusive. The actual

absorbance trend suggests a very strong binding between **54**·T, but this data implies that the **54** is bound with more thymine than is actually available due to the very sharp incline of the fitted curve at the low concentrations. The poor fit to the calculated data displayed by the actual absorbance indicates there is the presence of error. A possibility for this error can be attributed to inaccurate measurements with the μL syringes used to dispense the **54** and thymine stock solutions due to the high vapour pressure of the THF. On the other hand, auto pipettes proved to be even less accurate for the same reason. One possible way to increase accuracy that was not investigated at the time would be to weigh the solutions instead of measure by volume. It is also possible that THF of the stock solutions slowly evaporated over the course of the experiment, even though they were kept capped when not in use.

3.3 Cyclic Voltammetry of target compounds

3.3.1 Theory

Cyclic voltammetry is an electrochemical method that consists of a three electrode cell, namely the working electrode, the counter electrode, and the reference electrode. The potential of CV experiments are controlled and follow a triangular waveform, as shown in Figure 3-3, where the resultant current of the system is plotted against the potential. t_0 to t_2 is one complete cycle. The waveform may be manipulated in both the potential and the time. By adjusting the amount of time it takes to complete a cycle, the *scan rate* is changed.

CV experiments enable the investigation into the reduction and oxidation potentials of a compound which can then be translated into a number of other properties, such as the

number of electrons involved in an electrochemical process, the reduction potential, the rate of the electrochemical process, reversibility of a reaction, diffusion coefficients, and more.

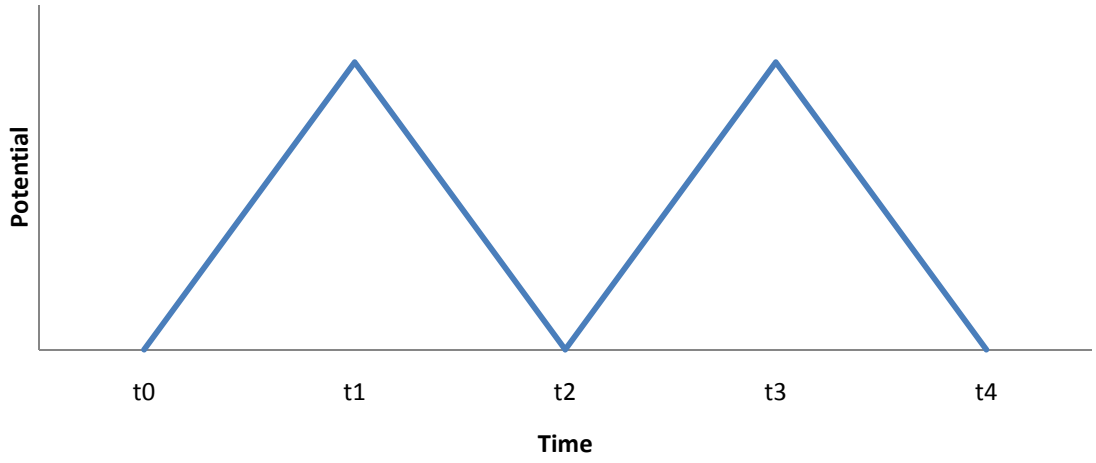

Figure 3-3: The waveform for a cyclic voltammetry experiment.

3.3.2 Instrumentation

Cyclic voltammetry (CV) experiments were performed on a commercial potentiostat (Autolab PGSTAT 302 Electrochemical Workstation) and data acquisition was controlled through software interface (GPES 4.9). All experiments were performed in a THF solution containing 0.1 M tetrabutylammonium hexafluorophosphate (TBAHFP) at 25°C. Three-electrode experiments were performed using a commercial Ag|AgCl|KCl_{3M} reference electrode (Bioanalytical Systems, Inc.), a Pt wire working electrode, and a Pt mesh counter electrode that were both flame annealed prior to each experiment. Solutions were purged with argon for 20 minutes prior to each experiment.

3.3.3 Analysis

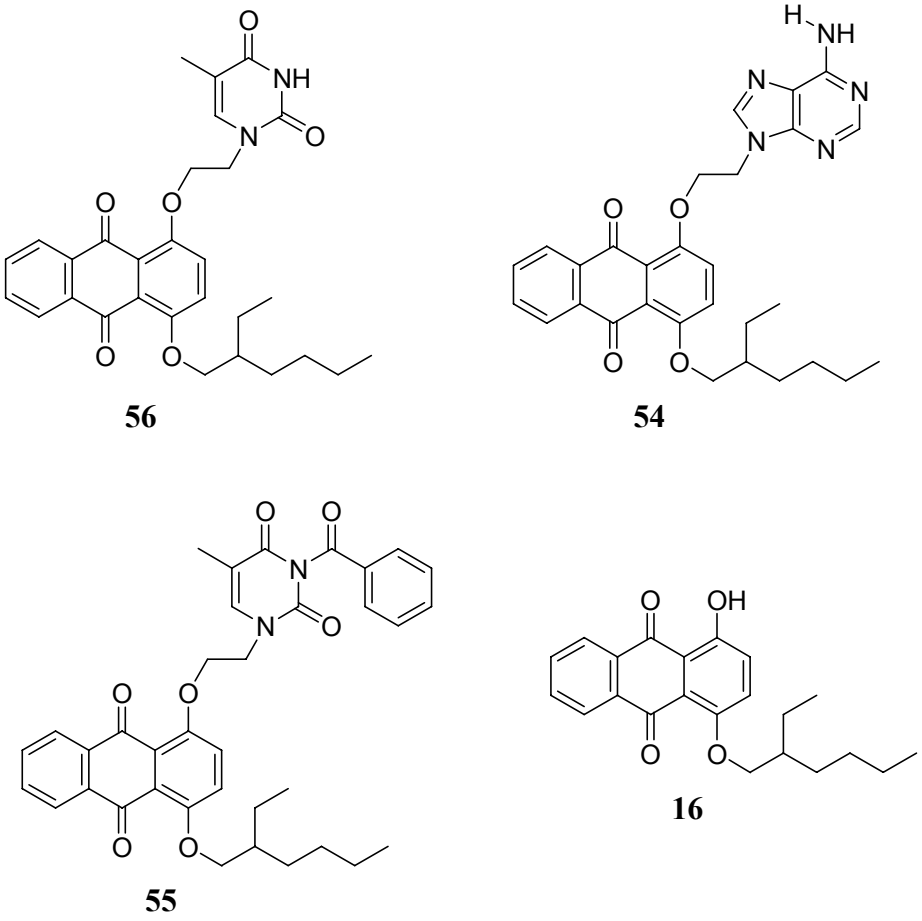

Scheme 3-2: The anthraquinone derivatives investigated in the cyclic voltammetry experiments.

The preliminary scans, shown in Figure 3-4, of the AQ derivatives, illustrated in Scheme 3-2, show some unexpected oxidation peaks between 0.1 and 0.7 V. To investigate these unknown peaks, additional CV experiments were preformed on thymine, and adenine as illustrated in Figure 3-5.

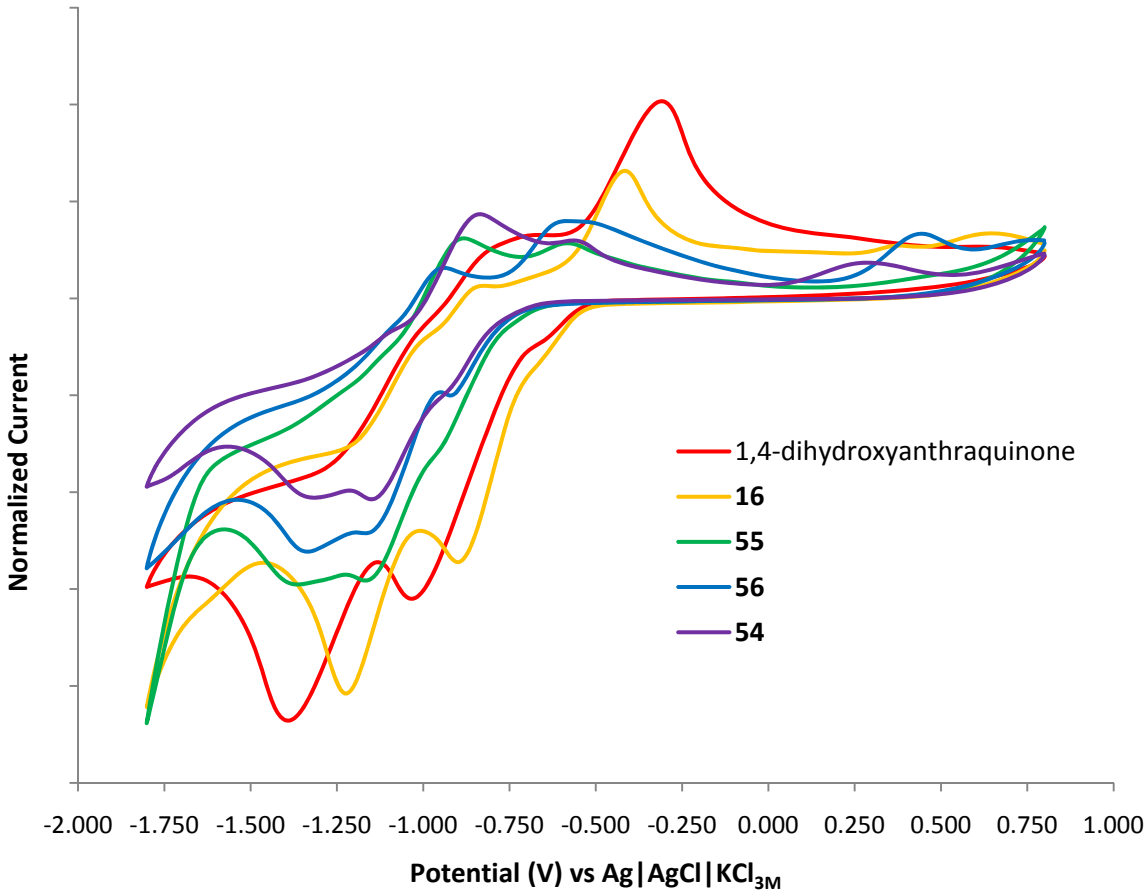

Figure 3-4: The plotted normalized cyclic voltammetry curves of 1,4-hydroxyanthraquinone and four derivatives in 0.1 M TBAHFP in THF at 25°C. 100 mV/s scan rate with a Pt wire working electrode and a Pt mesh counter electrode.

To determine the redox pair for adenine, the cathodic wave began at 0.8 V where the voltage was ramped to a more negative potential, until the anodic wave began at -0.75 V. This narrower waveform removes the both the reduction peak at -1.53 V and the oxidation peak at 0.10 V. For thymine, the cathodic wave began at 0.8 V and the anodic wave began at -1.1 V or at 0.25 V before further reductions were involved, the oxidation peaks at -0.26 V or at 0.59 V, respectively, could be isolated to see if it corresponded to the DNA base.

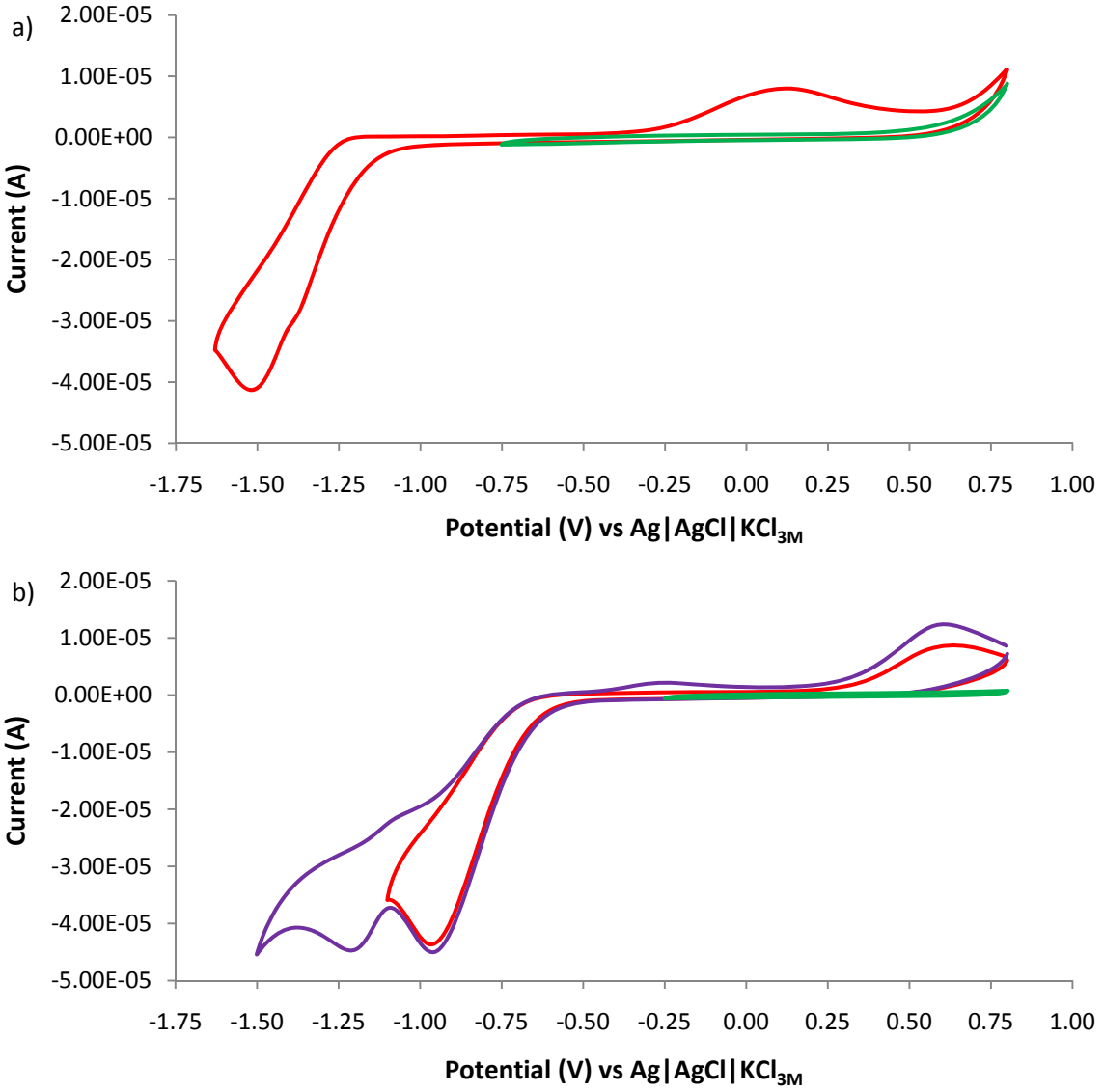

Figure 3-5: The cyclic voltammetry curves of saturated a) adenine and b) thymine starting at 0.8 V with different cut-off potentials in 0.1 M TBAHFP in THF at 25°C. 100 mV/s scan rate with a Pt wire working electrode and a Pt mesh counter electrode.

In all three cases, the oxidation peaks did not appear without the reduction of the nucleobases, indicating that the oxidation peaks were dependant on the reduction of the adenine or thymine. Because these two peaks are separated by more than 1.50 V, it is inferred that the reduction is irreversible, and that the oxidation peak therefore correlates

to another species (AS) that is derived from the reduced nucleobase (NB^{-}), as shown in the following equations:

$$NB \overset{\text{reduction}}{\rightleftharpoons} NB^{\cdot -} \qquad \text{(electrochemical reduction)}$$

$$NB^{\cdot -} \xrightarrow{\text{rearrangement}} AS^{\cdot -} \qquad \text{(chemical reaction)}$$

$$AS^{\cdot -} \overset{\text{oxidation}}{\rightleftharpoons} AS \qquad \text{(electrochemical oxidation)}$$

This hypothesis is further supported by the lack of the same peaks in the CV plot of both 1,4-dihydroxyanthraquinone and **16**. Interestingly, the protected **55** does not display these peaks, which suggest that the oxidation reaction is hindered by the addition of the benzoyl protecting group. The peaks correlating to the oxidized nucleobases were not further investigated.

Each of the AQ derivatives, including the starting material 1,4-dihydroxyanthraquinone, were examined in a solution of 0.1 M TBAHFP in THF at 25°C and the target concentration of the analyte was 10 mM. The exception to this ideal concentration was **54** which reached a saturated concentration below 10 mM, which suggests that an even larger alkyl group is necessary to fully solubilise these functionalized AQs.

The five AQ derivatives were scanned with varying scan rates, starting at 1000 mV/s, and then gradually slowing down the rate to 10-20 mV/s (Figures 3-6a – 10a). At the slower scan rates, the CV curves began to distort and in some cases, certain peaks were not observed. These missing or distorted reduction and oxidation peaks were not included in the following calculations to obtain the diffusion coefficient, D; the electron transfer rate, k; and the half-wave potential, $E_{½}$; (summarized in Table 3-1).

Before any of these aforementioned values are calculated, the peak current is plotted against the square root of the appropriate scan rates, shown in Figures 3-6b to 3-10b, and the slopes, m_i, of the formed lines are taken:

$$m_i = \frac{\Delta i_{pi}}{\Delta\sqrt{\upsilon}} \tag{3.8}$$

Where i_{pi} is the peak current and υ is the scan rate.

The slope, m_i, is inserted into a rearranged form of the Randles-Sevcik equation,[106] as shown in eq. 3.9, which determines the analyte's diffusion coefficient, D_i:

$$D_i = \left(\frac{i_{pi}}{(0.4436)nFAC_i\sqrt{\frac{n\upsilon F}{RT}}} \right)^2 = \left(\frac{m_i}{(0.4436)nFAC_i\sqrt{\frac{nF}{RT}}} \right)^2 \tag{3.9}$$

Where n is the number of electrons transferred, F is Faraday's constant (96 485 C mol^{-1}), C_i is the concentration of the analyte, R is the ideal gas constant (8.314 J K^{-1} mol^{-1}), and T is the temperature. A is the area of the working electrode surface which was determined by using the equation to find the surface area of a cylinder, shown in equation 3.10.

$$\begin{aligned} A &= A_{top} + A_{bottom} + A_{sides} \\ A &= 0 + \pi r^2 + 2\pi r h \end{aligned} \tag{3.10}$$

Where r the radius of the Pt wire, and h is the depth that the wire is submerged in the solution. It should be noted that the A_{top} is removed from the equation because it is not in contact with the solution.

From here, it is necessary to determine ψ_i from a graph presented by Nicholson[107] which is determined by the peak separation. The peak separation is the difference in potential

between the paired anodic peak and cathodic peak. This is then used to calculate the rate of electron transfer, k_i.[107]

$$k_i = \psi \sqrt{\frac{\pi D_i \upsilon n F}{RT}} \tag{3.11}$$

In the proceeding graphs shown in Figures 3-5 to 3-10, the peaks are labeled with i_{pxn}, where i_p indicates the current at the peak, the x denotes anodic ($x = a$) or cathodic ($x = c$) wave, which correlate to an oxidation or a reduction respectively, and the n simply numbers the peaks.

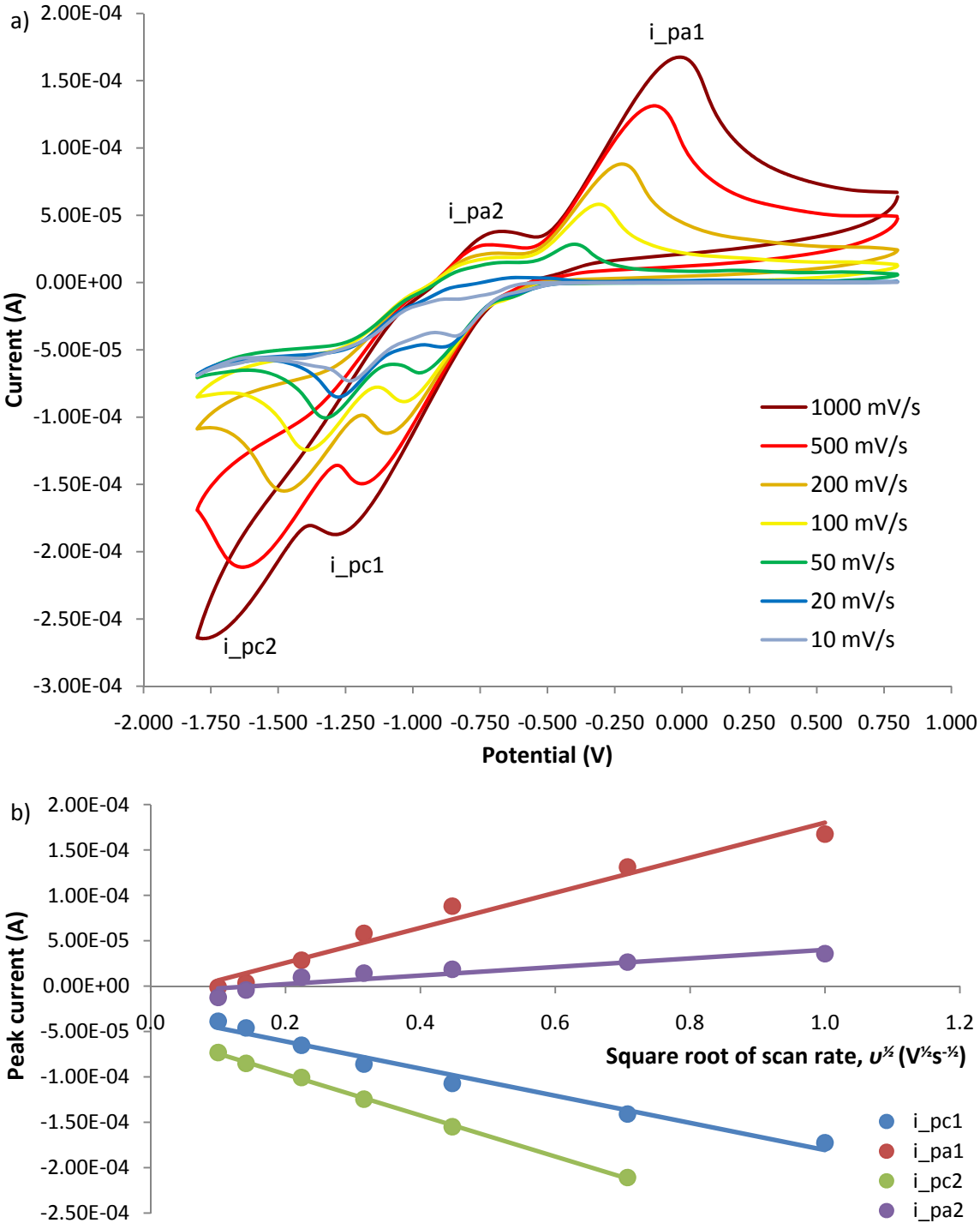

Figure 3-6: (a) The cyclic voltammetry curves of 1,4-anthraquinone at different scan rates; and (b) the peak currents, i_p against the square root of scan rate, $\upsilon^{½}$ plots

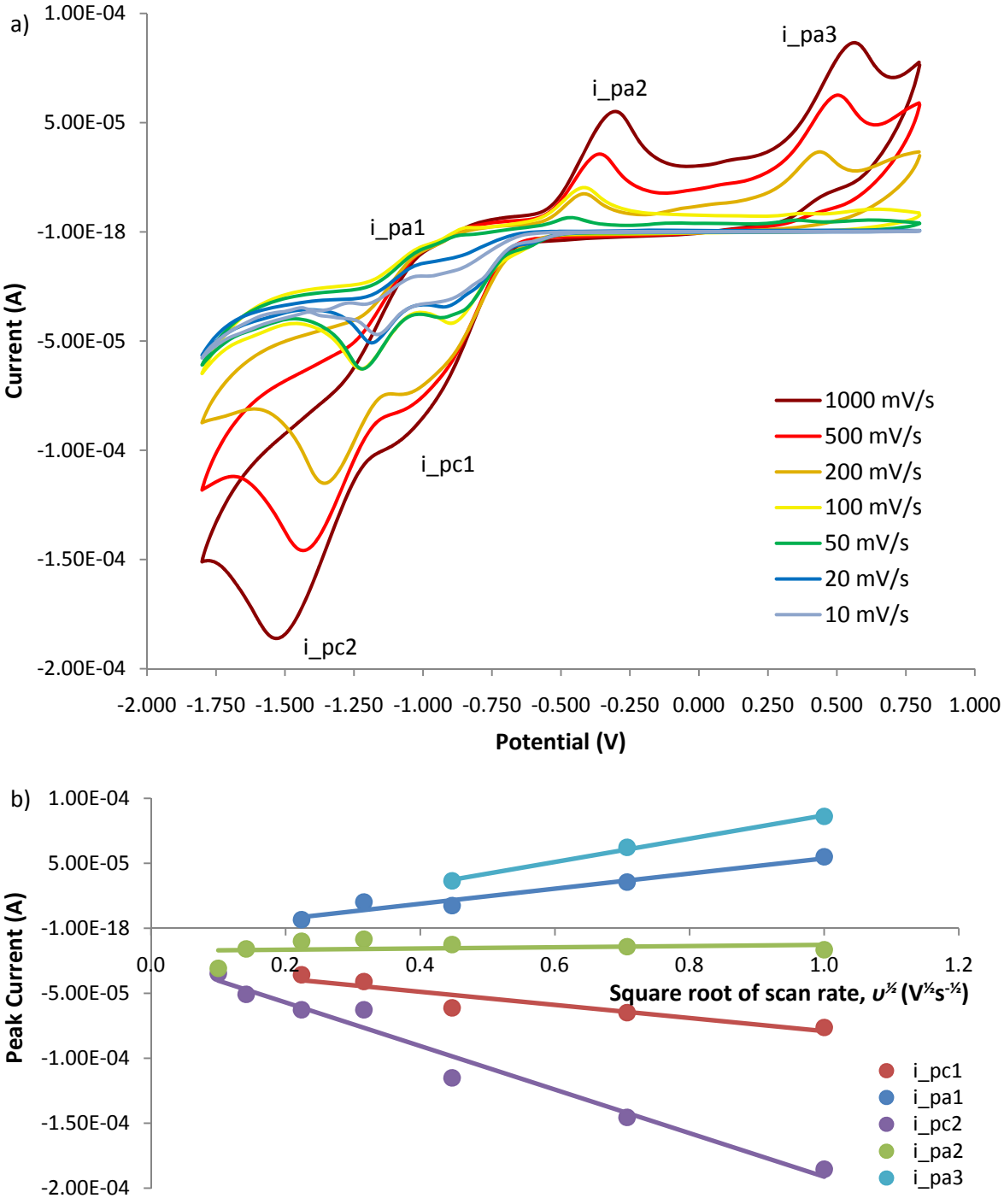

Figure 3-7: The cyclic voltammetry curves of 1-ethylhexyl-4-hydroxyanthaquinone at different scan rates; and (b) the peak currents, i_p against the square root of scan rate, $v^{½}$ plots

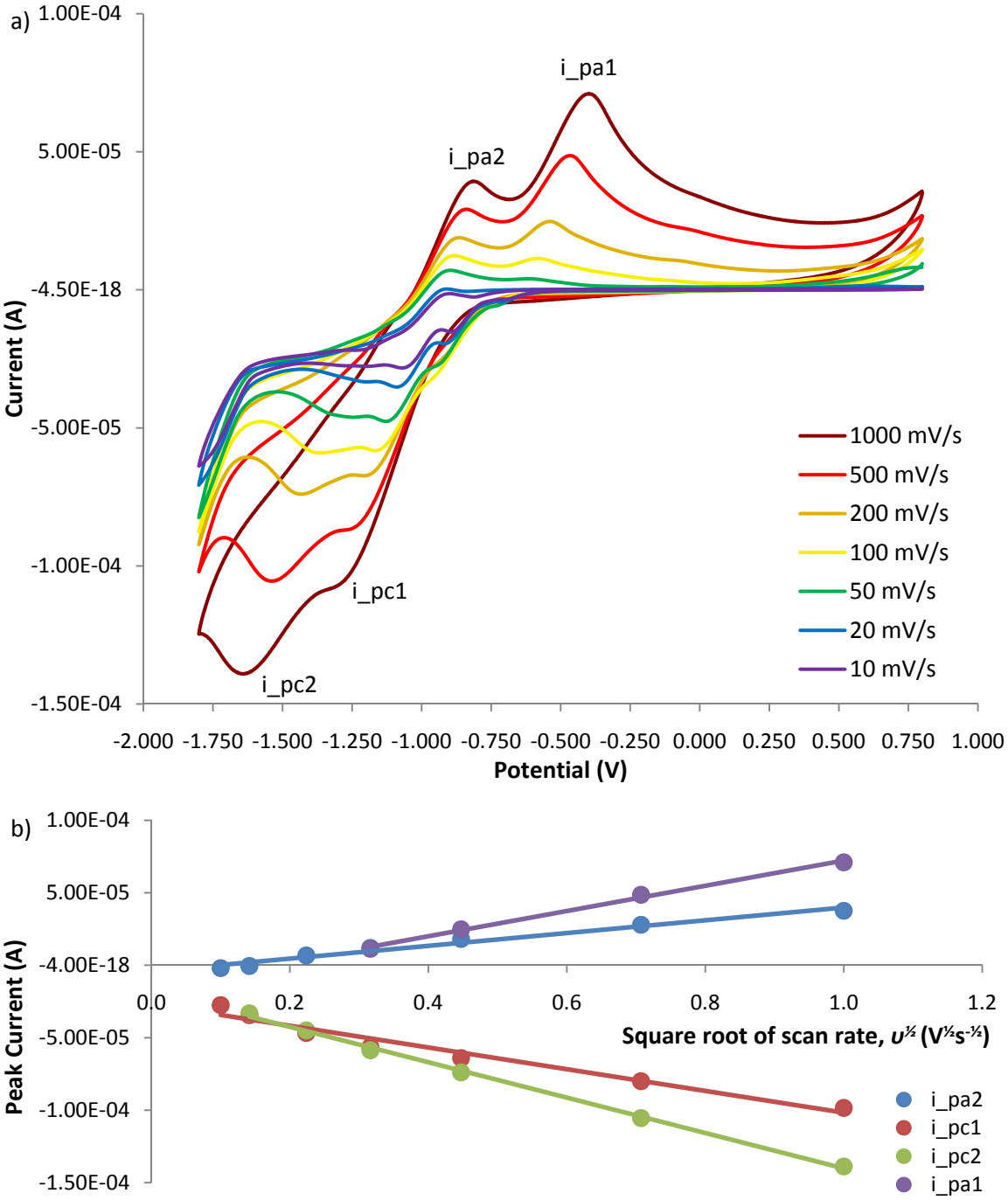

Figure 3-8: The cyclic voltammetry curves of 1-ethylhexyl-4-(2-ethyloxy(3-benzoylthymine))anthraquinone at different scan rates; and (b) the peak currents, i_p against the square root of scan rate, $\upsilon^{1/2}$ plots

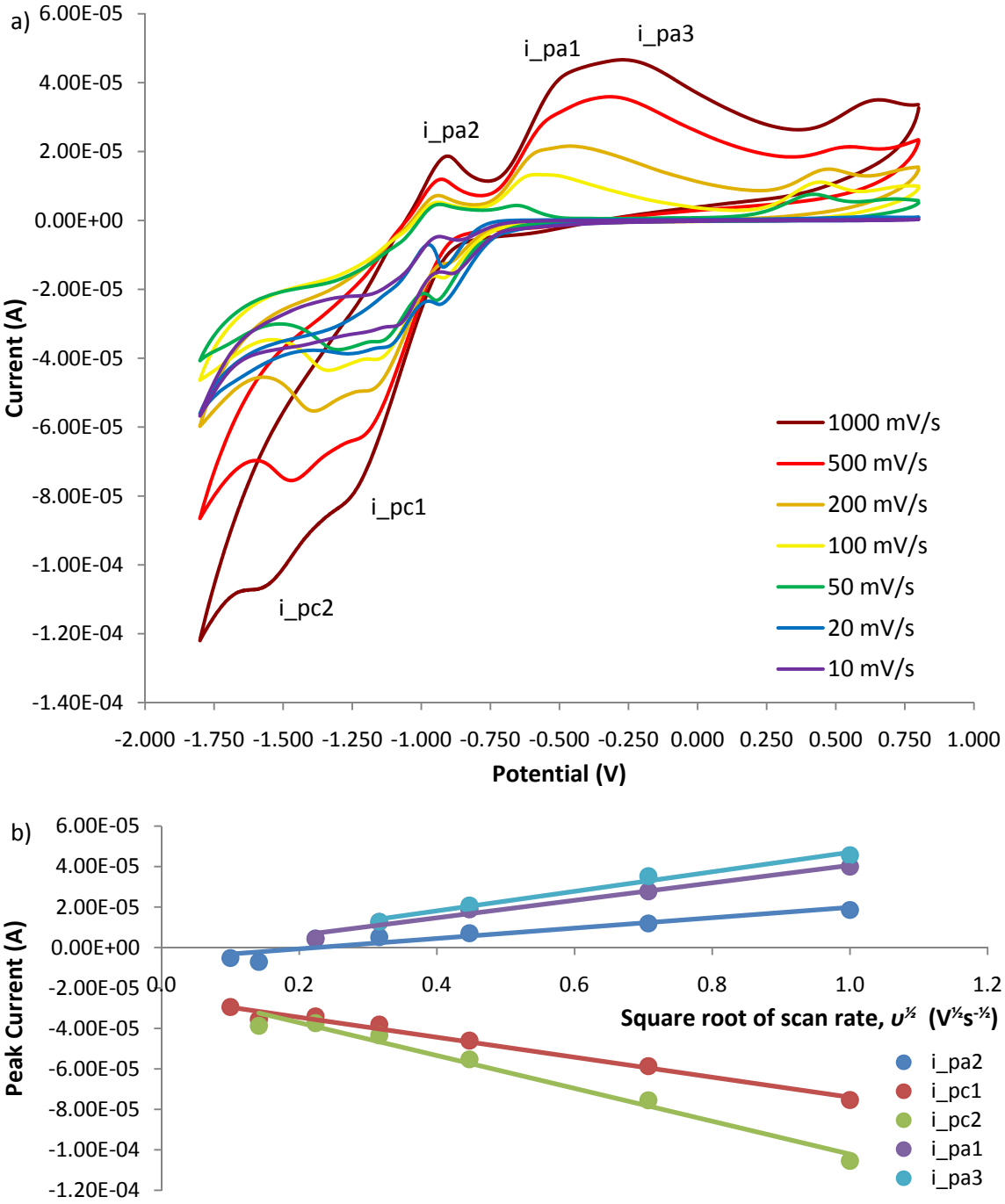

Figure 3-9: The cyclic voltammetry curves of 1-ethylhexyl-4-(2-ethyloxythymine)anthraquinone at different scan rates; and (b) the peak currents, i_p against the square root of scan rate, $v^{½}$ plots

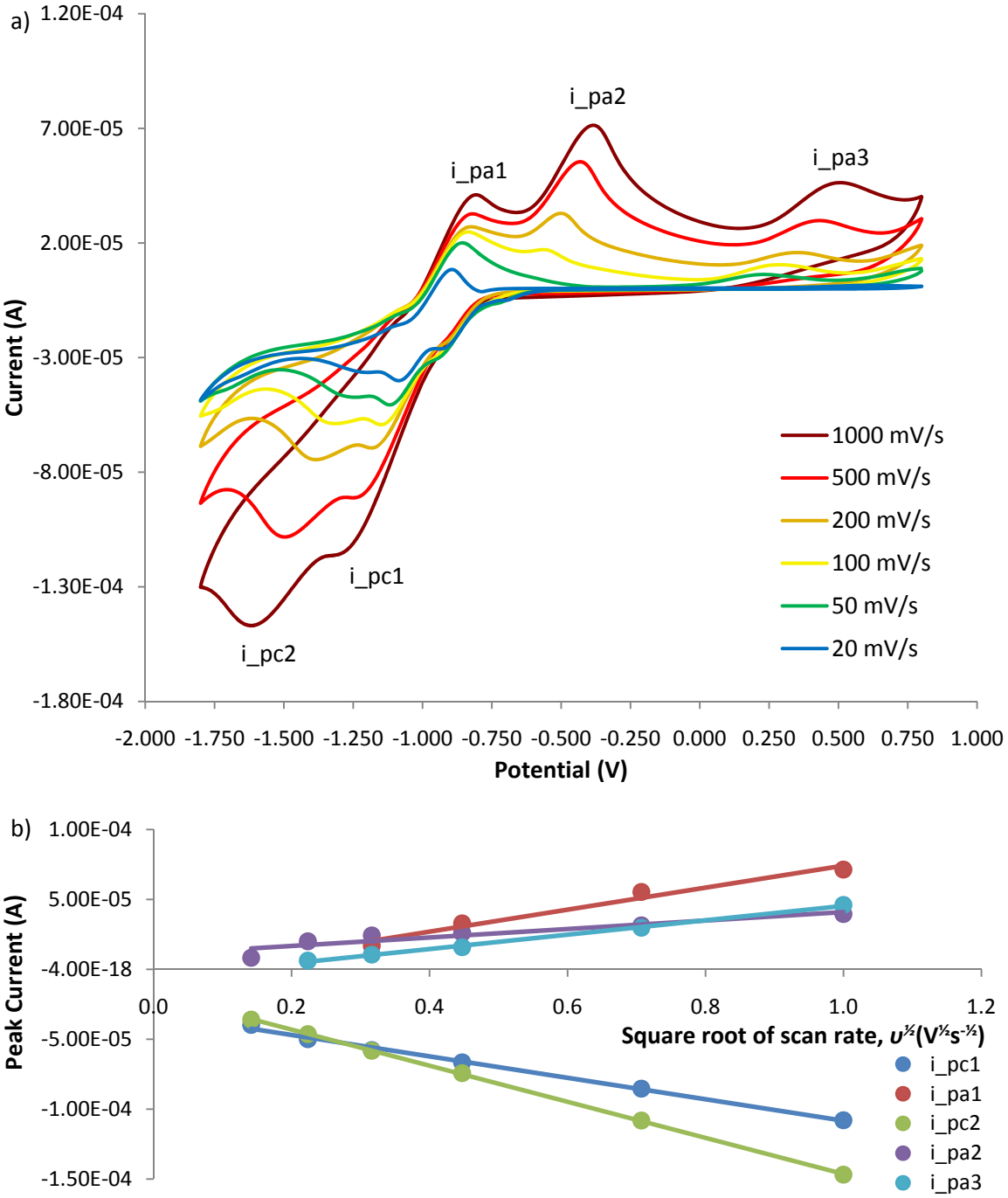

Figure 3-10: The cyclic voltammetry curves of 1-ethylhexyl-4-(2-ethyloxyadenine)anthraquinone at different scan rates; and (b) the peak currents, i_p against the square root of scan rate, $v^{½}$ plots

Table 3-1: The summarized calculated data from the i_p *vs.* $v^{1/2}$ plots of compounds 1,4-dihydroxyanthraquinone and four derivatives for comparison.

Compound	$E_{1/2\,(1)}$ (mV) (*vs.* Ag|AgCl|KCl_{3M})	$E_{1/2\,(2)}$ (mV) (*vs.* Ag|AgCl|KCl_{3M})	D_{O1} ($\times 10^{-8}$ cm^2/s)	D_{R1} ($\times 10^{-8}$ cm^2/s)	D_{O2} ($\times 10^{-8}$ cm^2/s)	D_{R2} ($\times 10^{-8}$ cm^2/s)	k_{O1} ($\times 10^{-5}$ cm/s)	k_{R1} ($\times 10^{-5}$ cm/s)	k_{O2} ($\times 10^{-5}$ cm/s)	k_{R2} ($\times 10^{-5}$ cm/s)
1,4-OH AQ	-660	-1102	90.9	54.5	5.45	42.0	14.2	11.0	2.66	7.39
16	-650	-1169	140	105	0.918	1160	22.5	19.5	1.69	60.1
55	-835	-1158	156	116	40.1	308	27.3	23.5	10.6	29.3
56	-872	-1168	75.5	99.0	26.7	268	16.5	18.9	8.63	27.3
54	-816	-1128	282	268	41.9	758	36.6	35.7	10.8	46.0

The diffusion coefficients of the five AQ species are quite different, depending on the charge of the AQ derivative, and the functional groups attached to the derivative. With the reduction and oxidation, the diffusion coefficients all seem to be in the same range of about 100 $\times 10^{-8}$ cm^2s^{-1}. The exception to this trend is the adenine functionalized AQ, **54**, which diffuses at a rate about 2.5 times faster. For the second reduction-oxidation set, the diffusion of the reduced species versus the oxidized species differs by a factor of 10, with the exception being **16** that differs by a factor of 1000. This difference may be caused by another reaction going on in solution, such as dimerization, or disproportionation.

The first half potentials ($E_{1/2\ (1)}$) of the AQ derivatives are most affected by the presence of the phenolic hydroxide substituent. There is very little difference between the $E_{1/2\ (1)}$s of 1,4-dihydroxyanthraquinone and **16**, which both possess a phenolic OH. Once the second OH is alkylated to a saturated ether, the $E_{1/2\ (1)}$ shifts to a more negative potential by 166-222 mV depending on the substituent. On the other hand, the second half potentials ($E_{1/2\ (2)}$) of the AQ derivatives differ significantly less than $E_{1/2\ (1)}$. By alkylating the last OH group, the $E_{1/2\ (2)}$ drops between 26-66 mV. This trend suggests that the OH substituent helps stabilize the added negative charge on the molecule, as shown in Scheme 3-3.

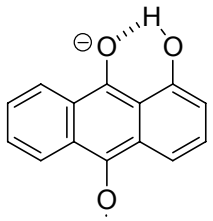

Scheme 3-3: The hydrogen bonded structure of a one electron reduced 1-hydroxyanthraquinone.

It is difficult to compare these values directly to those reported in other studies, as each set of conditions (i.e. solvent, and electrolytes) can greatly affect the half-potential and how it interacts with the reduced species.[108]

Chapter Four: **Conclusions and Future Work**

4.1 Conclusions

The synthetic portion of this thesis was largely successful; the solubility limitations of AQ and the DNA nucleobases (with the exception of guanine) were solved to develop novel, HBing capable, electro-active compounds. These challenges were overcome by functionalizing the AQ moieties with a racemic 2-ethylhexyl ether. The nucleobases were manipulated by using protecting groups that further increased their solubility in less polar, organic solvents. After investigating a variety of coupling methods, such as Pd catalysis and the Steglich esterification, the Mitsunobu reaction was found to give the highest yield and soluble products.

The binding properties of adenine (A) and thymine (T) functionalized AQs were investigated by UV-vis spectroscopy, but it was discovered that the two HBs between the A-T base pair is not strong enough in solvents such as THF at room temperature. This shortcoming does not allow us to further evaluate HBs within electro-active systems, and ultimately the application towards the organic solar cell (OSC). However, the electrochemical properties of the monomers were investigated using cyclic voltammetry, and it was found that they demonstrate typical AQ behaviour in an aprotic solvent, where there are two single electron reductions.[109] Additionally, at the more positive potential of the range investigated, the nucleobases were irreversibly oxidized, which, depending on the potential range necessary, can further limit the use of DNA nucleobases within electronic organic materials.

4.2 Pyrrole

Melfi *et al*. reported the synthesis of the 2-acid-5-ester pyrrole **59** from the 2-ester pyrrole **57** as shown in Scheme 4-1[110] using lead tetraacetate and lead dioxide to oxidize the methyl group in the 5- position to the aldehyde **58**, which is then taken to the acid with potassium permanganate.

Scheme 4-1: Synthesis of benzyl 4-methyl-3-(2-methoxycarbonylethyl)pyrrole-5-carboxylate 2-carboxylic acid

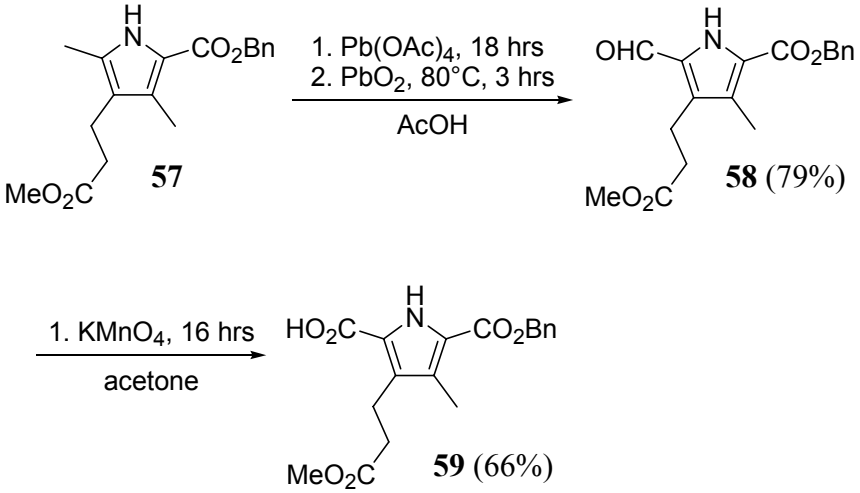

Melfi's synthesis, depicted in Scheme 4-1, shows promise for three reasons. The first, alternative esters (in this case benzyl) can be used besides the precursor diethyl malonate. Secondly, instead of functionalizing the 3- position of the 2,4-pentadione with alkyl groups, it can be functionalized with esters, as they have already proven to withstand the future reaction conditions such as the Zn reduction. By using two different esters on the 2- position and on the alkyl chain in the 4- position, shown in Scheme 4-2, the protecting groups can be selectively deprotected and further manipulated, without having to protect the carboxylic acid with a *t*-butyl ester like in Schmuck's work.[72] The third reason is that Melfi *et al*. have shown alternate oxidizing agents that can be used to convert the 5-

methyl group into the desired acid with an overall yield of 52%.[110] This oxidation can be used to replace the method used by Schmuck *et al*,[72] shown as step iii) in Scheme 4-2, where the same methyl group is first trichlorinated, and then converted into the acid by substituting the chlorides with water. This would allow the continuation of the synthesis with the group **X** which is equivalent to –OTBDMS, shown in Scheme 4-2.

Scheme 4-2: The retrosynthesis of Schmuck's pyrrole without having to protect the formed acid intermediate.

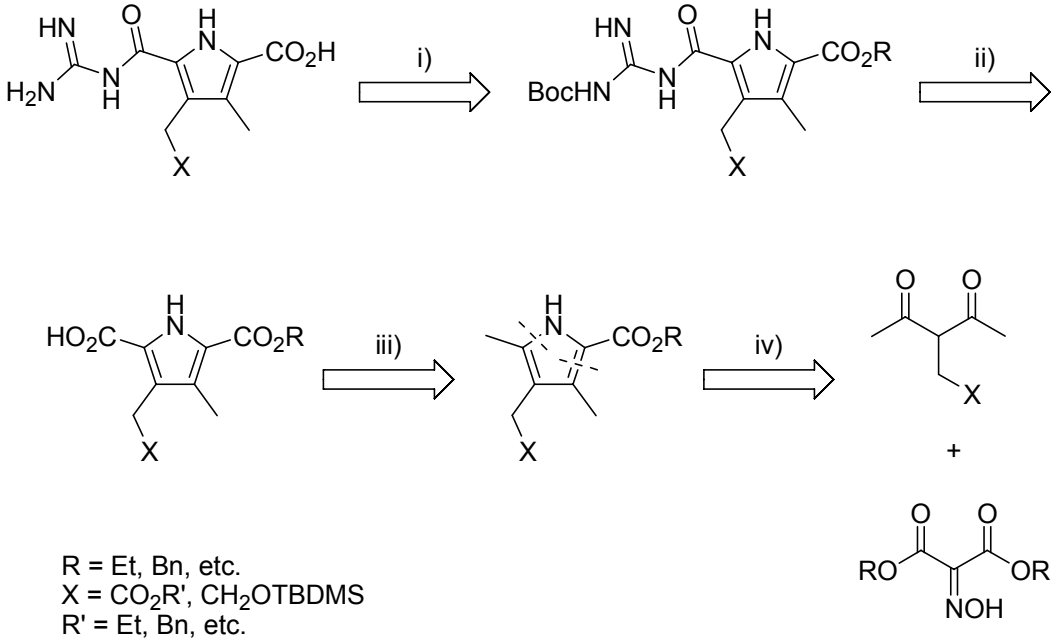

With the modified Schmucks pyrrole in hand, it is proposed that the TBDMS group can be removed to leave the alcohol, which can then be reacted with an AQ phenol under the Mitsunobu conditions. The last step in this synthesis would be to deprotect the carboxylic acid and the guanidinium portions of Schmuck`s dimer to yield the zwitterionic product.

4.3 Guanine

4.3.1 Protecting groups

The major problem with the guanine synthesis is its insolubility that prevents reactions under most conditions. In literature, the two most relied upon methods to overcoming this problem is to either add a solubilising protecting group,[50-56] or to convert the guanine into 6-chloroguanine[58,59] which is markedly more soluble and easier to manipulate, likely due to the weaker HBs of a chloride and a proton when compared to the oxygen and a proton. The 6-chloroguanine is easily converted back to guanine by using 2-thioethanol and sodium methoxide in methanol;[60-63] or by refluxing in a strong base[64] or acid.[65,66]

These longer chained amides can be created in the same fashion that Kang *et al.* have demonstrated by using hexadecanoyl chloride to regioselectively alkylate the N^2 shown in Scheme 4-3.[111] It is less common to work with small chains, especially the acetyl group as it offers a marginal improvement in guanine`s solubility.

Scheme 4-3: The formation of the N^2 amide protecting group using acyl halide.[111]

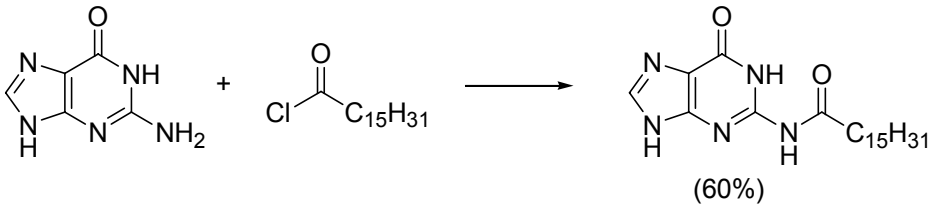

With the increased solubility of either 6-chloroguanine or a long-chain amide-protected guanine, the required manipulations, such as the hydroxyalkylation at the N^9 site, are expected to be more successful. The alkylation involving ethylene carbonate would be tried first, as it is cheaper and shorter than the Mitsunobu route required for thymine and uracil, but if necessary, the Mitsunobu method will be attempted.

4.4 Thymine and uracil

4.4.1 Protecting groups

Scheme 4-4: The numbering system of thymine.

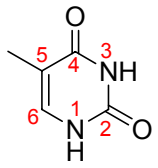

With the DNA/RNA bases thymine and uracil, the largest synthetic hurdle is with the selectivity of the alkylation between the N^1 and N^3 sites shown in Scheme 4-4. The benzoyl group chosen in this research project was suitable for the Mitsunobu coupling conditions, but not for the simpler and less expensive alkylation using ethylene carbonate which is cleaved in the presence of the catalytic amount of sodium hydroxide.

Utilizing other protecting groups (PGs) that are stable in the presence of sodium hydroxide, such as PG = benzyl (Bn), trityl (-CPh_3 or Tr) or tosyl (Ts)[112] will enable the alkylation of the protected thymine using ethylene carbonate, thereby eliminating the addition steps associated with the Mitsunobu route. These PGs can be removed, respectively, by a variety of methods that are outlined in Table 4-1.

These protecting groups, as they are expected to withstand the basic conditions, would be suitable for the alkylation conditions with ethylene carbonate. Their deprotections are also suitable for the thymine and uracil; and the AQ systems should be stable in all but the Pd-C deprotection for the Bn PG.

Table 4-1: The suggested protecting groups of thymine and uracil that are stable in basic conditions; and the appropriate methods of protection and deprotection.[112]

Protecting group	Protection and Deprotection (R = H, Me)
Benzyl (Bn)	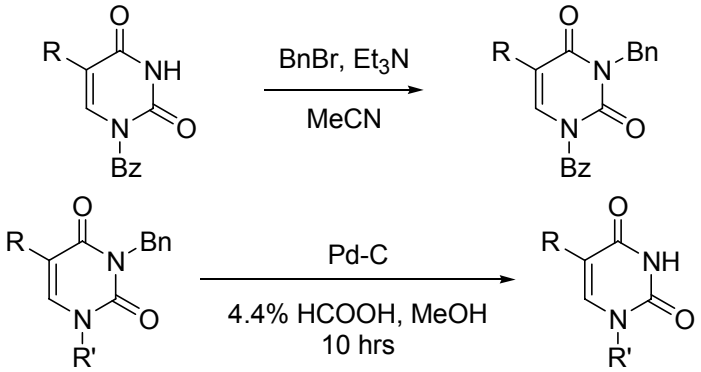
Trityl (Tr)	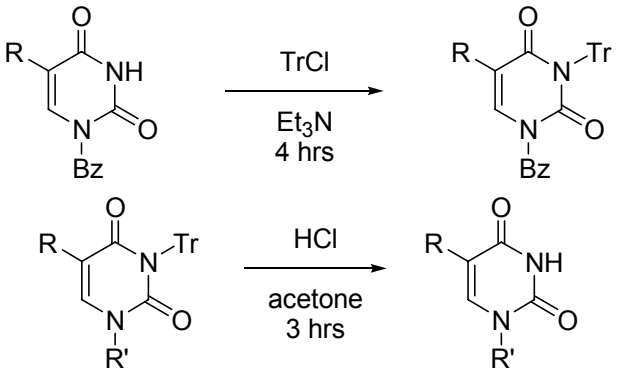
Tosyl (Ts)	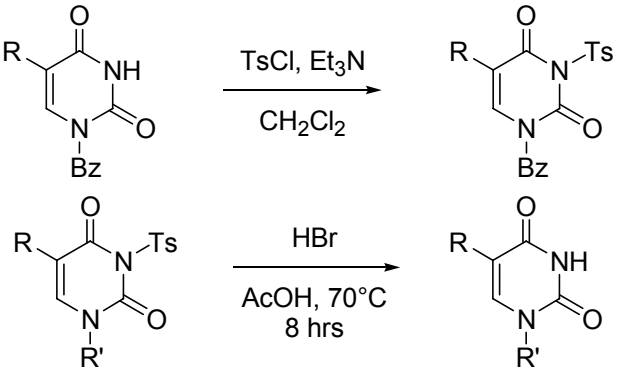

4.5 Anthraquinone

4.5.1 Different substitutions of di, tri, and tetrahydroxyanthraquinones

There are a large number of other commercially available hydroxylated AQs listed in Table 4-2 that can possess as many as six hydroxyl substituents, and the solubility of these AQs can be modified with the addition of various alkyl moieties. These can be modified in size and number, to see how this affects the rate of charge transfer between the AQ and the electrodes in electrochemistry experiments. It would be interesting to determine at what point the number of substituted alkyl ethers around the AQ begins to insulate the AQ during electrochemical experiments.

The alkyl ethers can be formed using the same method as with the 2-ethylhexyl AQ ethers were synthesized. The Williamson ether synthesis,[39] was carried out with potassium carbonate in DMF, and then purified by column chromatography on silica using a combination of hexanes and ethyl acetate, as described in Chapter 2.

An alternative method to obtain the resultant alkylated AQ with one remaining hydroxyl substituent is to try to protect one of the hydroxyl groups prior to alkylation.[112] This synthetic route would not be selective to either of the hydroxyl groups and consequently there would be a distribution of products.

There are a plethora of suitable protecting groups as the alkylation conditions are not especially harsh: even an acetyl group would be sufficient for this purpose, and would be easily deprotected after.[112] It should be noted that the hydroxyl groups in the 2-, 3-, 6-, and 7- positions are more nucleophilic compared to the 1-, 4-, 5-, and 8- positions.[113]

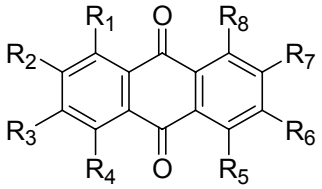

Table 4-2: Commercially available anthraquinones ranging from monohydroxy- to tetrahydroxy-anthraquinone.

Common Name	R_1	R_2	R_3	R_4	R_5	R_6	R_7	R_8
Alizarin	OH	OH	H	H	H	H	H	H
Purpurin	OH	OH	H	OH	H	H	H	H
(n/a)	OH	H	H	OH	OH	H	H	OH
Alizarin Bordeaux	OH	H	H	OH	OH	OH	H	H
Anthraflavic Acid	H	OH	H	H	H	OH	H	H
Chrysazine, Danthron	OH	H	H	H	H	H	H	OH
Anthrarufin	OH	H	H	H	OH	H	H	H
(n/a)	H	OH	H	H	H	H	OH	H
Xanthopurpurin	OH	H	OH	H	H	H	H	H
Anthragallol	OH	OH	OH	H	H	H	H	H
Anthrapurpurin	OH	OH	H	H	H	H	OH	H
(n/a)	OH	OH	H	H	OH	H	H	H
(n/a)	OH	H	H	OH	OH	H	H	H
(n/a)	OH	OH	H	H	H	H	H	OH
(n/a)	OH	H	OH	H	OH	H	H	H
(n/a)	OH	H	H	H	H	OH	OH	H

Frequently, strong bases, heat, or acyl halides are necessary to protect the latter positions with a simple acetyl PG,[114-117] while the former can be protected simply with acetic anhydride.[114]

4.6 Coupling

4.6.1 Heck coupling

The major downfall with the Heck reaction is that the allyl substituted DNA/RNA bases are not sufficiently electron withdrawing to the alkene as required for the type of catalyst used. For electron rich alkenes, the success of the reaction requires a different palladium catalyst that involves chelating phosphine ligands with aryl triflates.[118] The triflate will dissociate, leaving a positive Pd centre for the electron rich alkene to dock at, shown in Scheme 4-5. Two examples of chelating phosphine ligands that have been used include BINAP[119] and phosphinooxazoline[120] as shown in Scheme 4-5, where they are both added to the reaction solution. It is also possible to add a halide sequestering agent, like Ag^+ in the form of AgOTf, that will encourage the trans-product formation with electron rich alkenes.[100] This cation additive works by precipitating the bromide ion that results from the oxidative addition of the aryl halide, leaving a cationic palladium catalyst, depicted as int-B in Scheme 4-5. From here, the electron rich alkene, which is a good σ donor and a poor π acceptor, will now bond to the palladium centre in

Scheme 4-5: Two examples of chelating phosphine ligands.

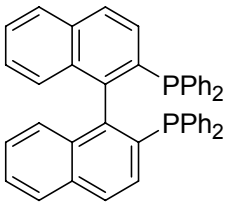

(R) or *(S)* BINAP

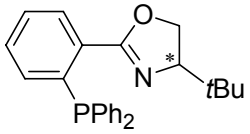

phosphinooxazoline

the way necessary to produce the desired *trans*- product, depicted as int-C in Scheme 4-5.[100]

It is also possible that some of the N atoms in the DNA/RNA nucleobases were coordinating to the Pd centre as well. To investigate this, the outcome of unsubstituted and protected allyl-substituted nucleobases will be investigated and the products compared.

Scheme 4-5: The catalytic cycle of the Heck reaction for alkenes containing electron donating groups (EDG) and aryl triflates.[100]

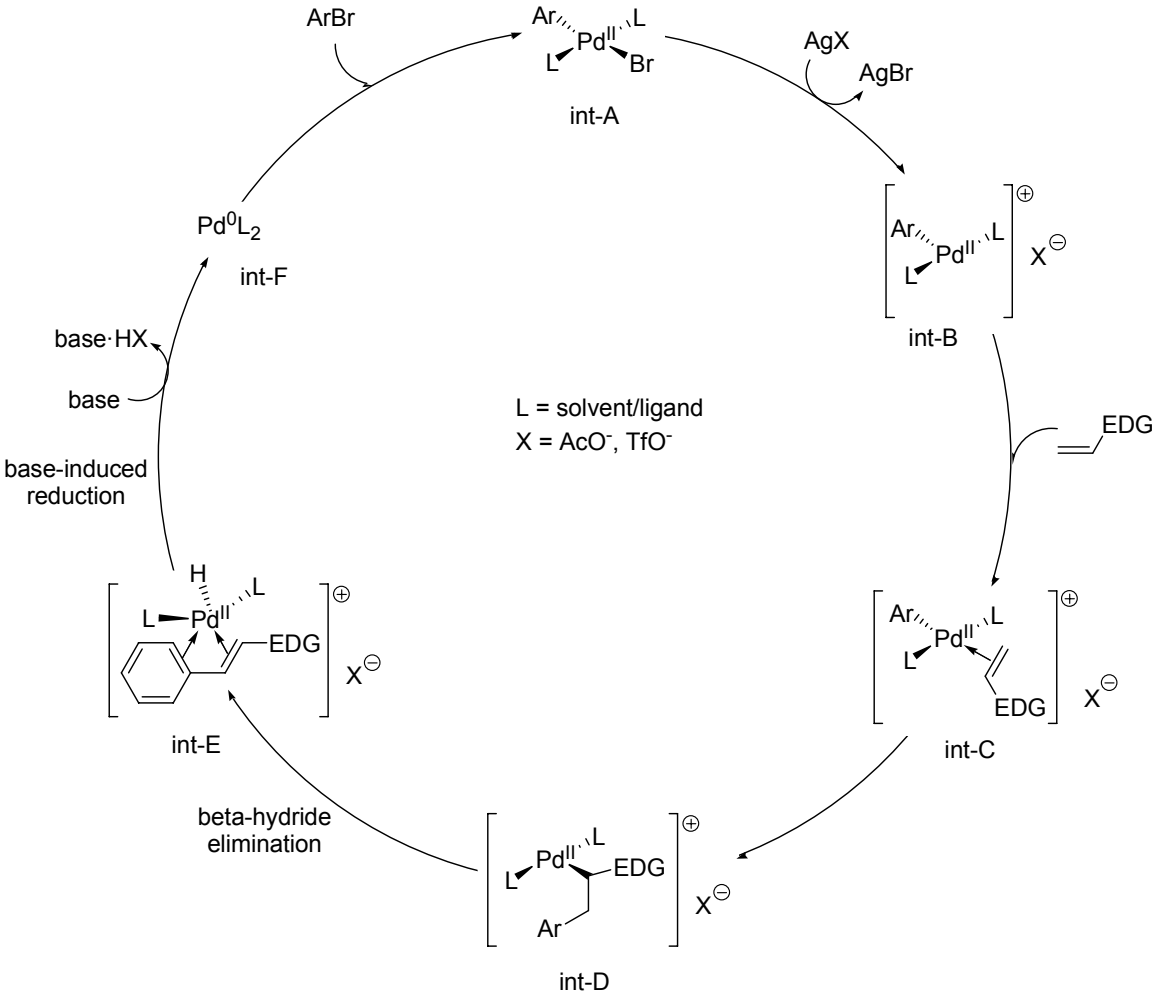

Chapter Five: **References**

(1) Lewis, N. S.; Nocera, D. G. *Proc. Nat. Acad. Sci. U. S. A.* **2006**, *103*, 15729-15735.

(2) http://www.eia.doe.gov/cneaf/alernate/page/renew_energy_consump/rea_prereport.html viewed August 28, 2009.

(3) Program, U. N. D. *World Energy Assessment Report: Energy and the Challenge of Sustainability*, United Nations, 2003.

(4) http://www.pv-tech.org/news/_a/solarmer_breaks_organic_solar_pv_cell_conversion_efficiency_record_hits_nre/ viewed July 4, 2010.

(5) Kazmerski, L.; Nat. Renewable Energy Laboratory (NREL): 2010.

(6) Luque, A.; Hegedus, S. *Handbook of Photovoltaic Science and Engineering*; Wiley, 2003.

(7) Geisz, J. F.; Friedman, D. J.; Ward, J. S.; Duda, A.; Olavarria, W. J.; Moriarty, T. E.; Kiehl, J. T.; Romero, M. J.; Norman, A. G.; Jones, K. M. *App. Phys. Lett.* **2008**, *93*, 123505-123505-3.

(8) O'Regan, B.; Graetzel, M. *Nature* **1991**, *353*, 737-40.

(9) Guenes, S.; Neugebauer, H.; Sariciftci, N. S. *Chem. Rev.* **2007**, *107*, 1324-1338.

(10) Halls, J. J. M.; Pichler, K. *App. Phys. Lett.* **1996**, *68*, 3120.

(11) Heremans, P.; Cheyns, D.; Rand, B. P. *Acc. Chem. Res.* **2009**, *42*, 1740-1747.

(12) Benanti, T. L.; Venkataraman, D. *Photosyn. Res.* **2006**, *87*, 73-81.

(13) Pivrikas, A.; Sariciftci, N. S.; Juska, G.; Osterbacka, R. *Progress in Photovoltaics* **2007**, *15*, 677-696.

(14) Sariciftci, N. S.; Smilowitz, L.; Heeger, A. J.; Wudl, F. *Science* **1992**, *258*, 1474-6.

(15) Singh, T. B.; Sariciftci, N. S. *Annu. Rev. Mat. Res.* **2006**, *36*, 199-230.

(16) Kroon, R.; Lenes, M.; Hummelen, J. C.; Blom, P. W. M.; de Boer, B. *Polym. Rev.* **2008**, *48*, 531-582.

(17) Segura, J. L.; Martin, N.; Guldi, D. M. *Chem. Soc. Rev.* **2005**, *34*, 31-47.

(18) Roncali, J. *Acc. Chem. Res.* **2009**, *42*, 1719–1730.

(19) Armstrong, N. R.; Carter, C.; Donley, C.; Simmonds, A.; Lee, P.; Brumbach, M.; Kippelen, B.; Domercq, B.; Yoo, S. *Thin Solid Films* **2003**, *445*, 342-352.

(20) Paniagua, S. A.; Hotchkiss, P. J.; Jones, S. C.; Marder, S. R.; Mudalige, A.; Marrikar, F. S.; Pemberton, J. E.; Armstrong, N. R. *J. Phys.Chem. C* **2008**, *112*, 7809-7817.

(21) Sijbesma, R. P.; Beijer, F. H.; Brunsveld, L.; Folmer, B. J. B.; Hirschberg, J. H. K. K.; Lange, R. F. M.; Lowe, J. K. L.; Meijer, E. W. *Science* **1997**, *278*, 1601-1604.

(22) Sanchez, L.; Rispens, M. T.; Hummelen, J. C. *Angew. Chem., InterNat. Edition* **2002**, *41*, 838-840.

(23) El-Ghayoury, A.; Schenning, A. P. H. J.; Van Hal, P. A.; Van Duren, J. K. J.; Janssen, R. A. J.; Meijer, E. W. *Angew. Chem., Int. Ed.* **2001**, *40*, 3660-3663.

(24) El-ghayoury, A.; Peeters, E.; Schenning, A. P. H. J.; Meijer, E. W. *Chem. Commun.* **2000**, 1969-1970.

(25) Beckers, E. H. A.; Schenning, A. P. H. J.; van Hal, P. A.; El-Ghayoury, A.; Sanchez, L.; Hummelen, J. C.; Meijer, E. W.; Janssen, R. A. J. *Chem. Commun.* **2002**, 2888-2889.

(26) Neuteboom, E. E.; Beckers, E. H. A.; Meskers, S. C. J.; Meijer, E. W.; Janssen, R. A. J. *Org. Biomol.Chem.* **2003**, *1*, 198-203.

(27) Sanchez, L.; Martin, N.; Guldi, D. M. *Angew. Chem., Int. Ed.* **2005**, *44*, 5374-5382.

(28) Segura, M.; Sanchez, L.; De Mendoza, J.; Martin, N.; Guldi, D. M. *J. Am. Chem. Soc.* **2003**, *125*, 15093-15100.

(29) Huang, C.-H.; McClenaghan, N. D.; Kuhn, A.; Bravic, G.; Bassani, D. M. *Tetrahedron* **2006**, *62*, 2050-2059.

(30) Sessler, J. L.; Sathiosatham, M.; Brown, C. T.; Rhodes, T. A.; Wiederrecht, G. *J. Am. Chem. Soc.* **2001**, *123*, 3655-3660.

(31) Harriman, A.; Kubo, Y.; Sessler, J. L. *J. Am. Chem. Soc.* **1992**, *114*, 388-90.

(32) Myles, A. J.; Branda, N. R. *J. Am. Chem. Soc.* **2000**, *123*, 177-178.

(33) Zhao, C.-C.; Tong, Q.-X.; Li, Z.-T.; Wu, L.-Z.; Zhang, L.-P.; Tung, C.-H. *Tetrahedron Lett.* **2004**, *45*, 6807-6811.

(34) Fang, H.; Wang, S.; Xiao, S.; Yang, J.; Li, Y.; Shi, Z.; Li, H.; Liu, H.; Xiao, S.; Zhu, D. *Chem. Mater.* **2003**, *15*, 1593-1597.

(35) Guldi, D. M.; Martin, N. *J. Mater. Chem.* **2002**, *12*, 1978-1992.

(36) Sun, H.; Steeb, J.; Kaifer, A. E. *J. Am. Chem. Soc.* **2006**, *128*, 2820-2821.

(37) Beard, E. E.; Lulek, R. N.; (E. I. du Pont de Nemours & Co.). US, 1935.

(38) Kislyi, K. A.; Samet, A. V.; Strelenko, Y. A.; Semenov, V. V. *J. Org. Chem.* **2008**, *73*, 2285-2291.

(39) Williamson, A. W. *Quart. J., Chem. Soc.* **1852**, *4*, 229-39.

(40) Lolk, L.; PÃ¸hlsgaard, J.; Jepsen, A. S.; Hansen, L. H.; Nielsen, H.; Steffansen, S. I.; Sparving, L.; Nielsen, A. B.; Vester, B.; Nielsen, P. *J. Med. Chem.* **2008**, *51*, 4957-4967.

(41) Ludek, O. R.; Meier, C. *Synlett* **2005**, 3145-3147.

(42) Tsai, J.-Y.; Bouhadir, K. H.; Zhou, J.-L.; Webb, T. R.; Sun, Y.; Shevlin, P. B. *J. Org. Chem.* **2003**, *68*, 1235-1241.

(43) Lee, Y.-S.; Hyean Kim, B. *Bioorg. Med. Chem. Lett.* **2002**, *12*, 1395-1397.

(44) Shatila, R. S.; Bouhadir, K. H. *Tetrahedron Lett.* **2006**, *47*, 1767-1770.

(45) Cruickshank, K. A.; Jiricny, J.; Reese, C. B. *Tetrahedron Lett.* **1984**, *25*, 681-4.

(46) Frieden, M.; Giraud, M.; Reese, C. B.; Song, Q. *J. Chem. Soc., Perkin Trans. 1* **1998**, 2827-2832.

(47) Lee, Y.-S.; Hyean Kim, B. *Bioorg. Med. Chem. Lett.* **2002**, *12*, 1395-1397.

(48) Uzunian, G. E.; Song, L. S.; Turner, D. F.; Lewis, R. A.; (Engelhard Corporation, USA). Application: US
US, 2005, p 5 pp.

(49) Pfeiderer, W. *Justus Liebigs Ann. der Chem.* **1961**, *647*, 167-73.

(50) Kobe, J.; Kjellberg, J.; Johansson, N. G. *Acta Chem. Scand., Ser. B.* **1987**, *B41*, 564-8.

(51) Biagi, G.; Costantini, A.; Costantino, L.; Giorgi, I.; Livi, O.; Pecorari, P.; Rinaldi, M.; Scartoni, V. *J. Med. Chem.* **1996**, *39*, 2529-2535.

(52) Grigorii , G. S.; Elena , N. K.; Igor , A. M. *Helv. Chim. Acta* **2007**, *90*, 1818-1836.

(53) Hudson, R. H. E.; Goncharenko, M.; Wallman, A. P.; Wojciechowski, F. *Synlett* **2005**, 1442-1446.

(54) Nasr, T.; Taniguchi, Y.; Sasaki, S. *Heterocycles* **2007**, *71*, 2659-2668.

(55) Taylor, E. C.; Kuhnt, D.; Chang, Z. Y. *J. Org. Chem.* **1991**, *56*, 6937-9.

(56) Hildebrand, C.; Sandoli, D.; Focher, F.; Gambino, J.; Ciarrocchi, G.; Spadari, S.; Wright, G. *J. Med. Chem.* **1990**, *33*, 203-6.

(57) Kjellberg, J.; Johansson, N. G. *Nucleosides & Nucleotides* **1989**, *8*, 225-56.

(58) Luo, L.; Chen, G.; Li, Y. *Heterocycles* **2008**, *75*, 2803-2808.

(59) Wu, J.; Xu, X.-Y.; Liu, K.-L. *Chin. J. Chem.* **2003**, *21*, 566-573.

(60) Kim, A.; Hong, J. H. *Nucleosides, Nucleotides & Nucleic Acids* **2008**, *27*, 121-130.

(61) Shen, Q.; Hong, J. H. *Nucleosides, Nucleotides & Nucleic Acids* **2008**, *27*, 213-223.

(62) Bremond, P.; Audran, G.; Monti, H.; De Clercq, E. *Synthesis* **2008**, 3253-3260.

(63) Moon, H. R.; Park, A.-Y.; Kim, K. R.; Chun, M. W.; Jeong, L. S. *Nucleosides, Nucleotides & Nucleic Acids* **2007**, *26*, 975-978.

(64) Vazquez-Romero, A.; Rodriguez, J.; Lledo, A.; Verdaguer, X.; Riera, A. *Org. Lett.* **2008**, *10*, 4509-4512.

(65) Oh, C. H.; Hong, J. H. *Nucleosides, Nucleotides & Nucleic Acids* **2008**, *27*, 186-195.

(66) Jeong, L. S.; Lee, J. A.; Kim, H. O.; Tosh, D. K.; Moon, H. R.; Lee, S.-J.; Lee, K. M.; Sheen, Y. Y.; Chun, M. W. *Nucleosides, Nucleotides & Nucleic Acids* **2007**, *26*, 1021-1024.

(67) Gao, H.; Mitra, A. K. *Syn. Commun.***2001**, *31*, 1399-1419.

(68) Zou, R.; Robins, M. J. *Can. J. Chem.* **1987**, *65*, 1436-7.

(69) Shibata, M.; Takenaka, A.; Sasada, Y. *Acta Crystallogr., Sect. C: Cryst. Struct. Commun.* **1985**, *C41*, 1501-3.

(70) Toucet, I.; Aponte, M. A. *J. Polym. Sci., Part A: Polym. Chem.* **1991**, *29*, 1883-8.

(71) Gottlieb, H. E.; Kotlyar, V.; Nudelman, A. *J. Org. Chem.* **1997**, *62*, 7512-7515.

(72) Schmuck, C.; Wienand, W. *J. Am. Chem. Soc.* **2003**, *125*, 452-459.

(73) Siedel, W. *Ann.* **1943**, *554*, 144-61.

(74) Eisner, U.; Lichtarowicz, A.; Linstead, R. P. *J. Chem. Soc.* **1957**, 733-9.

(75) Paine, J. B., III; Dolphin, D. *J. Org. Chem.* **1985**, *50*, 5598-604.

(76) Paine, J. B., III; Dolphin, D. *J. Org. Chem.* **1988**, *53*, 2787-95.

(77) Scarsella, M.; Sleiter, G. *Gazz. Chim. Ital.* **1988**, *118*, 757-62.

(78) Cho, D. H.; Lee, J. H.; Kim, B. H. *J. Org. Chem.* **1999**, *64*, 8048-8050.
(79) Johnson, A. W.; Markham, E.; Price, R. *Org. Synth.* **1962**, *42*, 75-6.
(80) Ueda, N.; Kondo, K.; Kono, M.; Takemoto, K.; Imoto, M. *Makromol. Chem.* **1968**, *120*, 13-20.
(81) Holy, A.; Kohoutova, J.; Merta, A.; Votruba, I. *Collect. Czech. Chem. Commun.* **1986**, *51*, 459-77.
(82) Kondo, K.; Iwasaki, H.; Ueda, N.; Takemoto, K.; Imoto, M. *Makromol. Chem.* **1968**, *120*, 21-6.
(83) Carey, F. A.Organic *Chemistry*; 5 ed.; McGraw-Hill: New York, NY, 2003.
(84) Drasar, P.; Budesínský, M.; Reschel, M.; Pouzar, V.; Cerný, I. *Steroids* **2005**, *70*, 615-625.
(85) Baik, W.; Luan, W.; Lee, H. J.; Yoon, C. H.; Koo, S.; Kim, B. H. *Can. J. Chem.* **2005**, *83*, 213-219.
(86) Henri, D.; Jean-Cyrille, H. *Angew. Chem. Int. Ed.* **2007**, *46*, 834-871.
(87) Frisch, A. C.; Beller, M. *Angew. Chem., Int. Ed.* **2005**, *44*, 674-688.
(88) Netherton, M. R.; Fu, G. C. *Adv. Synth. Catal.* **2004**, *346*, 1525-1532.
(89) Netherton, M. R.; Dai, C.; Neuschutz, K.; Fu, G. C. *J. Am. Chem. Soc.* **2001**, *123*, 10099-10100.
(90) Kirchhoff, J. H.; Dai, C.; Fu, G. C. *Angew. Chem., Int. Ed.* **2002**, *41*, 1945-1947.
(91) Frisch, A. C.; Shaikh, N.; Zapf, A.; Beller, M. *Angew. Chem., Int. Ed.* **2002**, *41*, 4056-4059.
(92) Ishiyama, T.; Abe, S.; Miyaura, N.; Suzuki, A. *Chem. Lett.* **1992**, 691-4.
(93) Molander, G. A.; Sandrock, D. L. *J. Am. Chem. Soc.* **2008**, *130*, 15792-15793.
(94) Lee, S. J.; Gray, K. C.; Paek, J. S.; Burke, M. D. *J. Am. Chem. Soc.* **2007**, *130*, 466-468.
(95) Gillis, E. P.; Burke, M. D. *J. Am. Chem. Soc.* **2008**, *130*, 14084-14085.
(96) Gillis, E. P.; Burke, M. D. *J. Am. Chem. Soc.* **2007**, *129*, 6716-6717.
(97) Abou-Elkhair, R. A. I.; Netzel, T. L. *Nucleosides, Nucleotides & Nucleic Acids* **2005**, *24*, 85-110.
(98) Liu, Q.; Burton, D. J. *Tetrahedron Lett.* **1997**, *38*, 4371-4374.
(99) Housecroft, C. E.; Sharpe, A. G. *Inorganic Chemistry*; 1 ed.; Prentice Hall: Harlow, England, 2001.
(100) Crisp, G. T. *Chem. Soc. Rev.* **1998**, *27*, 427-436.
(101) de Meijere, A.; Meyer, F. E. *Angew. Chem. Int. Ed.* **1995**, *33*, 2379-2411.
(102) Arjunan, P.; Berlin, K. D. *Org. Prep. Proced. Int.* **1981**, *13*, 368-71.
(103) Danishefsky, S.; Berman, E. M.; Ciufolini, M.; Etheredge, S. J.; Segmuller, B. E. *J. Am. Chem. Soc.* **1985**, *107*, 3891-8.
(104) Santhosh, K. C.; Balasubramanian, K. K. *Syn. Commun.* **1994**, *24*, 1049 - 1056.
(105) Du, H.; Fuh, R. C. A.; Li, J.; Corkan, L. A.; Lindsey, J. S. *Photochem. Photobiol.* **1998**, *68*, 141-142.

(106) Gosser, D. K. *Cyclic Voltammetry : Simulation and Analysis of Reaction Mechanisms*; Wiley-VCH: New York, NY, 1993.

(107) Nicholson, R. S. *Anal. Chem.* **1965**, *37*, 1351-5.

(108) Quan, M.; Sanchez, D.; Wasylkiw, M. F.; Smith, D. K. *J. Am. Chem. Soc.* **2007**, *129*, 12847-12856.

(109) Quan, M.; Sanchez, D.; Wasylkiw, M. F.; Smith, D. K. *J. Am. Chem. Soc.* **2007**, *129*, 12847-12856.

(110) Melfi, P. J.; Camiolo, S.; Lee, J. T.; Ali, M. F.; McDevitt, J. T.; Lynch, V. M.; Sessler, J. L. *Dalton Trans.* **2008**, 1538-1540.

(111) Kang, P.; Foote, C. S. *J. Am. Chem. Soc.* **2002**, *124*, 4865-4873.

(112) Green, T. M.; Wuts, P. G. M. *Protective Groups in Organic Synthesis*; Wiley-Interscience: New York, 1999.

(113) Karsten, K.; Jürgen, V. *Eur. J. Org. Chem.* **2004**, *2004*, 209-219.

(114) Nak Cheon, J.; Ji Sun, L.; Eunju Lee, T.; Young Ju, L.; Kyung Byung, Y. *Angew. Chem. Int. Ed.* **2008**, *47*, 10128-10132.

(115) Kissel, P.; Weibel, F.; Federer, L.; Sakamoto, J.; Schluter, A. D. *Synlett* **2008**, 1793-1796.

(116) Kharlamova, T. V. *Chem. of Nat. Compd.* **2007**, *43*, 391-394.

(117) Gattinoni, S.; Merlini, L.; Dallavalle, S. *Tetrahedron Lett.* **2007**, *48*, 1049-1051.

(118) Cabri, W.; Candiani, I. *Acc. of Chem. Res.* **1995**, *28*, 2-7.

(119) Ozawa, F.; Kubo, A.; Matsumoto, Y.; Hayashi, T.; Nishioka, E.; Yanagi, K.; Moriguchi, K. *Organometallics* **2002**, *12*, 4188-4196.

(120) Loiseleur, O.; Hayashi, M.; Schmees, N.; Pfaltz, A. *Synthesis* **1997**, *1997*, 1338-1345.